



National Defence
Research and
Development Branch

Défense nationale
Bureau de recherche
et développement

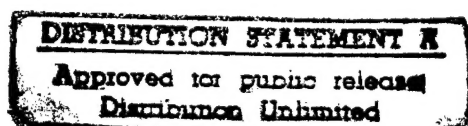
DREA CR/97/408

LASER BASED METHOD OF EVALUATING
THE BEHAVIOR OF SURFACES AND
SURFACE TREATMENTS AT TRANSIENT
HIGH TEMPERATURES AND PRESSURES.

by

V.E.Merchant, & J.A.Hewitt

THE LASER INSTITUTE
9924-45 Avenue
Edmonton, Alberta, Canada
T6E 5J1



CONTRACTOR REPORT

Prepared for

Defence
Research
Establishment
Atlantic



Centre de
Recherches pour la
Défense
Atlantique

Canada  DTIC QUALITY INSPECTED 3

19970804 043



National Defence
Research and
Development Branch

Défense nationale
Bureau de recherche
et développement

DREA CR/97/408

**LASER BASED METHOD OF EVALUATING
THE BEHAVIOR OF SURFACES AND
SURFACE TREATMENTS AT TRANSIENT
HIGH TEMPERATURES AND PRESSURES.**

by

V.E.Merchant, & J.A.Hewitt

THE LASER INSTITUTE
9924-45 Avenue
Edmonton, Alberta, Canada
T6E 5J1

Scientific Authority

Calvin Hyatt
Calvin V. Hyatt

W7707-5-3295/01-HAL
Contract Number

March 1996

CONTRACTOR REPORT

Prepared for

**Defence
Research
Establishment
Atlantic**



**Centre de
Recherches pour la
Défense
Atlantique**

Canada

DTIC QUALITY INSPECTED 3

Abstract

A set of experiments were performed in order to test the ability of a laser based system to simulate the chemical and thermal effects inside a gun barrel. It is expected that a laser based system would be a relatively inexpensive method for testing various materials and coatings for eventual gun barrel use, and to the present time, there are no publicly documented systems capable of such testing. An extensive literature review revealed that simulation of the mechanical effects would not be possible under the scope of this project, but thermal and chemical simulations could be done. A chamber was constructed to be used for both laser weld overlaying in an inert atmosphere, and for the simulations. Laser melting of titanium indicated that the chamber could provide an inert atmosphere in which no visual contamination of the titanium occurred. Parameters were developed to weld overlay titanium on AISI 4340 using 0.25 mm of preplaced powder, 1 ms pulses at a frequency of 50 Hz, and energy of 7.5 J/pulse, and a speed of 2.1 mm/s. This coating was then used as an interlayer for weld overlaying a 90tantalum-10tungsten alloy. Since titanium has a melting temperature close to the alloy steel, it was conjectured (correctly) that it could be more easily laser weld overlayed than the high melting temperature tantalum-tungsten alloy. Since Ta-Ti form a solid solution, rather than intermetallics formed by Ta-Fe, this was the best interlayer. The 90Ta- 10W alloy was overlayed using 0.25 mm of preplaced powder, 1 ms pulses at a frequency of 50 Hz, and energy of 7.5 J/pulse, and a speed of 5.2 mm/s. The coating was not continuous, but did appear to be melted and bonded in several locations. Other coatings were produced, including 0.25 mm of Stellite 6 on A36 mild steel, and 90 Ta-10W on commercially pure titanium. These coatings and their base materials were then subjected to thermal cycle testing. The testing involved using a frequency of 2 Hz corresponding to a firing rate of 120 rounds/minute, a pulse duration of 5 ms (typical of a gun), 5 shot bursts at 45 J/shot. A waiting period of 10 s between bursts was necessary for equilibrium temperatures to be reached. The process was calibrated using AISI 4340. Although the system was capable of over 2000 shots (400 cycles), the parameters were based on 10 cycles (50 shots) to cause visible melting on the surface. After 10 cycles, the poorest material was the A36 mild steel which contained extensive melting. The 90Ta- 10W alloy seemed to perform the best, with little visible damage after 10 cycles (50 shots). After 20 cycles (100 shots), damage/melting was more evident, but did not worsen up to 50 cycles (250 shots).

Résumé

Une série d'expériences a été menée afin de tester la capacité d'un système laser à simuler divers effets chimiques et thermiques sur les parois intérieures d'un canon d'arme à feu. La méthode de simulation laser employée pour tester divers matériaux et revêtements destinés à la fabrication des canons d'arme à feu semble relativement peu coûteuse. À l'heure actuelle, ce type de système n'est décrit dans aucun document public. Après un examen exhaustif de la documentation existante, il est ressorti que la simulation des effets mécaniques ne serait pas possible dans le cadre du présent projet, tandis que des simulations thermiques et chimiques pourraient être menées. Une enceinte a été construite aussi bien pour le rechargement laser sous atmosphère inerte que pour la conduite des simulations. La fusion laser de titane, au cours de laquelle aucune contamination du matériau n'a été observée, a démontré que l'enceinte pouvait effectivement offrir une atmosphère inerte. Le rechargement laser du matériau AISI 4340 au moyen de titane s'est effectué à l'aide d'une couche de 0.25 mm de poudre prédisposée sur le substrat, le laser délivrant des impulsions de 1 ms, à une fréquence de 50 Hz avec une énergie de 7.5 J/impulsion et une vitesse de balayage de 2.1 mm/s. Le revêtement ainsi obtenu a ensuite servi de couche intermédiaire en vue du rechargement au moyen d'un alliage de tantale- 90% tungstène- 10%. Comme le titane a une température de fusion voisine de celle de l'alliage d'acier, on a supposé (avec raison) qu'il pourrait subir le traitement laser plus aisément que l'alliage tantale-tungstène à température de fusion élevée. L'alliage Ta-Ti, qui forme une solution solide plutôt que des composés intermétalliques comme dans le cas du Ta-Fe, constituait une meilleure couche intermédiaire. L'alliage Ta-90% W-10% a été mis en place au moyen d'une couche de 0.25 mm de poudre prédisposée, le laser fonctionnant par impulsions de 1 ms, à une fréquence de 50 Hz, avec une énergie de 7.5 J/impulsion et une vitesse de balayage de 5.2 mm/s. L'opération a donné un revêtement non continu, mais apparemment fondu et lié en divers endroits. D'autres revêtements ont été réalisés, notamment une couche de 0.25 mm de Stellite 6 sur acier doux A36 et un alliage Ta-90% W- 10% sur du titane sous forme commerciale pure. Ces revêtements ainsi que leurs substrats ont ensuite été soumis à des essais de cycles thermiques.

Les essais laser ont été effectués à une fréquence de 2 Hz correspondant une cadence de tir de 120 coups/minute, avec une durée d'impulsion de 5 ms (durée type dans une arme à feu), par rafales de 5 coups à 45 J/coup. Il a fallu prévoir un délai de 10 secondes entre chaque rafale pour atteindre les températures critiques. L'étalonnage du procédé s'est effectué sur le matériau AISI 4340. Bien que le système pouvait reproduire 2 000 coups (400 cycles), les paramètres de traitement ont été établis en fonction de 10 cycles (50 coups) afin de provoquer une fusion visible sur la surface. Après 10 cycles, l'acier doux A36 a obtenu les moins bons résultats, montrant d'importants signes de fusion. L'alliage Ta- 90% W- 10% semble s'être le mieux comporté et n'a montré que très peu de dommages après 10 cycles (50 coups). Après 20 cycles (100 coups), on a observé plus de dommages/fusion, mais jusqu'à 50 cycles (250 coups), la dégradation n'a pas évolué.

Table of Contents
Phase I. Literature Survey

I. Introduction	1
I.1 Outline	1
I.2 Gun Tube Wear	2
II. Conditions in Gun Tubes and Mechanisms of Erosion	4
II.1 Erosion of Gun Tubes	4
II.2 Muzzle Wear	15
II.3 Gas Wash Phenomenon	15
II.4 Firing Conditions in Gun Barrels	17
III. Lasers to Stimulate Chemical and Metallurgical Changes in Surfaces	19
III.1 Metallurgical Effects	19
III.2 Alloying Effects	20
IV. Lasers Generated Plasmas, and Mechanical Effects in Targets	22
IV.1 Mechanism of Laser Interaction	22
IV.2 Laser Ablation of Material	25
IV.3 Surface Interaction with Laser Produced Plasmas	29
IV.4 Laser Interaction with AISI 4340 Discs	32
IV.5 Laser Interaction with Buffered Targets	34
V. Surface Engineered Coatings for Gun Tubes	38
V.1 Criteria for Materials	38
V.2 Chromium Plate	38
V.3 Laser Interaction with Chromium Plate	40
V.4 Coatings Other than Chrome Plate	42
VI. Analysis of Potential of Lasers to Simulate Gun Tube Wear	48
VI.1 Variables to be Simulated	48
VI.2 Previous Laser Simulation Studies	50
VI.3 Laser Driven Shock Waves	51
VI.4 Laser Simulation of Gun Tube Damage	53
VII. Project Definition	54
VII.1 Ambient Pressure Experiments	54
VII.2 Laser Irradiation Parameters	55
VIII. References	57

Table of Contents
Phase II. Experimental Work

I. Introduction	- 63 -
I.1 Background	- 63 -
I.2 Objectives	- 65 -
II. LASER WELD OVERLAYING	- 65 -
II.1 Experimental Apparatus	- 65 -
II.2 Experimental Materials	- 67 -
II.3 Experimental Procedures	- 67 -
II.3.1 Laser Melting of C.P. Titanium	- 69 -
II.3.2 Laser Weld Overlaying of Titanium on AISI 4340	- 70 -
II.3.3 Laser Weld Overlaying of Tantalum-Tungsten Alloy on C.P. Titanium	- 70 -
II.3.4 Laser Weld Overlaying of Tantalum on LWO Titanium (on AISI4340)	- 71 -
II.4 Description of Coatings	- 71 -
III. THERMAL CYCLE TESTING	- 74 -
III.1 Initial Trials	- 74 -
III.2 Calculation of Thermal Profiles	- 75 -
III.3 Experimental Apparatus	- 78 -
III.4 Experimental Procedures	- 79 -
III.5 Experimental Results and Observations	- 81 -
IV. Recommendations	- 88 -
V. Conclusions	- 90 -
VI. References	- 92 -
Appendix: Figures	- 93 -

Phase I. Literature Survey

I. Introduction

I.1 Outline

This is phase I of the project "LASER BASED METHOD OF EVALUATING THE BEHAVIOUR OF SURFACES AND SURFACE TREATMENTS AT TRANSIENT HIGH TEMPERATURES AND PRESSURES". The project is intended to develop procedures for using laser energy to simulate the wear on gun tubes, and to demonstrate that these procedures can be used for evaluating coatings with the potential to improve the service life of guns.

The first section of the report contains an examination of the literature for what is known about the firing conditions in gun tubes, such as the pressure and temperature history, and the mechanisms of erosion. The following section summarizes the use of lasers to induce changes in steel, and in particular in gun steel. Changes are of three types: (1) metallurgical changes in which the structure of the material is changed, (2) chemical changes in which the composition is modified, usually accompanied by a metallurgical change, and (3) mechanical effects, in which the pressure wave induced by the laser interaction with the metal surface damages the material.

Possible surface coatings for gun tubes are then discussed. Chromium plated surfaces have long been used for guns. There have been a few experiments in which laser radiation has been used to modify the chromium surfaces; these are briefly described. Coatings other than chrome plate are then discussed; it is anticipated that some of these coatings may be those evaluated once the laser simulation of gun tube damage has been verified.

The report concludes with an analysis of the potential of laser energy to simulate gun tube damage, and a definition of the parameters that have to be duplicated in qualifying the laser procedure as a means of testing gun coatings.

I.2 Gun Tube Wear*

During firing, the bores of high calibre, military gun barrels are exposed to extremely aggressive operating conditions, which cause extensive wear on the internal surface, and limit the gun life. Temperature and pressure fluctuations in excess of 2700 C and 550 MPa respectively, the presence of a variety of combustion gases produced during firing, and mechanical contact with the sliding projectile can produce severe wear patterns and microstructural modifications to the surface. The wear has been found to be dependent on the temperature produced by the explosive charge. Work by Thornhill (reviewed by Izod and Baker¹) determined wear per round as a function of predicted bore surface maximum temperature rise. For temperatures below 660C, there is no wear; between 660 and 1050 C, wear takes place relatively slowly; but above 1050 C, there is an accelerated rate of wear. Ward *et al.*² measured wear on a 37 mm blow out gun to be 1.1 ± 0.4 , 50.7 ± 6.0 , and 240.5 ± 15 mg/shot with explosives with flame temperatures of 2207, 2991, and 3443 °C respectively.

Ahmad³ states that the rate of erosion depends on the nature of the explosive. Picrate rich propellants are less erosive than non-picrate equivalent propellants. Propellants containing nitroamines are more erosive than the equivalent nitrocellulose base propellants. Izod and Baker¹ refer to experiments in which the wear decreased with increasing flame temperature, but in this case specially formulated propellants with different ballistic sizes were used to give the same muzzle velocity in a 30 mm test gun. These experiments imply that factors other than flame temperature may be significant in gun wear, but these factors have not been completely explored.

Ahmad³ summarizes methods to reduce the bore surface temperature, and hence wear, by external cooling of the barrels, by use of protectors and sleeves around the barrels, or by the use of a smear, an inert oil or grease (typically silicon oil), ahead of the propellant gas to

* A variety of different units are used to measure pressure; in this report they have all been converted to Pascal (Pa), kilopascal (kPa), Megapascal (MPa), or Gigapascal (GPa). One Pascal is a pressure of a newton/m². The conversion factors are as follows:

1 Atmosphere = 1.01 bar = 1.01×10^6 dynes/cm² = 1.01×10^2 Pa = 101 kPa = 14.6 psi.

provide a temporary thermal barrier. Various additives to the propellant have been used. Canadian workers used thin slices of polyurethane foam inside the cartridge, while others have used liners of TiO_2 , wax and dacron (or rayon), or WO_3 and talc. The liners leave a residue which insulates the bore surface in subsequent firings. Ahmad suggested that a residual film was left on the bore surface from all the inorganic additives used in either large or small calibre guns. The film at least partially reduced the heat lost to the bore surface and the subsequent erosion. Izod and Baker, in their summary of U.K. work, say that the use of polyurethane foam described above increased barrel life by a factor of four. They attribute the lifetime increase to injection of relatively cool gas from the liner into the boundary layer protecting the steel.

In spite of the above protective measures, gun barrels continue to erode, as will be discussed in the next section. The remainder of this report shall be devoted to permanent coatings on the barrel surface, and methods of testing them.

II. Conditions in Gun Tubes and Mechanisms of Erosion

II.1 Erosion of Gun Tubes

There are few, if any, studies of the wear during the initial stages because of the cost of the barrels of large guns. However, there are considerable analyses of damage of condemned guns. At this point, the guns have been subjected to a variety of different types of explosives, different charges, and different shells. As a result, there are not many cases of damage to guns that have been fired under well documented conditions, and much of the initial stage of damage remains a mystery.

Barrel wear is generally thought to be caused by three factors; thermal effects due to temperature variation, chemical interaction of the barrel surface with the propellant gases, and mechanical contact with the projectile⁴. The relative importance of each factor in contributing to the overall wear mechanism, the amount of wear, and the microstructural modification produced in the barrel surface is dependent upon the position along the length of the bore⁵, and on the temperature of the explosive. Generally, the amount of wear is determined by the rate of heat that is transferred to the bore surface. Typically, the wear decreases as one moves from the origin of rifling towards the muzzle, but can increase again in the vicinity of the muzzle itself, as will be discussed later.

The greatest wear rates are typically displayed at the origin of rifling where the barrel is exposed to the highest temperature, which causes softening and melting of the surface region⁴. The wear in this region is increased by the chemical interaction of the hot metal with propellant gases including CO, CO₂, H₂, N₂, and water vapour. This interaction produces a hard, white etching microstructure which melted at a lower temperature.^{1,2} Metallurgical examination of the white layer has revealed it to be the result of carburization by the propellant gases, and to consist of high carbon austenite and a eutectic structure of fine carbides⁵. The presence of Fe₃O₄ and Fe₂O₃ indicated oxidation to be occurring concurrently with carburization⁵. Ahmad *et al.* pointed out⁶ that the interaction of the gun steel with surface gases converted the surface to carbides and oxides. Some carbon and nitrogen diffused deeper in the heat affected zone (HAZ), stabilizing some of the austenite since the martensitic

transformation is inhibited by high carbon contents⁷. When a single base propellant* was used, Fe_3C was the predominant product. In advanced barrels, however, a double or triple based propellant has been used. Then, higher temperatures resulted in FeO being the major product.

The modified surface melted at a lower temperature, as low as 1150°C , whereas the base metal melted at 1450°C . The combination of the lower melting temperature of the carburized surface together with the high operating temperatures and high velocity propellant gases resulted in almost complete removal of the land at the origin of rifling, as well as considerable damage to the valleys⁸. This is sometimes referred to as the "gas wash" phenomenon.

Under at least some operating conditions, the white carburized layer and the thermally altered layer beneath it, as well as the presence of cracks extending through the thermally altered layer to the base metal, appeared after a single shot of the gun⁹.

Bulpett¹⁰ studied white etched layers from Chieftain and RARDE** barrels using a variety of methods including microscopy, hardness testing, scanning electron microscopy (SEM), transmission electron microscopy (TEM), electron microprobe analysis, electron probe x-ray microanalysis (EPMA) light element analysis, and secondary ion mass spectroscopy (SIMS).

Surface structure of samples from the region of the commencement of rifling region of the Chieftain gun showed a $10\text{ }\mu\text{m}$ thick, apparently structureless surface layer. Under this was a 110 to $150\text{ }\mu\text{m}$ thick white layer through which a network of cracks penetrated. The two layers were referred to as the thin and the thick white etching layers, respectively.

The microstructure of the thin layer consisted of large martensite grains with narrow lenticular twin features; there was an even distribution of fine M_3C and M_7C_3 carbides within the grains. The outer white layer contained a small amount of calcium, presumably originating from the propellant charge, a slightly increased level of nickel, and a decreased level of

* A single base propellant consists of one explosive material, usually nitrocellulose. Double and triple based propellants consist of nitrocellulose mixed with other explosive materials, for example nitroglycerine or dinitrotoluene. The multiply based propellants have a higher flame temperature. A list of the composition of common propellants used in the US is given by Ahmad³.

** Royal Armament Research and Development Establishment, U.K.

chromium relative to the matrix. Chromium and molybdenum were also depleted into the thick white etching layer. The carbon content of the thin etching layers, the thick etching layers, and the matrix were 2.8, 0.55, and 0.45 weight percent respectively. The measurement accuracy was ± 0.05 weight percent, so the observed enrichment of the thick etching layer was not significant. The thick etching layer consisted of martensite grains with a high density of dislocations and small M_3C and M_7C_3 carbide particles.

The 30 mm RARDE gun had apparently undergone 3750 rounds with a variety of propellants. TEM analysis of the surface of the samples from the RARDE gun revealed a thin, approximately 10 μm thick, surface white-layer containing 5.2 wt% C; it was a distinct band of homogeneous material composed of small equiaxed grains with no visible internal structure. Diffraction suggested that this layer was primarily composed of M_3C carbides in an austenitic matrix. Below this was an approximately 50 μm thick white-etching layer, severely cracked, which had been modified by the thermal cycling to produce a fine grain material containing a distribution of small M_3C and M_7C_3 carbide particles. It was not significantly enriched in carbon from the 0.4% level of the underlying steel.

The thick white-etching layers formed on the Chieftain and the RARDE barrels contained increased levels of hydrogen, nitrogen, and oxygen to a depth of 30 μm and 10 μm respectively, when compared to the underlying matrix. These thin surface layers had a lower hardness than the underlying thermally refined martensite. Elemental analysis showed the thin etching layer in samples from this gun were depleted in chromium, manganese and nickel and enhanced in molybdenum with respect to the matrix. The thick etching layer had no significant deviation in composition from the matrix.

Bulpett also referred to earlier work by Amos and Sheward (a UK Ministry of Defence report from RARDE) in which gun barrel white layers were found to consist of 70% ϵ -phase carbo-nitride and 30% α -ferrite. He also refers to 1939 work by Snair and Wood, in which a 50 μm thick white layer in the bore of machine gun barrels was attributed to nitrides in solution rather than a martensitic structure.

Lin¹¹ used Auger electron spectroscopy to analyze the surface of sections from three gun tubes manufactured from 4330 steel. The propellants and service conditions used with the guns

were not known. The surface of a 20 mm gun was eroded to a grey to black colour with no metallic lustre. It was so severely etched and cracked that no rifling pattern was distinguishable. Large circumferential cracks spaced about 1 mm apart penetrated 100 μm into the surface at an angle, interconnected by smaller cracks. Traces of chromium plating remained. Auger analysis of the surface layer found, in addition to iron, carbon and oxygen, the following elements: barium, sulphur, calcium, phosphorus, chlorine, nitrogen, chromium, and zinc. The barium was associated with sulphur and oxygen, and was conjectured to be due to BaSO_4 . The nitrogen was greater than expected from the composition of the steel, and thought to be from nitrates and nitrites in the propellants. Potassium and calcium were present in significant amounts, were found together, and had a depth profile similar to oxygen. The origin of the zinc was attributed to the gilding metal on the shells.

Sections from a still serviceable 47 mm gun were also analyzed. The rifling was well preserved, and no cracking or pebbling of the bore surface was visible. Two white reaction layers of 0.5 and 18 μm thickness were observed. Elements detected were sulphur, chlorine, potassium, calcium, carbon, nitrogen, oxygen, iron, chromium, nickel, copper,

zinc, and occasionally lead. The sulphur, potassium, chlorine and calcium were presumed to be from the propellant; the sulphur and potassium were on sublayers of the surface. The concentrations of nitrogen and carbon were high compared to the first gun analyzed. The top layer was extensively oxidized and carburized.

The third sections analyzed by Lin were from a 105 mm gun. They were severely cracked, but the rifling pattern was still visible. A 200 μm thick layer of chromium had been electroplated on the surface; cracks were observed to extend through the coating and into the

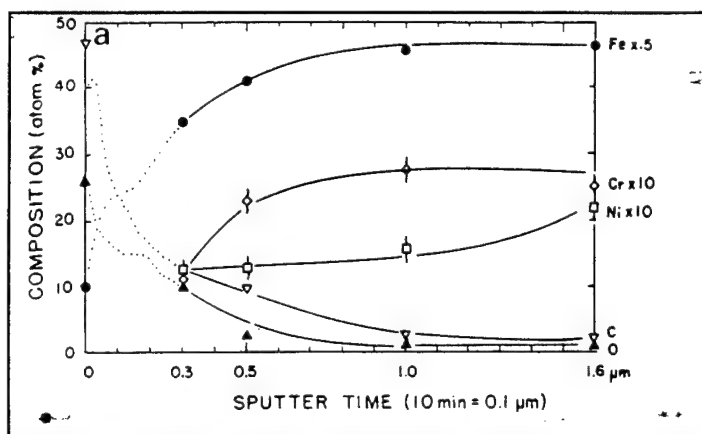


Figure 1. Depth profile determined by Auger in GS2. The first white layer is 0.5 μm thick, and the second white layer about 18 μm thick.

underlying steel. Elements detected were phosphorus, beryllium, chlorine, sulphur, potassium, calcium, chromium, oxygen, iron, copper, zinc, and aluminum.

In later work, Lin continued¹² the Auger analysis of the chemical constituents of barrel surfaces. He reported that accumulated deposits and residues from combustion gases were usually more than a few microns thick. The elements found depended on the propellants used in firing. Major features of gun tube erosion visually observed were extensive oxidation and thermal cracking. The combination of both features in varying degrees is a unique characteristic of the eroded surfaces regardless of the surface materials.

He proposed several stages of gun tube erosion, based on examinations of different gun tubes at different service intervals:

1. **Deposition of unburnt particles on the molten surfaces.** The "white" layers contained a uniform distribution of calcium, oxygen, carbon, nitrogen, and sulphur.
2. **Corrosion and cracking of the chromium coated surface.** Cracks of the chromium layer were 100-200 μm deep and 10-20 μm wide. Precipitates including carbon, potassium, sulphur, sodium, zinc and oxygen accumulated in the cracks. He suggested it was a mixture of oxides, but could only detect the individual atomic constituents.
3. **Severe erosion and the removal of the cracked Cr layer.** Cracking penetrated into the underlying steel substrate; platelets of the cracked chromium surface were missing. Iron was found on top of partially separated flakes, possibly from the projectile. Carbon was primarily in the cracks. Sulphur was found on top of a loosened platelet, together with oxygen and iron. Oxygen was distributed on the top surface layer of the chromium, suggesting the formation of metal oxide.
4. **Erosion of the steel substrate.** After the chromium was removed, wide networks of cracks penetrated into the steel. Major cracks were normal to the maximum temperature gradient, with small ones perpendicular to the major cleavage. Edges of cracks were rounded and smoothed. Carbon from unburnt propellant were found in the cleavages and cracks. There was more carbon in larger cracks; the accumulation depended on the orientation of the cracks. Oxygen distribution coincided with iron. Potassium and sulphur were primarily distributed in depressed regions formed by cracks.

The thickness of the oxide layer varied widely from 3 μm on the chromium surface exposed to the combustion gases to several tens of microns in the valleys of the steel cracks. Lin concluded that oxygen is the most important factor in the chemical erosion of the gun tubes. He proposed that the oxygen originated in gases such as water vapour, nitrous oxide, nitric oxide, carbon monoxide, and carbon dioxide presumably originating from additives of the propellant, which would react at high temperatures with the steel.

Lin suggested that the carbon that he observed was from soot, unburnt particles, or particles condensing from the exploding gases, rather than from interaction between the gases and the steel. The carbon tended to accumulate in cavities of the eroded surfaces such as pits, cracks, and depressions. The amount of carbon present in the cavities seemed to depend on the size as well as the orientation of the cavities. In micro-cracks with no direct exposure to precipitates, no carburization was observed. Auger showed the elements iron and oxygen occurred together.

Nitrogen was observed as a minor constituent on the eroded surface. Nitrogen was widely scattered in depressed areas of the surface, but was not found on the top surface layer. The presence of nitrogen was always accompanied by a large concentration of oxygen, so it was believed that nitrogen was present in the form of nitrate or nitrites.

Turley⁸ conducted an examination of a condemned 120 mm tank gun barrel, which showed slag in the rifling grooves. The term slag refers to a fused mass of material derived from the bore surface, the projectile driving band, and the propellant debris. Energy dispersive X-ray scans showed lead, iron, aluminum, potassium, silicon, phosphorus, and titanium in the slag; in some cases chromium from the electroplate was also observed. The lands of the rifling grooves were covered with craze cracks; the X-ray scans showed the cracks to be largely filled with copper.

A heat affected zone in the gun steel was seen in the eroded rifling grooves, but not in the lands where some chromium remained. Deep craze cracks were present in the chromium and extended into the underlying steel. In some cases, adhesion of the coating at the edge of the lands was poor, and erosive gases had penetrated through some craze cracks and then along the chromium-steel interface. In other cases adjacent to copper filled craze cracks,

separation was taking place within the chromium coating rather than at the interface, indicating good coating adherence. It was conjectured that during heating of the bore, the stress exerted on the chromium coating by thermal expansion of the copper in the craze cracks was of the same order as the tensile strength of the coating.

Recrystallization of the chromium electroplate was observed, indicating that temperatures near the melting point were reached, particularly near the edges of the lands where the friction with the projectile was assumed to be at a maximum.

In a later publication, Turley and coworkers¹³ continued the study of the metallurgy in a region of the condemned barrel using scanning Auger microscopy (SAM), SEM, and X-ray diffraction. The gun metal was 0.4% C, 1.5% Cr, 1.0% Mb, 2.5% Ni, with a tempered martensite microstructure of hardness ≈ 450 Hv. The bore surface was observed to be covered with a network of craze cracks. In the lands, the cracks contained copper and zinc; in the grooves, the cracks contained lead. Beneath the eroded bore surface in the commencement of rifling region, four distinct altered layers were identified:

1. an outer white layer consisting of cementite (Fe_3C). It was formed by carburization of the bore surface by hot propellant gases, and had a lower melting temperature (≈ 1150 C) than the gun steel (≈ 1500 C). During firing the outer white layer melted and was largely removed by the propellant gases. The thickness of the layer was $0.25 \mu\text{m}$.
2. An inner white layer of high carbon austenite. It was formed by carburization of the bore surface by hot propellant gases. The thickness of the layer was $1.3 \mu\text{m}$.
3. A TAL (Thermally Altered Layer) of lightly tempered fine-grained martensite, formed as a result of the gun steel being heated into the austenite range. Craze cracks extended through this region.
4. an overtempered layer of gun steel. Formed as a result of the gun steel being heated to below the AC_1 temperature.

In comparing the results of their work to other work in the literature; they comment that other workers have found the outer white layer to consist of ϵ -iron carbonitride, also on a tank gun barrel. In this work, nitrogen was detected primarily at background levels. The white layer was produced only when the metal was exposed to carbonaceous reducing atmospheres, in

particular 41% CO₂, 32% N₂, 20% H₂ and 7% CO, a mixture similar to that produced by burning propellant. The paper contained some discussion about how the carbon gets into the material. A solid state diffusion mechanism would not explain the observed depth. Solid state diffusion would lower the melting point, and liquid flow would result in a deeper penetration.

Griffin and coworkers⁹ describe experiments with an instrumented 5" gun at the U.S. Naval Weapons Center. Test plugs were inserted at different positions in the barrel. The plugs could be withdrawn after 1, 2 or 5 rounds. Due to erosion of the port holes, test plugs were exposed to a propellant atmosphere on their sides as well as on their faces. Erosion of the port holes resulted in alteration of the gas flow pattern, and the majority of metallurgical changes occurred at the specimen corners due to turbulent flow and stagnation. Even though the instrumented gun had promise as a test apparatus, the presence of the test plugs influenced the gas flow, producing results that were not necessarily representative of the gun barrel surface.

The propellants tested were (1) Naco, (2) Pyro, (3) M-26 plus talc, and (4) M-26 plus silicon oil. The materials tested were (1) gun steel, (2) 1018 carbon steel, and (3) Armco iron. Some of the projectiles had copper rotating bands, and some had plastic. The number of firing tests was insufficient for complete matrix study.

The authors described the zones in metal samples from a field fired cannon, which they subsequently related to samples from their trials:

1. Unaltered gun material
2. The thermally altered layer (TAL), which appears to be as-quenched martensite with an extremely fine grain size. There were fine precipitates of carbides in the structure, probably resulting from tempering.
3. The inner white layer; it was featureless except for a fine needle-like constituent which appeared to emanate from the thermally altered layer. There was no distinct boundary between the inner white layer and the TAL.
4. The outer white layer. There was a distinct boundary between the inner white layer and the outer white layer, which sometimes contained a parallel plate-like phase.

In test plugs with Naco propellant, white layers were visible after one round. White layers were most prominent for plugs near the origin of rifling, and less prominent as the distance

from this position increased. Regions of surface alteration became more prominent after two rounds. No cracks were seen, although surface cracks were seen for the other propellants.

The gun steel after firing was compared to 1018 steel, at the same position. In the gun steel, the inner white and TAL layer were seen; the TAL layer showed a much finer grain size than the base metal. A crack extended through the white layer into the TAL, after one shot. In 1018 steel, the white layer was described as very thin, and was not obvious in the micrographs provided in the paper. Patches of as-quenched martensite were rich in carbon as the heat of firing had dissociated the pearlite but the time-at-temperature was insufficient for diffusion of carbon to form a low carbon austenite.

Gun steel was compared to Armco Iron, fired under similar conditions. In the Armco iron, grain refinement was seen near the corner of the test plug, and evidence of a white layer was detected. There was a sharp transition between the TAL and the base metal, corresponding to the extent of austenite formation at a temperature of 900 C.

Firing with different propellants was compared. Naco, Pyro, and M-26 propellants have adiabatic flame temperatures of 1877, 1877, and 2830 C respectively. The major difference in the structural damage of the test plugs was in the extent of damage. Guns fired in the field with Naco explosives showed soft surface hardness associated with the inner white layer. At a depth of 80 μm there was a transition to the base metal hardness. The surface of the barrels of a gun fired with Pyro explosives had a peak hardness which was observed to a greater depth than that with Naco explosives; it was 180 μm before base metal hardness was achieved. A test plug fired with M-26 plus silicone explosive showed a hardness similar to those fired with Pyro in the field tests. The hardness of a test plug after five rounds was the same as that after one round.

The wear rate was correlated¹⁴ with the bore surface temperatures achieved with the different propellants, as shown in the Table I.

The formation of the surface layer effects the wear of the gun tube, and can act as a protective coating. Ward *et al.* measured² wear on a 37 mm blow out gun with alternating explosives, studying the conditions of the barrel by the previous discharges. Wear by an explosive with a given flame temperature depended on the flame temperature of the explosive

used previously in the gun. The effect of the previous explosive was greatest with the propellant with the lowest flame temperature, in which the wear was the least. The effect of the previous explosive was attributed to the thickness of the surface layer, assumed to be an oxide.

Propellant	Bore surface temperature	Wear rate ($\mu\text{m}/\text{round}$)
Naco	850 C	0.5
M6	980 C	2.5
M26	1230 C	250

Table I. Use of Different Propellants

Because the oxide has a different coefficient of thermal conductivity than the base metal, the heat flow into the barrel and subsequent chemical and metallurgical changes are affected. No diagnostics verifying the existence of the oxide layer were mentioned in the paper.

Montgomery¹⁵ has studied the friction of the projectile in the gun tube, and emphasized the importance of melt lubrication. The coefficients of friction between the shell metal and the base metal measured in the laboratory were considerably lower than the values observed in guns. This was attributed to a liquid layer between the projectile and the tube. Evidence for melt lubrication was provided, although photographic reproduction was poor.

Above a threshold value of the pressure-velocity product, the coefficient of friction dropped with increasing product value, but the wear rate increased approximately as the square of the product. The wear rate, for a particular value of heat generation at the interface, increased with decreasing melting point of interfacial materials, with the exception of aluminum and copper which have higher thermal conductivities.

An investigation was undertaken¹⁶ of possible corrosion of high alloy materials if used in barrels of rapid fire aircraft weapons. These tests included AISI 4340 steel to provide a base point. The tests included hot plate tests, in which copper instantaneously wet the surface of the steel, at 1200C. The surface to a depth of 5 or 10 μm contained 1 wt% copper. Copper penetrated to a depth of 50 μm along grain boundaries. Several of the nickel based alloys reacted strongly with the copper.

Shells were also fired through a preheated barrel attachment, with removable test barrel sections, which were preheated to simulate the rapid fire operation. Some copper was transferred to the simulated 4340 steel barrels, but there was no detectable interpenetration of

copper into the iron.

Fisher and colleagues¹⁷ examined fired cannon tubes using scanning and transmission electron microscopy and electron diffraction (EDX) as well as Auger, Mossbauer, and secondary ion mass spectroscopy. They also presented brief results on simulation samples heated in a vacuum or in a methane atmosphere by capacitive discharge. The EDX spectrum from barrel samples from a cannon fired with additives in the explosive showed the presence of titanium aluminum, sulphur, potassium and copper. The copper was associated with abrasion marks, caused by the rotating copper rotating band. There was a heat checked "corn cob" pattern, with alternating shallow, deep, and very deep cracks. Copper and lesser amounts of aluminum and sulphur were found right to the tip of the crack.

Samples from a cannon fired without additives in the propellant had a somewhat different appearance, with cementite at surface confirmed by electron diffraction, roughly 0.25 to 0.5 μm thick. The subsurface 2 to 10 μm of austenite contained 2% C at the surface, decreasing to 1% C in the interior of the layer.

Examination of the white layer lead to conjecture that a carbon-saturated liquid iron formed on the surface and solidified rapidly after firing to form a thin layer of fine eutectic of Fe_3C and Fe with a considerable amount of retained austenite. The martensite start temperature was depressed because of the high C content. Carbon diffusion into the metal resulted in formation and retention of a layer of relatively soft austenite and an altered ferrite region hardened by the precipitation of alloy carbides. The paper stated that no white layer formed on surfaces protected by chrome plating, although the thickness of the chrome layer was not given.

Heat checking was presumed to result from the very different expansion coefficients of ferrite and austenite, so the surface layer was subjected to tensile strains. Rapid cooling results in quench cracks. Stresses would be relieved by an initial stage of crack formation, but build up during further cooling, causing secondary cracking which resulted in a network of coarse and fine cracks. Without additives to the propellant, an average wear rate of 25 μm per round was observed. This was comparable to the depth crevices between the heat-checked pattern elements. The authors postulated that each kernel was removed during each firing cycle,

perhaps by melting and being swept away.

Although the authors presented no photographs to support their observations, they also said that cracks 0.2 to 1 mm deep form parallel to the rifling, which they called fatigue cracks. These cracks contain easily detected copper, and some sulphur and aluminum, to very near the crack tip. The copper is likely transferred from the rotating band on the shell. The authors suggest that embrittling agents are forced into the cracks by the explosion pressure, which enhances the cracks. Moreover, the cracks allowed passage of exhaust gases contributing to subsurface carburization.

II.2 Muzzle Wear

Montgomery¹⁸ conjectured that improvements in erosion at the origin of rifling may lead to muzzle wear being a limitation in the lifetime of armaments. Muzzle wear would result in significant range and azimuth dispersion. Muzzle wear was different from the more extensively studied wear at the origin of rifling. It was confined entirely to the lands of the rifling grooves, usually asymmetric in the bore with the region of maximum wear spiralling down the bore with the rifling grooves. There was little evidence of the white etching layer on the steel surface, and the propellant burning temperature has no effect on muzzle wear. It is conjectured that compressed gas escaping past the shell misaligns it; the shell remains misaligned as it travels down the barrel.

The wear in the muzzle region has different characteristics and causes than that near the origin of rifling. The wear in this region is confined to the lands of the rifling, while the grooves usually show no appreciable wear. The presence of a hardened steel surface layer in this region together with the absence of a white etching layer suggests the predominant damage mechanism to be mechanical wear by the projectile with little or no involvement of the propellant gas. The presence of copper filled cracks in the hardened surface layer indicates the generation of sufficient frictional heat to partially melt the projectile rotating bands, and produce the surface heat affected zone in the steel.

II.3 Gas Wash Phenomenon

During the firing sequence of the gun, the exhaust gases from combustion and friction created by the moving projectile produce enough heat to reach the melting temperature of the

gun barrel material for a short period of time. As discussed below, the on-rush of gases in the confined space behind the projectile, and a chemical reaction of the molten steel with the propellant gases act to lower the melting temperature of the surface allowing for a small amount of molten material to be removed and swept away. After a number of shots, this erosion of material is evident as deep pockets at the origin of rifling.

Izod and Baker¹ postulated that the wear is due to gas flow around the shot. A good correlation of wear with a theoretical calculation was obtained, assuming the surface being eroded has hardness dependence on temperature typical of a 0.2% steel. They described the high speed filming of firing of a projectile, at 20,000 frames per second with the projectile lit by Xenon flash lamps. The filming showed that the projectile experienced vibration at charge firing and immediately before and during engraving (contacting the rifling grooves). Prior to engraving, cool non-luminous gas leaked past the projectiles and was pushed along with the shot. Later, this gas was compressed by the accelerating motion of the shot and ignites due to the heat of compression.

Jenning *et al.*¹⁹ studied the effect of a heated gas wash on metal surfaces. An explosively fired cylinder compressed gas in a chamber; the gas heated as it passes through a metal aperture. The aperture was fabricated from the metal being studied, and was examined after the tests. The gas used was an argon-nitrogen mixture. Pressures of 160 to 200 MPa were obtained, and temperatures of 3700 to 5200 C reached.

In an orifice of AISI 4340 steel, nodules 30 μm in size were formed, which contained carbon and, in some cases, oxygen. An Auger depth profile of the overall surface showed carbon at the surface and oxygen beneath it, both presumably originating from contaminants in the gas.

It is thought that turbulent eddies of gas behind the projectile sweep the hot gas around the rough heat-checked surface, causing localized melting around the grains in the white layer¹⁴. The melting results in the grains' susceptibility to being picked up by gas flow. In chrome plated tubes, propellant gas flow carried along by the moving projectile flows through the cracks and the spalled areas in the chrome plate and attacks the base metal. This undermines the integrity of the coating resulting in greater loss of chrome.

Johnson *et al.*²⁰ studied erosion of an orifice made of gun steel in a similar apparatus, but with a variety of different gases. Weight loss from the orifice was the indicator of whether erosion had taken place. There was no significant erosion when compressed nitrogen gas escaped through the orifice, even at temperatures of 2880C. With argon gas, temperatures of 4030C were reached, and some surface melting occurred on the orifice although there was little weight loss. Similarly, little weight loss was observed in carbon dioxide/argon mixtures, or using carbon monoxide. When oxygen-nitrogen mixtures were used, significant weight loss occurred, proportional to the fraction of oxygen in the mix in excess of 0.15 mole fraction. This was attributed to the extra heat from the oxidation reaction with the steel. Significant weight loss occurred with hydrogen, attributed to its greater thermal heat transfer coefficient. Increased weight loss was observed in gas mixtures containing water vapour, with the amount of weight loss increasing with increasing water vapour content. This was attributed to the decomposition of water vapour releasing oxygen which reacted with the metal surface. The increase with increasing water content in hydrogen/water mixtures was minimal; this was attributed to the presence of hydrogen depressing the decomposition reaction and hence the availability of oxygen.

Johnson and coworkers proposed that the mechanism of erosion was partial melting of the steel surface, either through chemical reactions or enhanced heat transfer. The molten metal and reaction products are swept away by the gas flow.

II.4 Firing Conditions in Gun Barrels

The firing of a gun results in a very aggressive environment, and there are few documented studies of the details of the environment. Where temperature and pressure data is presented, there is seldom a description of the type of transducers used, their sensitivities, and their response times. The following paragraphs detail what has been determined from a study of the literature.

Bulpett¹⁰ studied the metallurgy of sections of the barrel of a 30 mm RARDE gun. Thermocouples situated in the rifling grooves had indicated the surface temperature reached 1000C one millisecond after firing, dropping to 500C after 8 ms. A peak pressure of 400 MPa was apparently observed. Although a variety of different charges were used, this data is

presumably applicable to only one unspecified charge.

Izod and Baker¹ refer to a temperature rise and gas pressure pulse lasting 5 ms, but no details are given. Botstein and Arone report that temperatures exceeding 2700C and pressures of 550 MPa are "commonly" encountered. Turley and colleagues¹³ studied a condemned barrel that had undergone 220 effective full charges. With high energy rounds, flame temperatures exceeded 2700 C, pressures were up to about 520 MPa, producing muzzle velocities of 1520 m/s. No details of the temperature or pressure measurements were given.

Griffin *et al.* present data⁹ for temperature and pressure. This data is quoted in other publications referenced here. An instrumented 125 mm (5 inch) gun at the Naval Weapons Center contained test plugs at various distances along the barrel. Data for bore surface temperature as a function of time, measured 66 centimeters from the

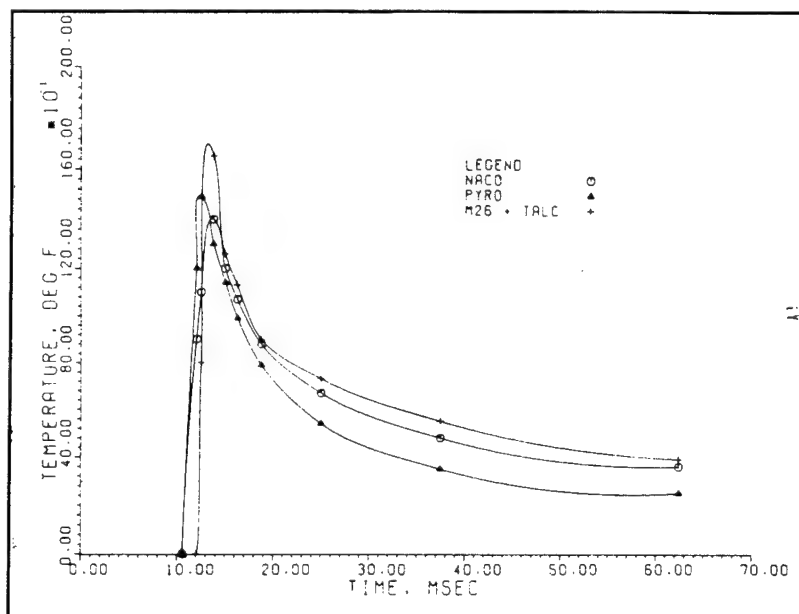


Figure 2. Recorded bore surface temperatures in a five inch gun, with different explosives.

commencement of rifling, are given in Figure 2 for different propellants. Peak pressures are also given in the reference. The pressures depend not only on the explosive charge but also on whether the shell has copper or plastic rotating bands, and on the lubricant used. Peak pressures when using talc wax and silicon oil lubricants with the M26 explosive were observed to be 350 MPa and 390 MPa, respectively.

III. Lasers to Stimulate Chemical and Metallurgical Changes in Surfaces

Gun tube failure is at least partially the result of extreme carburization of the steel and failure of this brittle highly carburized steel under the conditions of transient high pressure of gun firing, the friction of the moving projectile, and the subsequent "gas wash". Laser interaction with metal surfaces can produce both high pressures and high temperatures, and consequently there have been a multitude of attempts to use lasers to simulate the erosion in gun barrels. These experiments will be described in this section.

Possible relevant surface interactions induced by a laser beam can be one of three types: (1) metallurgical modification of the steel, (2) modification of the alloy content of steel, and (3) mechanical effects resulting from a laser produced shock wave.

III.1 Metallurgical Effects

Metallurgical effects are phase transformations including the thermally induced martensitic transformation, without any change of the steel composition. This is a well known and industrially used effect²¹. Bulpett studied¹⁰ white etched layers on laser treated steels as well as on gun barrels, digger teeth from a gravel extraction plant, and mechanically deformed steel plate. The laser specimens had been produced by scanning a continuously operating CO₂ laser at 1.5 kilowatts of power, focused to a spot size of 6 mm, at speeds of 25 mm/s to 100 mm/s. This produced a white etching layer.

The characteristics of the layer produced by the laser thermal treatment were quite different from the thermo-mechanical surfaces of the gun barrel. The gun barrels had a network of surface cracks, whereas the laser treated steels were relatively smooth, except for porosity due to escaping gases when surface melting occurred. The microstructure of the laser treated steel was M₃C carbides in an acicular ferrite matrix, while the microstructure of the gun steel was

Material	Chieftain gun steel	817M40
C	0.4	0.4
Si	0.2	---
V	0.2	---
Cr	1.0	1.2
Mn	0.5	0.6
Ni	3.0	1.5
Mo	0.5	0.3

Table II. Composition in Wt% of Materials studied by Bulpett

large martensite grains with narrow lenticular twin features and an even distribution of fine M_3C and M_7C_3 carbides within the grains. The white etched layers in the laser treated specimens showed no significant change in elemental composition, while the gun barrels contained increased levels of carbon, oxygen, hydrogen and nitrogen to a depth of 10 μm . The original chemical compositions of the steels were similar, as shown in the attached table.

The work in this thesis shows that metallurgical phase transitions resulting from scanning a continuous laser across a metal surface did not replicate the changes in gun steel resulting from firing.

III.2 Alloying Effects

There have been a number of studies in which laser produced carburization of the material was deliberately performed to modify the material properties. In some cases the alloy addition had been applied to the metal surface in solid form prior to the laser treatment. In other cases it was added from the gas phase during the laser treatment. For example, scanning a continuous CO_2 laser over the surface of graphite coated steel in a vacuum resulted in a significant increase in hardness of the steel²² and an increase in the carbon content of the steel, measured with EPMA. Carbon alloying also occurred in laser melting in a helium, argon, or nitrogen atmosphere, but no alloying occurred in an air or oxygen atmosphere. Coated steel samples with carbon content prior to irradiation of 0.14, 0.23, 0.36, 0.44, and 0.52% were irradiated with a 1.8 kw beam of size approximately 4 mm, scanned at 200 mm/min; cracks appeared in the latter three alloys during the irradiation, attributed to high hardness.

Walker and colleagues²³ passed a continuous laser over steel coated with colloidal carbon, and studied effects associated with the absorption of the carbon into the steel. The steel composition was 1.0%C, 0.29 Si, 0.42 Mn, 1.39 Cr, and 0.17 Ni, with 0.005 P and 0.005 S. Five passes at 25 mm/s were made with a 5 mm diameter beam from a 1.7 kW CO_2 laser over the metal surface, which was recoated with carbon between passes. The molten region had a heterogeneous microstructure due to incomplete mixing; it was largely eutectic with some Fe_3C crystals. In the interface between the melt zone and the heat affected zone, there was a light etching region 20 μm thick with micro-hardness ≈ 350 Hv. This interface region contained large equiaxed grains, interpreted as mostly austenite with some martensite. The structure was

attributed to solid-state diffusion of carbon leading to depression of the M_s temperature. As would be expected, the HAZ was martensitic, with ≈ 900 Hv.

A stationary 400 watt beam, focused to a diameter of approximately 0.75 mm, was fired at metal samples with a stream of gas directed at the interaction zone, by Mordike *et al*²⁴. With acetylene gas, hardnesses of 1000 HV were achieved to the depth of melting, about 100 μ m, in 3 seconds after irradiation. For shorter irradiation times, or if the stream of gas was air, argon, or nitrogen, the hardness typical of martensite in 0.1% C steel (350 HV) were observed. Hardening was also observed in a carbon dioxide gas steam. Further descriptions are given in other references^{25,26}.

This alloying work was performed with a relatively well characterized alloying additions. No work has been uncovered which has resulted in a multicomponent inhomogeneous surface such as observed in gun barrels.

IV. Lasers Generated Plasmas, and Mechanical Effects in Targets

IV.1 Mechanism of Laser Interaction

This section presents a general overview of the effects that can occur when a laser beam interacts with a target. The following section will discuss laser ablation, or evaporation of material, and measurements of the pressure impulse into the workpiece as a result of the ablation. The following section, IV.3, contains a discussion of measurements of the pressure pulse into the material when a plasma forms above the surface. A series of measurements of the mechanical and metallurgical effects on laser irradiated 4340 steel discs are described in the following section. The discussion of mechanical effects of laser radiation concludes with a description of experiments in which the expansion of the plume or plasma above a laser irradiated metal surface is buffered by a layer of liquid.

A high energy laser pulse incident on a solid surface can cause explosive evaporation of surface material or, if the intensity is sufficiently high, the creation of an ionized plasma on the surface. Recoil forces due to ablation of the surface material and/or expansion of the plasma can cause a compression wave to propagate into the solid surface. Laser induced shock waves have been investigated for a variety of purposes:

1. Research in laser fusion. The shock wave created by the laser compresses matter to one hundred times solid density. At this density, neutrons produced in thermonuclear reactions would stimulate other reactions, leading to rapid burning of the fuel.
2. High pressure physics. At ultrahigh pressures, atoms interact by a different regime of interatomic forces than do atoms at normal density. Investigations of the "equations of state" study these material interactions.
3. Strength of materials. Pressures typical of laser produced shock waves are a method of investigating the ultimate strength of materials.
4. Non-destructive testing (NDT). Laser produced impulses and shock waves are used to excite vibrations for mode analysis of industrial components, and are used for non-contacting NDT (in which the shock waves would reflect from sub-surface defects).
5. Fusion reactor applications. Laser solid interactions are used to study the properties of candidate materials for the "first wall", the chamber wall subject to very large heat fluxes

from a magnetically confined or inertially confined nuclear fusion reactor.

6. Laser shock hardening. Residual strains induced by shock waves are used to increase the fatigue properties of materials. These include Hadfield manganese steels and aluminum alloys²⁷.

Ready²⁸ describes two mechanisms by which pressure pulses are produced in laser targets. The first is material evaporation, causing recoil of the heated material against the surface. This would cause motion of the target as a whole. The second is a thermo-mechanical effect. Laser radiation is absorbed by a thin layer near the surface. The internal energy of that layer increases. The heated layer will expand by thermal expansion. If the thermal energy is deposited very rapidly, as would be the case for a short laser pulse, a compressive shock wave travels through the material. When the stress wave reaches a free surface of the material, it is reflected as a tension wave. If the tension wave becomes large enough and exceeds the ultimate strength of the material, fracture or spallation at the free surface could occur. Measurements of the maximum tensile stress induced in a piece of glass by absorption of the defocused output of a 70 MW Q-switched ruby laser pulse of a few nanoseconds duration were of the order of 10^6 dynes/cm². No spallation on the surface of the target was reported. When a series of pulses of 10^{-12} to 10^{-11} seconds duration and total energy 20 to 50 J from a mode-locked Nd-glass laser was absorbed in a metal film deposited on the end of a 5 cm long crystalline bar of fused quartz, the shock waves destroyed the bar. The high rate of heat input associated with the shorter pulses produced a shock wave intense enough that the ultimate strength of the material was exceeded.

Chan and Mazumder provided an overview²⁹ of laser produced material damage. The heat flux produced by laser absorption in a solid can produce a molten layer on the solid surface with vaporized material above the surface, depending on the intensity of the laser. Hot vapour will expand rapidly away from the target. The recoil pressure from the gas expansion exerts a force on the liquid and can expel it sideways. Thus, the materials are removed from the target both in vapour and liquid forms, causing permanent damage to the substrate. This type of damage is denoted as "thermal damage".

For a intense short pulse, evaporation may be rapid enough that a shock wave is created

in the gas surrounding the target. For a sufficiently intense and short, laser pulses, the recoil generates a shock wave in the solid target, in addition to that in the gas. Intense pulses will also ionize the vapour above the target, producing a plasma which strongly absorbs the laser energy. Rapid expansion of the superheated plasma can enhance the shock waves in the solid and in the gas. The shock waves can travel through the material causing fracture if there is enough shock energy. This type of damage is denoted "mechanical damage".

The formation of a plasma complicates the interaction between the laser radiation and the target material. Depending on the laser intensity, the plasma can give rise to combustion waves or detonation waves. In a laser driven plasma, energy is entirely supplied by the laser, usually uni-directionally incident on the plasma. Weakly absorbing, subsonically expanding plasmas are known³⁰ as "laser supported combustion waves".

By contrast, a laser supported detonation wave results from the coupling of an absorbing plasma layer and a shock wave. The shock wave is intense enough that thermal ionization accompanying the pressure impulse results in the formation of a sufficient number of free electrons that an avalanche breakdown can occur immediately behind the shock front. The breakdown plasma absorbs all the incident laser radiation via the inverse Bremsstrahlung process*. The additional energy enhances the shock wave, which usually expands towards the radiation source leaving behind an expanding volume of low density hot gas.

The laser supported detonation wave effectively shields the target from the incoming beam, as all the energy is absorbed in the incoming plasma. Interaction can resume under special circumstances. As the shock wave propagates towards the focussing lens, the laser intensity becomes weaker and may become too weak to sustain the plasma. As the plasma is extinguished, a new one forms at the laser focal point and a new laser supported detonation wave begins.

Zhirakov *et al.* used a streak camera to observe³¹ the laser produced plasma above a laser

* Inverse Bremsstrahlung is a process in which an electron and a neutral atom or molecule collide in the presence of an intense electromagnetic field, transferring energy from the electromagnetic field to the electron. The neutral atom is necessary for simultaneous conservation of momentum and energy.

irradiated target, using a PZT piezoelectric transducer to monitor the recoil pressure in the target. Sixty Joule laser pulses at 1.06 μm were focussed by a 4 cm focal length lens to a spot diameter of 1.5 mm. After the recoil pressure had undergone an initial spike, it decreased as a plasma formed above the workpiece, but increased again when the plasma was extinguished at the end of the laser pulse as the power decreased. At lower pulse energies, the plasma was observed to be repeatedly extinguished and re-ignited, and recoil pressure surges were loosely correlated with times of extinguishing.

Laser supported detonation wave almost always have a negative impact on laser material interaction, preventing the beam from efficiently coupling into the target. Under a special set of circumstances, Sturmer and von Allmen were able to avoid the detrimental effects by choosing parameters such that after the decay of the first LCD wave, the gas pressure above the metal surface was too low to support a second wave³². Laser radiation was then coupled into the workpiece, heating it beyond the melting point, and allowing the formation of a stationary plasma above the metal surface. A low density of gas above the target as well as long laser pulses were required to initiate these conditions and get significant coupling into the target.

IV.2 Laser Ablation of Material

Matthias and Dreyfus³³ summarized the physical processes taking place in the interaction of nanosecond pulses with metals in the Table III. Note that the authors consider only nanosecond pulsed beams; for pulses of a different length, the intensity at which the different effects occur may be different. This review article summarizes work by a number of prior researchers. Ablation usually resulted in a pressure wave travelling away from the target, as

Intensity	Effect
$\geq 1 \text{ MW/cm}^2$	Non-thermal desorption of neutrals and ions
$\geq 10 \text{ MW/cm}^2$	Ablation
$\geq 100 \text{ MW/cm}^2$	Explosive eruption and shock wave damage
$\geq 1 \text{ GW/cm}^2$	Plasma formation

Table III. Laser-Metal Interaction at Different Intensities

discussed above.

The energy of the shock wave can be determined by deflection of a helium-neon beam aimed parallel to the surface. The refractive index of the gas is proportional to the gas density, so the deflection was proportional to dp/dt as the wave propagates through the probe beam. The time integral of the deflected signal was proportional to the amplitude of the pressure pulse, and the energy is proportional to the square of the pressure. The article referred to work by Petzoldt *et al.*, who have shown that the energy of the shock wave generated by a high power laser pulse impinging on a surface was correlated to the volume of the removed material.

In other referenced work by Petzoldt, the photo-acoustic signal had a threshold, with the signal above the threshold observed to increase not linearly with an increase in intensity but as a power of intensity; that is, intensity squared or intensity cubed, depending on the material and the wavelength. It was suggested that this was evidence of multiphoton ionization playing a major role in the surface "damage" of material, while the bending at higher intensity signalled the onset of plasma formation.

The article also referenced work by Jee *et al.* in which it was shown that the damage threshold for copper surfaces depended on the crystallographic orientation of the crystals. The threshold for (110) orientation was higher (10.7 J/cm^2) than that for (100) or (111) orientation (9.2 J/cm^2). Jee *et al.* also observed that the damage threshold decreased with the number of shots (and hence would also depend on the laser pulse duration, since a long duration pulse at high intensity must be equivalent to using many shots.) For example, the damage threshold on the (111) plane decreased from the single shot threshold of 9.2 J/cm^2 to 6.5 J/cm^2 at ten shots. The decrease in damage threshold was attributed to increased absorption accompanying an increase in surface roughness due to plastic slip deformation. This detail is mentioned to point out that a measurement of ablation or damage threshold of an uncharacterized surface is of phenomenological interest only. Much of the physics of laser surface interaction is hidden by the averaging over many micro-features of an engineering surface.

The shock wave is distinct from the plume of heated gas emitted from the region of laser-target interaction on the surface. Measurements of laser ablation of polymer surfaces with a

KrF excimer laser at 248 nm were undertaken³⁴ with a deflected HeNe laser beam in conjunction with pulsed Schlieren diagnostics. There was a variable delay between the excimer pulse and the Schlieren analysis. Laser energy deposition on the surface heated the adjacent gas and created a high temperature plume. If the plume was sufficiently energetic, it acted like a piston and drove a shock wave. The shocks were observed for approximately the first 20 μ s after the laser pulse. The plume of hot gas expanded at about 1% of sound velocity. It detached from the surface after about 1 millisecond, and was visible for about 7 milliseconds if created by a 100-150 mJ/cm² laser pulse. This was long after the shock waves have died away. The size of plume was 20 to 30% larger if the laser irradiation was carried out in air as compared to in nitrogen or argon; this suggested a chemical reaction added additional energy.

There was a threshold energy at which the sound waves generated by the plume of expanding gas moved faster than the speed of sound and became shock waves. Ventzek *et al.* correlated this threshold with the threshold for ablation from the surface, for laser irradiated PET (polyethylene-terephthalate) and PMMA (polymethyl-methacrylate), as shown in the Table IV. It is not clear that the same correlation would exist in laser irradiation of metals.

Above the threshold for formation of shock waves, the velocity of shock increased linearly with increasing laser fluence.

Below the ablation threshold, the plume presumably consisted of gas heated by contact with the laser-target interaction region. Above the threshold, the plume would also contain the ejected material.

Aden *et al.* considered vaporization of aluminum and steel surfaces³⁵. Theoretically, one

	PET	PMMA
Transition from sound to shock wave	20-30 mJ/cm ²	500-600 mJ/cm ²
Ablation threshold	20-30 mJ/cm ²	650 mJ/cm ²
Plasma (observed visually and photographically)	6-10 J/cm ²	6-10 J/cm ²

Table IV. Excimer laser interaction with plastic materials

dimensional heat flow into the substrate without a phase change was used to calculate the surface temperature. Gas expansion was accounted for by conservation of mass, momentum, and energy flow, put into non-dimensional form, and numerically integrated to find (1) the surface temperature, (2) the pressure ratio, as a function of irradiance for different irradiance levels and beam diameters, and (3) the location of the shock front at different times.

Experiments were performed with a Nd:YAG laser of 1.6 J with a square pulse of 100 μ s and a gaussian beam shape of radius 170 μ m. A double pulse ruby laser with adjustable delay was used to take Schlieren photographs of the shock fronts. Rather impressive agreement with the theoretical calculations was achieved. Aden *et al.* were concerned primarily with gas flow into the ambient atmosphere, and although information was given allowing a calculation of the back pressure into the target, this was not done.

The pressure wave induced by laser interaction can cause spallation and damage of the target. A Nd:Glass laser of 80 Joule capability, producing a 4.3 ns pulse with a 0.4 ns risetime, was focused onto an aluminum foil target³⁶. At

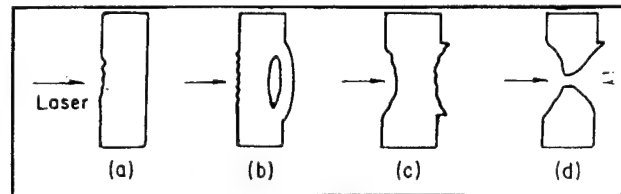


Figure 3. Stages of material failure, with increasing irradiance

moderate intensities, a crater formed on the front of the target due to material ablation. As the pulse intensity was increased, an internal crack developed causing a swelling of the back surface. At higher intensities, the material beyond the spalled plane was severed from the back of the target, leaving a crater on the rear surface. The crater depth increased with increasing pulse power until the back and front side craters meet and target perforation occurs. The adjacent figure shows these different stages of material failure. The reference also gives good photographs of damage, but makes no mention of specific laser conditions. Note that this mechanism for producing substrate damage required a planar shock wave being transmitted into the material.

The damage can be significantly enhanced, and the nature of the damage altered, if the surface is coated with an absorbing liquid. The laser energy is then absorbed at the surface of the liquid, rather than at the metal surface. This is a different effect than that to be

discussed later in which the surface is covered with a transmitting liquid, and the laser energy is absorbed at the interface between the liquid and the solid. With an absorbing liquid, a significantly larger fraction of the laser energy was absorbed in the liquid than in the solid, in which there can be a substantial room temperature reflectivity for the laser light. Moreover, the liquid was more easily evaporated than the metal surface, so a given laser energy produces a larger volume of vapour, and hence more recoil. Siegrist and Kneubuhl observed³⁷ hole drilling in quartz required a significantly fewer number of pulses (23 versus 230) when the quartz was covered with a layer of water which absorbed the CO₂ strongly. Without the water, the drilling appeared to take place by melting and vaporization, but when the quartz was covered by water, drilling took place by fracturing of the surface without melting.

IV.3 Surface Interaction with Laser Produced Plasmas

Considerably higher forces can be generated when a plasma is created on the surface, but if the plasma frequency (the oscillation frequency of the electrons in the plasma) matches the laser frequency, the beam is totally absorbed in the plasma and does not reach the target surface. Marcus *et al.* studied the "thermal coupling coefficient" (the ratio of the thermal energy absorbed per pulse to the laser pulse energy) using a 500 J CO₂ laser producing a 15 μ s pulse consisting of a 2 μ s peak and a decaying tail. The results³⁸ are shown in the attached

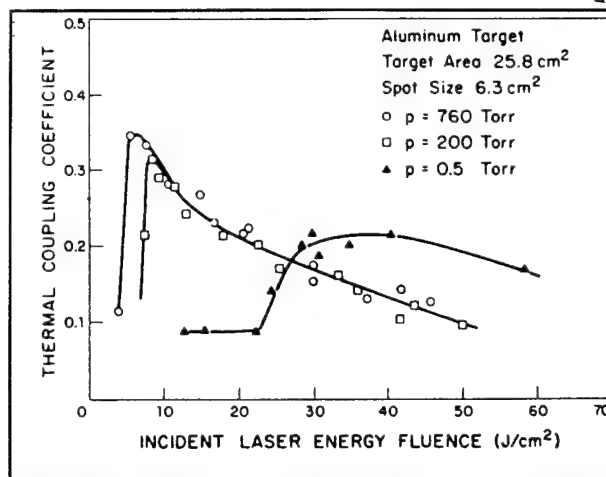


Figure 4 Pressure dependence of thermal coupling to aluminum targets

figure. As the laser fluence increased over the threshold for breakdown, coupling decreased. This was attributed to propagation of an air plasma away from the target toward the laser. At greater laser fluences, the plasma became more dense and receded faster from the target, thus decoupling the laser energy from the target more effectively.

As pressure decreases, the threshold for breakdown increased (presumably because electron loss from the focal area increases) and maximum coupling of the laser energy into

the target decreased. Some energy reaching the target is from re-radiation from the plasma, as ascertained by the temperature increase of the target as target size varied. Surface heating was observed to continue after the end of the laser pulse, by transfer of heat from the hot plasma to the surface.

Diaci and Mozina used a model for a point explosion combined with measurements of shock velocity to determine³⁹ the energy in a shock wave created by laser irradiation of aluminum and steel targets in air. The shock velocity was measured by deflection of second laser beam propagating parallel to the surface. Nd:YAG pulses of diameter 0.5 mm and of duration 12 or 60 ns were used. At low pulse energies (10 mJ) the conversion of laser energy into shock energy was greatest for the shortest pulses (i.e., 12 versus 60 ns pulses). At greater pulse energies (>20 mJ), a maximum of 20% energy conversion was observed, independent of the pulse length and of the material. Although the existence of a plasma wasn't explicitly mentioned in the publication, an energy of 20 mJ corresponds to power densities where a plasma would be formed above the surface. The plasma isolated the target from the beam, and energy deposition into the plasma driving the shock wave would be expected to be independent of the nature of the target, as was observed. For example, samples of 2024 aluminum were irradiated by a Nd:Glass laser producing 20 to 30 nanosecond pulses of an unspecified energy, with diameters in the range of 0.7 to 3 cm. Peak pressures in the range of 10 gigapascals resulted in hardening of the aluminum alloy to 180 VHN, from a base hardness of 140 VHN, with a slight increase in yield strength and in ultimate strength. The shock hardening and strengthening was attributed to a dislocation substructure produced by the shock waves. The fretting fatigue life of fastener joints of 7075-T6 was increased by orders of magnitude by inducing shocks around the fastener hole.

Pirri used formulae from the literature to evaluate the impulse on a solid target as the laser initiated detonation wave expands, and compares the results with experimental data⁴⁰. He separated the phenomenon into a regime of one-dimensional expansion, which occurred for a time determined by the beam diameter and the expansion velocity, and two-dimensional or cylindrical expansion which occurred after this time interval. Formulae for planar blast waves and cylindrical blast waves respectively were used to describe the two phenomenon; during

the regime of one-dimensional expansion the pressure decayed as $1/t^{2/3}$ and during the 2D expansion the pressure decayed as $1/t$. The total impulse depended on the duration of the 1D expansion phase as compared to the duration of the laser pulse. In the case of a target much larger than the beam dimensions, all the impulse of the cylindrically expanding plasma was applied to the target surface. The calculations indicated the maximum impulse on the surface occurs when the pulse duration was equal to the time duration in which the 1D expansion was relevant. Results were expressed in terms of the specific impulse; or, the ratio of the total impulse (force x time) applied at the surface, to the laser pulse intensity in Joules. Results of the derivation were compared to the author's previous experimental results, in which the impulse transmitted to the surface of target discs by a high energy CO₂ laser (50J in 100 μ s) was (1) independent of the target material (tungsten, graphite, or aluminum), (2) dependent on the target diameter, and (3) inversely proportional to the pulse duration. Moderate agreement with the experimental data was obtained. The specific impulse varied from 0.2×10^{-5} to 8×10^{-5} Newton-sec per Joule of laser energy.

Unless the plasma significantly expands or propagates in the duration of the laser pulse, decoupling the laser from the surface, the presence of a plasma can significantly enhance the absorption of laser energy in the vicinity of the metal surface. This enhanced absorption causes a pressure impulse that can cause metallurgical effects in the substrate. Gerland and Hallouin⁴¹ used a Nd:Glass laser with pulse duration 0.3 ns, focal spot size 3 to 6 mm, and intensities of 2×10^{11} to 2×10^{12} W/cm², to irradiate 304 stainless steel targets. The hardness of the shocked sample had increased from an initial value of 190 kg/mm² to a value of 400 kg/mm² with laser irradiation of 5×10^{11} W/cm², corresponding to a calculated pressure of 25 GPa. TEM analysis showed the presence of twins in the laser affected region.

In an experiment in which the shock resulting from plasma formation was expected to result in hardening of a metal surface, softening was observed instead. Pulses of 2.7 ns duration from a 1.06 μ m Nd:YAG laser or of 1.9 ns duration at the second harmonic at 0.53 μ m were used to irradiate samples of carbon steel in air. Pressures up to 10 GPa were observed with 50 GW/cm² pulses⁴². For the same power, slightly higher pressures were observed using the second harmonic wavelength, presumably because of greater transmission

at the wavelength through the plasma generated above the metal surface. In a sample of martensitic steel with 0.35% carbon, irradiated with a 2.7 ns 26 GW/cm² pulse, the Vickers hardness was measured to be 568, 610, 651, and 700 at the surface, 25 μ m below the surface, 50 μ m below the surface, and at a reference depth respectively. The softening of the surface was attributed to a tempering of the steel by thermal conduction or thermal re-radiation from the hot plasma, rather than a mechanical effect due to the shock.

IV.4 Laser Interaction with AISI 4340 Discs

In several references, the interaction of laser energy with 4340 steel has been studied. Caldor and Cornell⁴³ irradiated AISI 4340 steel discs with the output of a Nd:YAG laser. The discs were 19 mm diameter, 1.6 mm thick, and prepared by sanding with 600 grit paper. When the laser was operated in the Q-switched mode, producing 9J pulses of 30 ns duration, measurements with strain gauges indicated that the plate vibrated back and forth at its natural frequency (38,800 hertz). This was due to the laser produced impulse on the front surface, and analogous to ringing of a gong. In spite of the plume emitted from the surface of the sample, there was no evidence of a shock wave transmitted through the sample. Such a shock wave was calculated by this reviewer to have a ringing period of about 0.5 μ s. Temperature changes induced by sample irradiation with normal mode pulses of 40 J and 600 μ s duration resulted in thermal distortion of the disc on a relatively slow time scales. There was some evidence of ringing at the natural frequency superimposed on the thermal distortion.

A higher power resulted in surface damage. Goldberg and Cornell⁴⁴ used 600 μ s pulses from a Nd:YAG laser with 100J capability to simulate degradation of metal surfaces when subjected to high temperature excursions. The laser output was partly focussed to a 6 mm diameter. Nineteen mm diameter AISI 4340 steel disks were instrumented with thermocouples or strain gauges. The thermocouples showed that absorption of the laser radiation into the samples increased with multiple shots over that observed with only a single shot. Strain gauges mounted on the samples showed oscillations at the natural frequency of the sample, excited by the laser pulse.

On a single pulse, there was localized melting due to "hot spots" in the beam, but after ten shots the surface was completely melted. A microstructural analysis showed three regions

of heating: (1) a melt zone in which a martensitic transformation had taken place on solidification and cooling, (2) a region which had been heated to the austenite region, resulting in a martensitic transformation, but without melting, and (3) a region with partial martensitic structure which had been heated to the point of only partial formation of austenite. Two of the regions were white etching. There was distortion and "tearing" in a region around the beam spot, attributed to the stresses involved in heating, melting, and the martensitic transformation. A sample subjected to ten 88 J pulses showed a surface hardness of 653 VHN, compared to 176 VHN in the annealed base metal structure, with cracking in the white etching region.

Samples coated by chemical vapour deposition with 250 μm of tungsten on top of an electroplated 2 to 10 μm thick nickel interlayer were laser irradiated to test the coating's response to temperature excursions. Barely perceptible cracking was observed on samples with a 9.7 μm thick nickel interlayer, after ten pulses of 88 Joules of laser energy at 30 second intervals. Extensive cracking was observed on samples in which the nickel was 2.7 μm thick. It was conjectured that yielding of the relatively soft nickel layer accommodated the stresses due to differential thermal expansion. The extent of crazing was related to the extent of localized melting. Melting was least and the cracking was greatest when the nickel layer was thinnest. No change in the steel microstructure was observed in the laser irradiated coated samples.

Price⁴⁵ caused chemical effects in the steel discs by irradiating them in the conditions similar to those mentioned above, but in atmospheres including CO, CH₄, 10% CH₄ in argon (to prevent soot formation), NH₃, N₂, and air. The targets were 12.7 mm diameter, 3.2 mm thick discs made of (1) pure iron, (2) 4340 steel, quenched and tempered to produce a tempered martensite microstructure, and (3) tungsten coated 4340 steel. A lens focused a 600 μs beam from a Nd:Glass laser with 100 J capability to a 3.2 mm spot diameter on the targets. Analysis of the irradiated region included SIMS, SEM, and optical metallography.

The SIMS analysis showed significant increase in the carbon content as the number of pulses increased, for pure iron targets. The depth profiles are shown in the attached figure. No significant increase in carbon content was observed in 4340 steel targets, however.

When surface melting occurred, two different zones were observed by optical microscopy.

The first was in the region where melting occurred, producing a light etching, as-quenched martensite. There was also a zone of intermediate etching martensite, in which it was supposed that A_{c3} was exceeded, resulting in complete transformation to martensite without melting. The martensitic structures in the AISI 4340 targets did not appear to be sensitive to the gaseous environment.

There was an apparent absence of interstitial diffusion in specimens pulsed with conditions insufficient for surface melting. In addition, there was a good correlation between the depths of interstitial penetration determined by SIMS depth profiles and the damage layers revealed by optical microscopy.

The depth of carburization is increased by (1) plastic deformation caused by the pressure wave induced by the laser pulse, and (2) dilatation strain imposed by the martensitic transformation.

In irradiation of the tungsten coated targets, the resulting density of cracks appeared to decrease as the beam energy decreased. The earlier results where increasing the thickness of the intermediate nickel layer reduced the tendency of the tungsten overlay to crack, were confirmed. Price reported that effect was relatively small. He concludes that the viability of the laser system for testing the mechanical integrity of coatings was confirmed by the experiments on the tungsten coated steel specimens.

IV.5 Laser Interaction with Buffered Targets

Several researchers have investigated the mechanical effects in solids as a result of laser irradiation of the solid surface immersed in a liquid. For these studies, the liquid transmits the

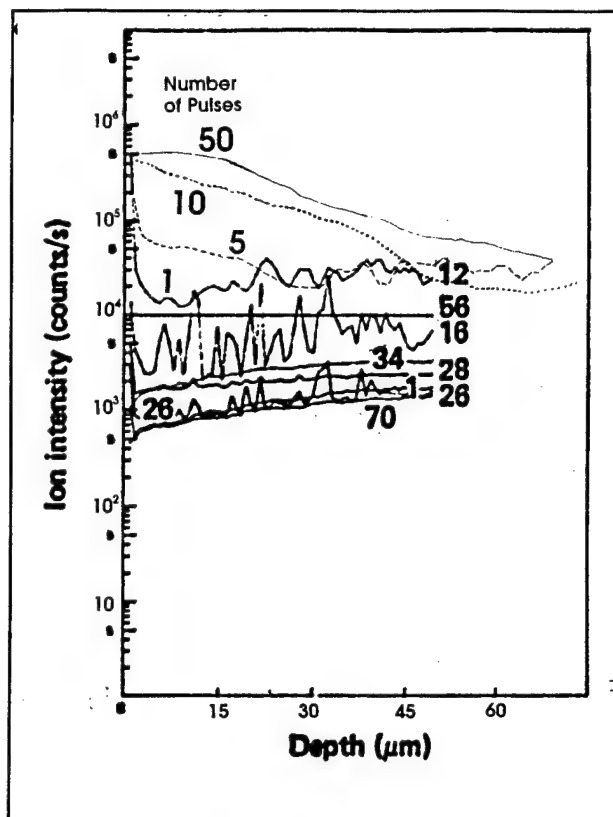


Figure 5. SIMS depth profile of iron target irradiated in Ar-10%CH₄; all counts are normalized to that for iron (mass 56)

laser radiation so that the energy is absorbed at the liquid-solid interface. The inertia of the liquid inhibits the expansion of vaporized material away from the surface. Moreover, as the liquid is more easily vaporized than the metal target, more vapour is produced by the laser radiation from a liquid covered metal surface than for a metal surface alone. These two effects combine to produce a larger and longer pressure impulse into the metal target.

A shock wave created by a laser in water⁴⁶ has a velocity about 1.5 mm/ μ s. The overpressure created by the laser at the laser solid interface moves away relatively rapidly, carrying away energy. A pressure surge will remain in the presence of the liquid-solid interface until the vapour, or the pressure due to the presence of the vapour, can be dissipated. This will require a certain time interval simply because the liquid has sufficient inertia (inertial confinement) that it can't accelerate rapidly. A pressure wave, a sound wave, or a shock wave doesn't correspond to a physical motion of the liquid. It remains to be seen if the pressure pulse remains for a sufficient length of time to be meaningful for simulation of gun barrel wear.

The dynamics of laser plasma formation in liquids (in the absence of a solid target) by a pulsed laser was studied by Felix and Ellis⁴⁷. Three Joule Q-switched Nd laser pulses of 50 ns duration were used to generate plasmas in tap water, de-ionized water, and methyl alcohol. Schlieren photographs were taken with a Xenon flash-lamp, the output of which was switched with a Kerr cell to produce 75 ns exposures with a controllable delay. Local breakdown occurred within the liquid, presumably at impurities or dust particles. Light accompanying the breakdown indicated a hot plasma was produced locally at these impurity centres. Shocks formed around these hot spots were initiated by the rapid expansion of the gas or vapour. The compressive shocks propagated spherically outward from the point of origin. A cavity or bubble was formed around each hot spot at the focal point during the 50 ns laser pulse duration, but was observed to continue to grow rapidly for 20 μ s. Thereafter the pressure dropped within the cavity, and the rate of growth decreased, resulting in a rarefaction wave which propagated outward. The rarefaction wave was intense enough to cause many small bubbles to appear in the region around the focus. The small bubbles grew slightly and remained for 100 to 200 μ s, then collapsed and disappeared. The large cavity became fully

grown, with a 6 mm diameter after 300 μ s, then it collapsed after 650 μ s.

Although plasma formation did occur in deionised water and methanol, fewer bubbles were observed, presumably due to fewer impurities to nucleate bubble formation. Bell and Landt⁴⁸ used a shadowgraph to observe shock waves in water induced by focussed Q-switched ruby and Nd:YAG laser radiation. A measured shock velocity of 0.7 cm/ μ s corresponded to a shock pressure of 23 GPa. Shocks were not observed using distilled filtered water, indicating the sources of the plasmas were impurities in the water.

Irradiation of a metal coated with an absorbing layer which was in turn covered by a confining material resulted in the imparting of residual stress to the metal surface, with no increase in microhardness⁴⁹. As a result of the coating of absorbing material, the material was affected only by the shock wave conducted through the absorbing layer, with no direct thermal effect. An Nd:glass laser producing 80 J, 25 ns (FWHM) pulses was used to produce shock waves in 0.55% C steel of yield stress (0.2% strain) 600 MPa. Residual stresses were determined by X-ray diffraction, and impact pressures were measured by piezoelectric quartz gauges.

When the laser produced plasma was confined by a layer of distilled water, the observed maximum pressure was 3 GPa for a laser fluence of 5 GW/cm². A maximum **compressive** residual stress of 250 MPa was achieved, produced by a 4 GW/cm² pulse that resulted in stresses of 2.5 GPa. The plastically deformed region had a depth of 800-1100 μ m.

When the plasma was confined by a sheet of BK7 glass, maximum pressures of 5 GPa were observed for the same fluence at which the maximum pressure with the water overlay was observed. The greater pressure was attributed to the difference in acoustic impedance between glass and water. The maximum compressive residual stress was approximately the same, but achieved at the lower fluence of 1.7 GW/cm².

No modification of Vickers microhardness scans was found as a result of the laser treatment. Roughness and depression measurements were taken. The roots of gear teeth, inaccessible to other treatment techniques, was proposed as an application area in which the residual stresses might lead to an enhanced lifetime.

In similar work, the output of a 50J laser with pulse duration 20 to 50 ns was directed at

the surface of a bearing steel⁵⁰, painted to protect the target from the laser, but under water to cushion the shock. The temperature at the interface between the water and the protective coating reached 8000 C, resulting in thermal ionization and formation of a breakdown plasma. Power in the range 1-10 GW/cm² produced pressure impulses of 1 to 5 GPa. The metal surface was depressed by a few microns due to compressive stresses, but the surface roughness was better than using shot peening for inducing compressive stresses.

The use of shorter wavelengths increased the energy transmitted to the target. This is because electron avalanche causing the plasma to form occurs by the Inverse Bremsstrahlung mechanism in which the breakdown threshold is proportional to the square of the wavelength. The 2nd harmonic of the Nd:YAG produced greater shock impulses than the Nd:YAG laser itself, for the same laser energy.

V. Surface Engineered Coatings for Gun Tubes

V.1 Criteria for Materials

Gun tubes can be protected by internal liners, coatings, or both. Ahmad's list⁶ of criteria for ideal liners and coatings is presented in Table V.

V.2 Chromium Plate

Chromium plate is the most widely accepted method of coating for protection of the bore of gun tubes. Izod and Baker¹ claimed that chrome plate doubled the life of barrels. They refer also to "Low contractile" chromium plate, in which careful control of plating bath temperature and rate of deposition resulted in a surface that was relatively free from

Material Criteria for Liners	
Melting Point	> 1500 C
Elastic Modulus	high
Fracture toughness	same or lower than jacket
... and impact strength	
Hot Hardness	high
Chemical resistance	high
... to propellant gases	(unless protected by a coating)
Coefficient of	
... thermal expansion	low (< that of barrel)
Reaction with rotating band	inert (unless coating is used)
Phase transitions	none
Material Criteria for Coatings	
Melting Point	>1500C
Elastic Modulus	high
Fracture toughness	
... and impact strength	same or lower than substrate
Hot Hardness	high
Chemical resistance	
... to propellant gases	high
Coefficient of	
... thermal expansion	compatible with substrate
Reaction with rotating band	inert
Phase transitions	none

Table V. Material Criteria

micro-cracks and has high resistance to flaking. They specified that the coating thickness should be such that steel substrate temperature rise doesn't exceed 725C at which point a phase change occurs. This thickness for Chromium is 0.1 mm, which with a safety factor leads to flaking. The flaking is possibly due to the different coefficient of linear expansion to that of steel.

Cracks are also formed from firing and engraving stresses. A thick coating (0.13 to 0.25 mm) is needed not only to thermally insulate the substrate, but also to prevent the substrate from deforming under the engraving stress of the rotating band, which results in coating

cracks. Once cracks are formed, hot gasses can penetrate the cracks and attack the underlying steel. According to Ahmad, the rate of damage is frequently higher than in an uncoated gun.

Montgomery and Sautter, in discussing chromium plating, said⁵¹ that phase transformation, with the attendant volume increase, of the underlying steel is the chief cause of spalling of the coating. A thicker electroplated coating prevents the underlying steel from reaching the transformation temperature. As a consequence, the useful life of the plated cannon tube is much increased. They attempted to measure mechanical stresses in the absence of thermal stresses of chromium plated onto gun steel (modified SAE 4340). Tests on heavily loaded but unfailed chrome plated rollers showed cracks in the steel just below the interface. Durability decreased to about half as the thickness of the electroplate was increased from 0.15 to 0.41 mm. Residual compressive effect in the steel produced by sandblasting significantly enhanced the durability.

Since gun barrel wear appears to be an inverse function of the melting temperature of the barrel material⁴, electroplated chromium is typically used as a coating to reduce damage. Although the wear resistance of chromium plating is very good, spalling of the coating during operation eventually occurs. It has been suggested that the microcracks typically present in the hard chrome plate link up during thermal cycling, and eventually form craze cracks. Subsequently, copper from the projectile rotating bands becomes deposited within the cracks and acts as a wedge to spall off the chrome plating during thermal cycling⁸. Attempts have been made to improve the durability of hard chromium plating by melting the plating onto the substrate using CO₂ laser energy, as described below.

There are ongoing research efforts to characterize the chromium-electroplating process, to improve gun wear. In one research study⁵², two 30 mm diameter rifled liners were plated under different conditions (current level, solution composition)

Requirements for chromium coating

1. thick enough to thermally protect the steel
2. no built-in microcracks
3. coating has some deformability so that it does not crack due to mechanical fatigue or thermal shock

from *Potential Erosion Resistant Refractory Metal and/or Alloy Coatings for Gun Tubes*, Ahmad, I, Greco, P., D'Andrea, G., and Barranaco, J., Proceedings of the 1978 Tri-Service Conference on Corrosion, Ed. Levy, M., and Brown, J. (available from the Metals Ceramics Information Center, Battelle Laboratories, Columbus,

designed to give a wide range in mechanical and microstructural properties. Prior to plating, the liners were internally electropolished in an acid solution in the same plating jig, and rinsed. The liners were shrunk fit into "stub receiver" barrels, through which were then shot 100 nylon banded rounds.

The breech area of the liner did not come into contact with the driving band, so damage in this area was attributed to hot gases. Examination of both liners showed them to be covered with fine craze cracks, more visible (hence wider) in the liner plated at the lower current. Apart from the cracking, the liner plated at the higher current was completely smooth, but the liner plated at a lower current was covered in small pits where areas of chromium had been removed.

Other work on improving the quality of chromium plating is being performed at Watervliet Armoury in the U.S., where special "electroactive" additives in the chrome bath are being investigated⁶.

V.3 Laser Interaction with Chromium Plate

There have been several instances where laser energy has been applied to chromium plated steel in attempts to measure or improve its properties. Much of the work described in this section was done with military involvement or military funding. Laser heating has also been proposed as a method of non destructive evaluation of electroplated chromium layers⁵³.

Montgomery successfully fused chromium electroplate⁵⁴ to AISI 4340 coupons using 7.5 kW of output power and processing speeds of 6.3 to 17 cm/sec. Although none of the conditions produced full melting of the chromium layer, fusion occurred via the production of an intermetallic layer between the plating and the steel. The size of the intermetallic layer became greater with higher heat input. Although the majority of surface cracks in the electroplated chromium were eliminated, recrystallization produced considerable softening from values of approximately 920-1140 KHN to 150-289 KHN. Application of the process to chromium electroplated rollers manufactured from modified AISI 4340 gun steel failed to produce an improvement in the durability of the coating under conditions of pure rolling. The laser fused rollers lasted approximately 14-47 seconds before the coating spalled

Cr-25Fe-15Mo	<ul style="list-style-type: none"> - developed during WWII - less erosion than stellite - liners applied by shrink fitting - brittle 	Mo	<ul style="list-style-type: none"> - elastic modulus > that of steel - prepared by forging → anisotropic properties - poor transverse strength → cracked during firing - good North American supply, cheap - performed best in IITRI study (pre 1970)
Mo-0.1%Co	<ul style="list-style-type: none"> - excellent erosion resistance - technology of liner fabrication not well developed - liners failed by cracking 	Ta-10W	<ul style="list-style-type: none"> - performed best of Ta,Nb,W, Mo in small calibre guns. - good hot hardness - Ahmad considers this a material with potential - performed second best in IITRI study - showed promise in Calspan study - best performance in Battelle study
Ta	<ul style="list-style-type: none"> - elastic modulus < that of steel - behaved well as liner, transfers load to barrel - expensive - selected by Watervliet for further investigation - conventional deposition is a fused salt bath technique which requires high temperature, so used only as a coating on a liner, not on steel - deposited by Magnetron sputtering by Turley - Stellite 22 used as liner material - less successful than the promise in initial tests - ongoing experiments to improve hardness 	Ta-Cr	<ul style="list-style-type: none"> - codeposition of Cr with Ta from a fused salt bath - hardness of Ta increases with Cr - Ta-Cr alloy expected to maintain its hardness at elevated temperatures
Nb	<ul style="list-style-type: none"> - elastic modulus < that of steel, transfers load to barrel - behaved well as liner - expensive - deposited by magnetron sputtering by Turley 	TZM	<ul style="list-style-type: none"> - good hot hardness - Ahmad considers this a material with potential
W	<ul style="list-style-type: none"> - cracked like chromium - elastic modulus > that of steel - imported, no North American suppliers 	Nb-Cr	<ul style="list-style-type: none"> - deposited by Turley with alternate magnetron sputtering units - spalled in service
		Ta-12W-1.0Re-0.025C	<ul style="list-style-type: none"> - GE Burlington considered this had best combination of properties for erosion resistance in barrels
		Nb-1%Zr	<ul style="list-style-type: none"> - one of the best in Calspan study

Table VII. Candidate Coating Materials

off, compared to approximately 17 minutes for the untreated chromium plated rollers. In the case of the laser treated rollers, failure occurred in the coating, while failure occurred in the

steel roller for the untreated roller. The authors suggested that the poor performance of the laser treated coating may have been due to nitrogen embrittlement that occurred during processing, resulting from inadequate gas shielding.

Christodoulou and Steen⁵⁵ investigated a wider range of processing conditions to generate three distinct melting regimes in chromium electroplate on mild steel: 1) complete melting of the chrome plate and dilution with the steel, 2) partial melting of the chromium and the production of an intermetallic interface, and 3) no melting of the chromium but transformation hardening of the underlying steel. Once again, considerable softening of the chromium electroplate was observed in the unmelted material due to recrystallization and grain growth, while microcracking was eliminated. Complete melting produced a smooth surface layer consisting of an iron-chromium alloy with a hardness of approximately 320 VHN. Unfortunately, wear testing to determine the suitability of the laser processed materials for gun barrel applications was not performed.

Other research on laser melting of electroplated chromium has been done by Molian⁵⁶. In addition, there has been other preliminary work⁵⁷ in which laser deposition of chromium powder has been investigated as an alternative to electroplating.

V.4 Coatings Other than Chrome Plate

Steel has been recognized since the 19th century as a good material for guns. According to Ahmad³, the impetus of a propellant is given by

$$F = R T_f / M$$

where R = gas constant, T_f = flame temperature (measured in Kelvin), and M = molecular weight of the products of combustion. As long as carbon, hydrogen, nitrogen, and oxygen compounds are the energy source, the limiting value of M is 17 or so. The flame temperature is limited by melting point of steel.

The successful deployment of high melting point materials such as chromium, Ta-10W, molybdenum, tungsten, and niobium alloys would allow the "steel barrier" to be broken, such that it should be possible to use propellants with a flame temperature a few hundred degrees higher, giving increased impetus, muzzle velocity, range and accuracy.

Ahmad describes a number of materials used or considered for use in coatings or liners.

The information from Ahmad and other sources is summarized in Table VII. TZM is titanium-zirconium-molybdenum, containing 0.5% Ti, 0.08% Zr, 0.02% C, and balance molybdenum. Stellite 21, a Ni-Co alloy, was developed during 1940-45. It is still used as liner in machine gun barrels. Ahmad said that Stellite 21 has excellent erosion resistance, hot hardness, ductility, and machinability, but unfortunately a relatively low melting point of 1280C. Failure occurs by surface melting. Stellite 21 has provided only marginal improvement in guns with higher muzzle velocity (>1070 m/s).

Alloys of Cr-25Fe-15Mo were developed during WWII, and had excellent erosion resistance, and have been shrink fit into steel barrels. They have shown less erosion than stellite. Molybdenum hardened with 0.1% Co has been tried, but suffered from cracking of joints due to poor fabrication technology. Ahmad suggests this material should be examined in terms of modern fabrication techniques such as powder metallurgy.

Ahmad summarized erosion studies undertaken at The Illinois Institute of Technology Research Institute (IITRI)⁵⁸, on tungsten, tantalum, molybdenum, niobium, hafnium, and zirconium alloys. These tests showed that these molybdenum alloy performed the best and Ta-10W second best. This was pre-1970 work. Ahmad also refers to a study by personnel at GE Burlington⁵⁹ of the physical and mechanical properties and erodibility of refractory alloys. This study concluded (in 1973) that Ta-12W-1.0Re-0.025C had the best combination of properties for erosion resistance in barrels.

Personnel at Calspan⁶⁰ conducted an investigation of fourteen materials for high velocity guns, and determined that Ta-10W and Nb-1%Zr showed a substantial improvement over the barrel material currently in use in 75 mm high velocity cannon. Montgomery and Sauter⁴ also refer to Calspan's erosion data, which was correlated with the melting point of the alloys; erosion decreased dramatically for alloys whose melting points were above 1500C.

Ahmad also describes a Battelle study, in which A-286 steel barrels were fitted with co-extruded liners of TZM, Mo-0.5Ti, Ta-10W, and L605 alloys. Ta-10W gave best performance. No further details were given. At Rock Island Arsenal, work was conducted on a number of liners of Cr-Mo-V steel. HS25 steel and Ta alloy T-222 liners fired the greatest number of rounds before failure.

At Watervliet Armoury, an investigation was undertaken on chromium, cobalt, Co-Al₂O₃, Co-Re, and Cr-(Co-Al₂O₃) coatings. Coatings of 0.25 mm thick chromium out-performed 0.13 mm Cr-(Co-Al₂O₃). Chemical Vapour Deposition Coatings of tantalum, tungsten, and Ta-10W were prepared by CVD, but more work on the CVD deposition is needed. Tungsten coatings cracked during firing, but still performed better than chromium plating.

Ahmad divides erosion resistant refractory metals and alloys into two classes depending on whether the elastic modulus is less or greater than that of steel. Those in which the elastic modulus is greater than steel include Cr, Mo, and W. These materials performed well in erosion gauge testing, but failed by cracking during firing; they do not effectively transfer the load to the substrate during firing. The problem was aggravated by thermal mismatch. Chromium was partially successful since its modulus is close to that of steel.

Materials in which the elastic modulus is lower than gun steel include Ta and Nb. With coatings of these materials, stress is effectively transferred to the jacket. They are also more ductile and less prone to cracking. Unfortunately, they are not as good as the first class of materials in terms of gas erosion.

Refractory Oxides have good erosion resistance, and as raw materials are considerably cheaper than refractory metal alloys. Cracking is potentially avoided if they can be mounted with the required compressive stresses. However flaws in the ceramics lead to stress concentrations.

Ahmad describes the need for development work to optimize technology (e.g. chemical vapour deposition and molten salt hydrolysis) to deposit coatings of materials such as Ta-10W and TZM that maintain their hot hardness at temperatures even higher than 1000C. These materials are expensive and would be used only as liners or coatings.

The refractory metals such as niobium and tantalum cannot be deposited from aqueous electrolytes⁶¹. Electrolysis in a molten salt bath (the FLINAK process) is used, but the bath temperature is around 800C which is considerably above the tempering temperature of the gun steel. The resulting weakening of the steel has limited consideration of the use of these coatings to liners, rather than to the tube bore itself. Alternative deposition techniques such as magnetron sputtering are being developed.

Stobie *et al.*⁶² described the use of a 37 mm blowout gun as a means to test coatings or platings for gun barrels, and used the guns to test sputtered coatings that included niobium, Cr-5Mo, chromium, Ta-W/Ta, Ta-16W, Ta-3Cr, Ta-9Cr, Co-40Cr-4Al-1.3Y. Different propellants were used. They conclude that the gun firing conditions can be adjusted to screen gun barrel coatings or platings in a reasonable number of shots. Tests on chromium electroplate coatings resulted in cracks which extended through to the base metal. In some cases there were transverse cracks in the base metal. Mass loss rate was low for the first few shots (less than steel), then accelerated mass loss occurred (greater than for unprotected steel). The electroplated chromium coatings protected better than sputtered chromium coatings. Of the sputtered coatings, Ta-16W seemed the most resistant to the combustion gases. In general, the sputtered coatings showed poor adhesion to the substrate; failure occurred at the interface.

Izod and Baker also refer to the difficulty in manufacturing tungsten or molybdenum coatings. The attractive means of deposition are chemical vapour deposition (CVD) and physical vapour deposition (PVD). The high temperature inherent in CVD tends to degrade the mechanical properties of the substrate, whereas coatings prepared by PVD have a slow cooling rate which doesn't provide the optimum properties.

Turley has investigated magnetron sputtering as a means of depositing chromium, niobium, and tantalum coatings⁶¹. They were prepared on rifled coupons for which the composition is shown in the Table VIII, and on the interior bore of a 30 mm rifled liner. The surfaces were precleaned with a fast ion beam (6 kV, 5 mA) prior to the sputtering. Defects in the form of nodular growths were present on the sputtered coupons. The nodules were "virtually" eliminated by coating at high deposition rates or oscillating the substrate between magnetron sputtering and fast ion beam irradiation. On the rifled coupons, the deposition was non-uniform between the lands and the sides of the lands of the rifling.

The tube bore was coated from the ends, as the coating could take place by line of sight only. Deposition rates were slower and deposition times up to 6 hours had to be used. The

Table VIII	
Composition of gun steel substrates coated by Turley:	
C:	0.36%
Mb:	0.52%
Ni:	2.70%
Cr:	0.72%

coating occurred at different rates depending on the distance up the tube. Coarse columnar grains were created; they were densified by irradiation with the fast ion beam to prevent diffusion between the grains.

Different alloys were deposited by alternating between two magnetron sputter units, each with a target of a specific material. In this way Nb-Cr and Nb-Ta alloys were deposited. These appeared to give denser coatings but it was acknowledged that this work was preliminary.

An Nb-Cr coating was deposited on a rifled 30 mm liner which was subsequently shrink fitted into a 30 mm barrel and 10 rounds fired. The coating time was 20.5 hours after 16 hours of cleaning with the fast ion beam. Visual and SEM examination of the coating after firing showed the remaining coating was about 5 μm thick, corresponding to the deposited thickness, but pieces of the coating had spalled. Below the coating was a martensitic heat affected zone around 35 μm thick. A thicker coating was recommended as being more resistant to spalling. Spalling was attributed to differential thermal expansion in the heating-cooling cycles during firing and stresses due to the volume changes in the austenitic and subsequent martensitic transformations.

Ceramics have been applied¹⁴ in a number of cases as gun tube liners. Many ceramics are ideal materials in that they have a high hardness and high melting temperatures. Unfortunately, ceramics are in general brittle, and fail catastrophically at tensile stresses significantly lower

Table IX. Candidate Ceramic Materials for Gun Tube Applications

Alpha SiC	2800C	B ₄ C	2347
Reaction bonded SiC	2800	AlN	2527
Hot pressed Si ₃ N ₄	>1900	HfC	3950
ZrO ₂	2715	LaB ₆	2717
Al ₂ O ₃	2050	NbC	3617
Mullite (3Al ₂ O ₃ -2SiO ₂)	1870	TaB ₂	3037
MgO	2800	SiC fibre-lithium aluminosilicate glass-ceramic matrix	1000*
Graphite fibre-borosilicate glass matrix	600*	* glass softens	

than the yield strength of gun steel. Criteria for successful employment of ceramic materials for this application are as follows:

1. high melting temperature
2. thermal expansion to match the outer jacket to ensure a continual fit of the insert during the large temperature change incurred on firing
3. high thermal diffusivity to reduce peak surface temperatures
4. high strength in tensile tests (high fracture toughness, but resistance to the growth of small flaws can be much different from that determined by normal fracture mechanics tests)
5. high hardness, maintained to high temperatures, to reduce effects of erosion by particle impact

Candidate ceramic materials, and their melting points in degrees C, are given in the Table IX. By contrast with these materials, tungsten melts at 3410 C. Use of most liner and coating materials will require considerable **tube design effort** to accommodate mechanical stresses imposed by thermo-mechanical property differences. In other words, eventual use of ceramic coatings or liners may not occur by a simple retrofit of existing guns with ceramic components, but may come about because of a redesign the gun from the start to make use of the new materials.

VI. Analysis of Potential of Lasers to Simulate Gun Tube Wear

VI.1 Variables to be Simulated

This project is aimed at developing a means of rapidly testing potential coatings for gun tubes. The variables to be simulated shall be identified in the following paragraphs. Unfortunately, detailed information about the gun barrel environment during firing is not available, but the available information was summarized in Section II.4. Details of the diagnostic equipment were not presented in any of the surveyed literature. The conditions in a gun barrel are as follows:

Temperature, and

thermal cycle: Bulpett reports that the RARDE gun experienced temperatures of 1000 C, dropping to 500C in 8 ms. Griffin *et al.*, in the

Table X. Comparison of Temperatures

Propellant	Flame Temperature K (C in brackets)	Bore Surface Temperature C
Naco	2239 (1966 C)	850
M6	2570 (2297 C)	980
M26	3132 (2860 C)	1330

data presented in figure 2, shows peak temperatures of 760 to 920C, depending on the explosive, falling to half of the maximum value in 15 ms. Many others report the flame temperature of the explosive rather than the bore temperature in the gun. Table X shows¹⁴ the two temperatures have no direct correlation. Izod and Baker refer to a temperature rise lasting 5 ms, but they give no details.

Pressure: The pressure surge in the barrel is given by various workers as

400 MPa	(Bulpett, RARDE gun),
550 MPa	(Botstein and Arone)
520 MPa	(Turley)
350-394 MPa	(Griffin <i>et al.</i>)

The duration of the pressure pulse has not been given, but is most likely closely linked to the temperature cycle. Griffin measured the dependence of the pressure pulse on the nature of the explosive and other factors.

Chemical Environment: The chemical environment depends on the nature of the explosive,

and some of the elements found in the cracks in damaged coatings have been identified with additives to the explosives. Efficient use of the explosive requires it to be reduced to low atomic and molecular weight constituents, hence the main constituent gases will be carbon monoxide, carbon dioxide, hydrogen, nitrogen, and water vapour, regardless of the nature of the explosive.

Gas Wash: It is not clear that the gas wash is responsible for initiating damage. The accepted doctrine is that the gas worsens damage after it has occurred, with turbulent hot corrosive gases being swept into cracks in either the chromium plate or the gun steel, causing further reactions. Erosion, especially near the origin of rifling, causes loss of obturation by the rotating band. Additional heat flux occurs by gas blow-by, and very high localized temperatures can occur. Thus the presence of damage can give rise to a situation where the rate of damage is accelerated. Perhaps the best expenditure of effort is to work on coatings which would extend the damage incubation time, the time before which the damage becomes severe enough that accelerated wear due to the gas wash becomes significant.

Chemical attack, oxidation and carburization, with the relative importance depending on the temperature of the explosive, leads to formation of the "white layer". In

Table XI. Thickness of the White Layer		
First layer	Second layer (if any)	
30 μm		Bulpett (Chieftain gun)
10 μm		Bulpett (RARDE gun)
0.5 μm	18 μm	Lin
0.25 μm	1.3 μm	Turley

some cases this is a two fold white layer, as discussed earlier. Table XI summarizes the information on thickness of the white layers, as discussed in section II.1. The diffusion coefficient of carbon in .46% carbon steel is⁶³ approximately $D = 4 \times 10^{-6} \text{ cm}^2/\text{sec}$ at 1300C. In a thermal burst lasting $t = 20$ milliseconds, carbon will diffuse a distance $\sqrt{(D \times t)} \approx 2 \mu\text{m}$. This is an order of magnitude shorter than the observed thickness of the white layer. A time period two orders of magnitude longer would be required for carbon to diffuse the observed distance, since the distance is determined by the square root of time or of the number of shots. As the guns being damaged had an uncertain history, with the exception of the RARDE gun which was known to have fired 3750 rounds, it is not unlikely that a sufficient number of rounds had been fired to produce the observed depth of the white layer by solid state diffusion

of carbon.

Energy flux: A review article by Montgomery and Sauter⁴ describes work by Ward and Brosseau, in which they correlate erosion with the heat transferred to the gun barrel.

There was no erosion for heat input to the gun less than 350 J/mm (120 J/cm² for the calibre of gun that they used). Erosion increased faster than linearly with heat input for heat inputs over this threshold value. This figure might be a good starting point for the laser experiments.

The review article refers to other work using a uniquely instrumented 60 mm research cannon in which a simplified correlation was found relating material loss to the rate of energy generation for steel cannon bores. There was no significant erosion for energy generation below 1.0 BTU-ft²sec⁻¹; that is, 10 MW/cm². Above this energy flux, the erosion increases somewhat faster than linearly with energy generation. The rate of erosion varies somewhat from gun-to-gun with different calibers and with different explosives. The article does not state clearly whether the energy inputs refer to energy generation *per unit area of the bore* or *per unit area of the surface of the gun tube*. Moreover, it is not clear whether the term "heat generation" refers to the heat transferred to the bore or the total heat generated in the gun. Some of the heat is transferred to the projectile, some of it escapes with the exhaust gases, and only some fraction of the heat generated is actually transferred to the gun barrel. It is more likely "heat generation" refers to the total heat, since the figure of 10 MW/cm² differs substantially from the figure of Ward and Brosseau, referred to above, for thermal pulses of the order of 10 milliseconds.

VI.2 Previous Laser Simulation Studies

This section summarizes previous attempts to use lasers to simulate the wear and corrosion of gun barrel tubes, as described in more detail in earlier sections of the report.

As described in section III.1, Bulpett studied samples in which a laser had been scanned across steel samples, producing a white etched layer without inducing surface melting. The microstructure was considerably different than the white etched layers in damaged gun steel (carbides in acicular ferrite versus carbides in a coarse-grained martensite), and the laser treated steel showed no change in elemental composition. It is concluded that this treatment is not a good simulation of the wear in gun steel.

Alloying of laser treated steel has been observed with alloying additions provided by coating the surface with graphite and/or spraying the surface with a carburizing gas, as described in section III.2. In the experiments described there, significant alloying did not take place unless surface melting occurred, and in most cases carbon enrichment occurred only in the molten area. In the experiment of Walker *et al.*, however, a white zone was observed below the molten layer, attributed to solid state diffusion of carbon. The thickness of the molten layer was 20 μm , of the same order as the thickness of the white layer in gun steel.

Irradiation of AISI 4340 steel discs with a pulsed Nd:YAG laser produced surface melting, white etching layers, and formation of martensite, as described in section IV.4. There was cracking of the white etching regions and "tearing" of the softer microstructure surrounding the region that had undergone the martensitic transformation. SIMS analysis of Iron discs that had been laser irradiated in a carbonizing atmosphere showed an increase in carbon content. AISI 4340 samples coated by tungsten and nickel were irradiated. The viability of the laser system for testing the mechanical stability of coatings has been clearly demonstrated.

VI.3 Laser Driven Shock Waves

Section IV.2 has described experiments in which a pulsed laser evaporates surface material producing a shock wave which causes metallurgical changes or damage in the material. Pressure impulses of 10 to 25 GPa induced shock hardening of various target materials. These pressures are 20 to 50 times that observed in guns, as described above. The damage produced by the laser-shocks is parallel to the surface, rather than perpendicular. This is shown, for example, in the Figure 6⁶⁴. By contrast, the craze cracks observed in the gun barrels are perpendicular to the surface. Moreover, damage from shocks is invariably at the rear side of the workpiece, where reflection has turned



Figure 6. Plastic Deformation of a Spall Layer

the pressure wave into a tensile wave.

The data in the literature does not indicate the duration of the pressure burst in a gun tube, or how long the pressure remains at its peak value. To the first approximation (ideal gas law, neglecting transit times), the pressure can be considered proportional to the temperature. For a particular explosive tested in Griffin *et al.*, referred to above, the temperature of the bore tube rose to its maximum value in 1.6 milliseconds, and thereafter fell to half its peak value in 7.6 milliseconds. These time scales differ by factor of a thousand from the transit time of an energetic shock through the thickness of a gun barrel. For example, Ng *et al.*⁶⁵ have measured shock speeds of the order of centimetres per microsecond, generated by 2 ns, frequency doubled Nd:Glass laser pulses. Because the characteristics of damage produced by irradiating targets in air by short pulsed lasers differs from that in a gun, and because the time scales in which the damage occurs is nanoseconds instead of milliseconds, the study of laser driven shocks in air is not relevant to the study of metallurgical failures in gun material.

In firing of the gun, there are thermal transients on a millisecond time scale set up in the gun metal. These transients result in thermal expansion and subsequent contraction and associated thermo-mechanical stresses, which can be duplicated using lasers. This would not however be done with the very short pulsed lasers that produce shock damage in materials irradiated in air.

Section IV.5 describes experiments in which lasers irradiate liquids or solids immersed in liquids. The absorption of laser energy, primarily in dust particles in the liquids, leads to vaporization of the liquid, plasma formation, and a high pressure shock wave, when an intense beam of nanosecond duration is focussed into the liquid. Experiments were described in which a laser was focussed onto a metal target immersed in a liquid. The shock wave resulting from the plasma formation caused plastic deformation of the metal and left residual stresses with potential beneficial properties. For the reasons given above for irradiation of targets in air, it is not felt that these experiments are relevant to the current research effort.

The literature search failed to turn up any instances in which high pressures were generated by millisecond thermal pulses, as distinct from nanosecond pulses with extremely high rates of energy input generating extremely high pressure bursts.

VI.4 Laser Simulation of Gun Tube Damage

As described above, laser irradiation of discs at atmospheric pressure, performed with a pulsed laser of a pulse duration corresponding to the thermal pulse at the gun barrel surface, was felt to be a viable method of testing the mechanical integrity of coatings. With the exception of the pressure burst, the variables involved in firing the gun can be simulated by varying the laser operating parameters. Once a laser energy is chosen, the energy flux can be matched to that observed in the gun by choosing the distance from the focussing beam to sufficiently concentrate the beam. The laser pulse duration can be chosen to match the duration of the temperature cycle in the gun. The gas wash can be simulated using a heater, such as a GTE Sylvania hot air heater, to direct a stream of hot oxidizing or inert gas at the sample as it is being laser irradiated. Covering the target with carbon DAG or a transmitting liquid may provide the chemical constituents found in the steel from the damaged gun tubes.

The next section describes a proposed experiment, in which laser energy is used to simulate the surface damage.

VII. Project Definition

VII.1 Ambient Pressure Experiments

The laser is a thermal heat source that can be readily cycled. As a heat source, it will cause thermal distortion of the workpieces or coatings, thermal chemical reactions, and thermal diffusion of impurities into the surface. These thermal phenomenon may simulate many of the conditions leading to gun wear.

As described above, experiments in which lasers have been used to generate high pressure impulses required a pulse duration that is inconsistent with heat input to targets that simulates the thermal cycle in the firing of a gun. It is proposed that a special apparatus be constructed that allows the simultaneous application of pressure and heat to targets, over a millisecond time period. This will be described in the following sections. It may happen that the damage to guns can be simulated without the application of pressure to the target. A preliminary set of experiments will be conducted in an ambient atmosphere, and if these yield satisfactory results the expense of building the special apparatus will be avoided.

The preliminary set of experiments will involve irradiating metal targets in a variety of different circumstances. In each case, the laser pulse duration will be controlled to simulate the heat input during the firing of the gun, as discussed in the next section. The laser will be focussed in a manner that produces a uniform and well characterized surface irradiance. The irradiance will be controlled to produce a range of values near 120 J/cm^2 , as discussed above. Three sets of experiments will be conducted, as follows:

1. Laser irradiation of AISI 4340 steel coupons, coated with a layer of graphite. The principle variables here are the energy density, varied by controlling the position of the target with respect to the laser focus, and the number of pulses. When multiple pulses are used, the samples may be recoated between shots.
2. Laser irradiation of AISI 4340 steel coupons, either covered with a thin layer of liquid that transmits the laser energy, or sprayed with the liquid between laser pulses. The latter is more amenable to accumulating a substantial number of shots on the target. The laser energy will be absorbed at the liquid-solid interface, heating both the liquid and the solid. Decomposition products from the liquid may chemically attack the surface, resulting in

oxidation or carburization that simulates the corrosive effect in gun tubes. Candidate liquids are 2-propanol⁶⁶ or methanol⁶⁷, both of which have been used by other researchers.

3. Laser irradiation of AISI 4340 steel coupons, being simultaneously blown by gas from a hot air or an inert gas heater. The gas flow simulates the effect of gas wash, as described in section II.3. It is very likely that the hot gas flow will be inconsistent with either an absorbing carbon coating or a liquid spray of the target surface. The gas flow can be chosen to be either air, a relatively inert gas such as argon or nitrogen, or a carburizing gas such as carbon dioxide. The gas flow velocity can be chosen to match the projectile velocity at the position of the origin of rifling. To a first approximation, the velocity of the gas wash will be the same as that of the projectile. Other variables include the laser pulse energy density and the number of shots.

For each of the above cases, the laser irradiated targets will be sectioned and mounted, followed by a visual examination and a microhardness traverse. SEM analysis will be appropriate, because of the expected narrow width of the white etching layer. EDX or alternative techniques will be used to determine the depth profile of contaminants or alloying additions to the materials. The results will be correlated with calculated temperature profiles in the material.

VII.2 Laser Irradiation Parameters

Laser transformation hardening is a process in which a steel sample must be held above the austenitic phase transition temperature for a long enough period of time for the carbon to be evenly distributed around the matrix. Sandven has demonstrated⁶⁸ that transformation hardening proceeds more efficiently if the laser pulse applied to the material surface has an initial spike followed by a lower level of power. The initial spike ensures the material is quickly brought above the A_3 temperature, while the lower level of power maintains the material at a high temperature long enough for the carbon to diffuse and form a uniform structure. In the gun barrel, the heat impulse from the detonation of the propellant follows a similar sequence, rising fairly rapidly to a peak value, followed by a gradual decay as the projectile accelerates down the tube. This pulse shape will maintain the surface at a

temperature at which diffusion can take place longer than if the energy was presented came in a uniform burst.

The Nd:YAG laser at The Laser Institute consists of two rods which can be independently excited, provided that the average energy delivered to the two rods is identical. It is proposed that the rods be triggered simultaneously, with one rod producing a fairly short intense pulse. This will serve to bring the target material quickly to a temperature at which diffusion of carbon into the material can readily occur. The duration of this pulse will be chosen to coincide with the peak of the temperature pulse during the firing of a gun, as discussed above. The second rod will be fired with the same energy of excitation, but with a time period typical of the decay time of the temperature pulse in the gun. The two rectangular pulses will superimpose to simulate the time variation of temperature seen in a gun.

If the target is uniformly illuminated, there is a uniform one dimensional heat flow from the surface into the bulk of the material which acts as a heat sink. If, however, the radiation striking the target has considerable transverse structure, a two or three dimensional heat flow may result, with a thermal history that is not easily characterized. When a laser is delivered through a large core fibre optic, the mode structure of the laser is largely lost, and the light at the delivery end of the fibre is essentially uniform. The light emerging from the fibre is diverging, but it is re-imaged onto the workpiece. The workpiece is then irradiated considerably more uniformly than if the laser was used without the fibre, and a heat flow that more closely approximates the one dimensional heat flow results. Moreover, the intensity at the workpiece surface has less variation and can be more easily determined. The fibre-optic-delivered beam will be used in the proposed experiments, to allow better control of the spatial distribution of the laser energy delivered to the workpiece.

VIII. References

1. *Gun Wear: An account of recent UK Research and New Wear Mechanisms*, D.C.A. Izod and R.G. Baker, Proc. Tri-service Gun Tube Wear and Erosion Symp., Dover NJ, Oct 25, 1982. Section III, pg 221.
2. *Effect of Surface Oxide on Gun Barrel Wear*, Ward, J.R., Stobie, I.C., Kaste, R.P., and Bensinger, B.D., Corrosion, 39, 384-385 (1983)
3. *The Problem of Gun Barrel Erosion - an Overview*, Ahmad, I. Proceedings of the Tri-Service Gun Tube Wear and Erosion Symposium, Dover, N.J., March 1977.
4. *A Review of Recent American Work on Gun Erosion and its Control*, Montgomery, R.S. and Sautter, F.K. Wear, 94, 193-199 (1984)
5. *The Microstructural Changes in the Surface Layer of Gun Barrels*, Botstein, O. and Arone, R. Wear, 142, 87-95 (1991)
6. *Potential Erosion Resistant Refractory Metal and/or Alloy Coatings for Gun Tubes*, Ahmad, I, Greco, P., D'Andrea, G., and Barranaco, J., Proceedings of the 1978 Tri-Service Conference on Corrosion, Ed. Levy, M., and Brown, J. (available from the Metals Ceramics Information Center, Battelle Laboratories, Columbus, Ohio).
7. Boyer, H.E., and Gall, T.L., *Metals Handbook*, Desk Edition (American Society of Metals, Metals Park, Ohio, 1985), pgs 28.6 and 28.24.
8. *Erosion of a Chromium-Plated Tank Gun Barrel*, Turley, D.M. Wear, 131, 135 (1989)
9. *Metallurgical Examination of Bore Surface Damage in a 5-inch Gun*, Griffin, R.B., Pepe, J., and Morris, C. *Metallography*, 8, 453-471 (1975).
10. *The Characterization of White-Etching Layers Formed on Engineering Steels*, Bulpett, R., Ph.D Thesis, Brunel University 1992.
11. *Auger Electron Spectroscopic Study of Gun Tube Erosion and Corrosion*, Lin, S-S., *Appl. Surf. Sci.* 15, 149-165 (1983)
12. *Chemical Constituents of Eroded Gun Barrels*, Sin-Shong Lin, *Applications of Surface Science* 21 (1985), 112-124.
13. *A metallurgical study of erosive wear in a 105 mm tank gun barrel*, D.M. Turley, G. Cumming, A. Gunner, and I.McDermott, Wear, 176, pg 9-17 (1994)

14. *Application of Nonconventional Materials to Guns and Gun Tubes*. Report No. NMAB-423 (National Materials Advisory Board, 2101 Constitution Ave., N.W., Washington, D.C. 20418, USA, 1986).
15. *Friction and Wear at the Projectile Tube Interface*, Montgomery, R.S. Proc. Tri-service Gun Tube Wear and Erosion Symp., Dover NJ, Oct 25, 1982. Section III, pg 446.
16. *Interaction of Copper-containing rotating band metal with gun bores at the environment present in a gun tube*, Montgomery, R.S., Wear, 33, pg 109-128 (1975).
17. *Metallographic Studies of Erosion and Thermo-Chemical Cracking of Cannon Tubes*, Fisher, R.M., Szirmai, A., and Kamdar M.H. Technical report ARLCB-TR-83022 (US Army Armament Research and Development Command, Watervliet, N.Y. 1983)
18. *Muzzle wear of Cannon*, Montgomery, R.S. Wear, 359-368 (1975)
19. *Material Degradation under Pulsed High Temperature and High Pressure*, Jennings, L.D., Lin, S., and Marotta, A.S., Proceedings of the conference Materials Characterization for Systems Performance and Reliability, (Plenum Press, New York, 1986)
20. *Hot Gas Erosion of Gun Steel*, Johnson, J.W., Caveny, L.H., and Sommerfield, M., Proceedings of the 1978 Tri-Service Conference on Corrosion (New Orleans, 1978), Levy, M., and Brown, J., Editors.
21. *Laser Surface Transformation Hardening*, Sandven, O., in Metals Handbook, Ninth Edition, Volume 4. (American Society for Metals, Metals Park Ohio, 1981)
22. *Study on Laser Surface Melting of Carbon Steels in Controlled Atmospheres*, Masumoto, I., Kutsuna, M., and Honda, Y., Trans. Japan Welding Society, Vol 20, No. 2, pg 84-90 (1989)
23. *Laser surface alloying of iron and 1C-1.4Cr steel with carbon*, Walker, A., West, D.R.F., and Steen, W.M., Metals Technology, Vol. 11, pg 399-404 (1984)
24. *Gaseous Alloying with Laser Heating*, Mordike, B.L., Bergmann, H.W., and Groß, Z. Werkstofftech, 14, 253-257 (1983)
25. *Laser Gas Alloying*, Mordike, B.L. in ; pg. of 389-412. Laser Surface Treatment of Metals, ed. Draper, C.W., and Mazzoldi, P. (Martinus Nijhoff Publishers, Dordrecht, Netherlands, 1986), pg 389-412.
26. *Surface Alloying of Iron Alloys by Laser Beam Melting*, Mordike, B.L., and Bergmann, H.W. in Rapidly Solidified Amorphous and Crystalline Alloys, Kear, B.H., Gleassen, B.C., and Cohen, M. (Elsevier Science Publishing Co., Inc., 1982), pg 463-483.

27. *Interaction of Laser-Induced Stress Waves with Metals*, A.H. Clauer, A.H., and B.P. Fairand, B.P. pp 229-253 of Source Book on the Applications of the Laser in Metalworking, Ed. E.A. Metzbower, E.A. (American Society for Metals, Metals Park Ohio, 1981), pg 229-253.
28. Effects of High Power Laser Radiation, by J.F. Ready (Academic Press, 1981)
29. *One-dimensional steady-state model for damage by vaporization and liquid expulsion due to laser-material interaction*, Chan, C.L. and Mazumder, J., J.Appl.Phys., 62, 4579-4586 (1987).
30. Laser-beam Interaction with Materials, von Allman, M. (Springer-Verlag Berlin, 1987), pg 175.
31. *Influence of a plasma on the interaction of laser radiation with a metal*, Zhirakov, B.M., Popov, N.I., and Samokhin, A.A. Soviet Physics JETP, 48, 247-252 (1978)
32. *Influence of laser-supported detonation waves on metal drilling with pulsed CO₂ lasers*, Sturmer, E. and von Allman, M. Journ. Appl.Phys. 49, 5646-5652 (1978).
33. *From laser-induced desorption to surface damage*, Matthias, E., and Dreyfus, R.W., pg 89-128 of Photoacoustic, Photothermal, and Photochemical Processes at Surfaces and Thin Films, Editor Hess, P. (Springer-Verlag, Berlin, 1989), Volume 46 of the Springer Verlag Series "Topics in Current Physics".
34. *Schlieren measurements of the hydrodynamics of excimer laser ablation of polymers in atmospheric pressure gas*, Ventzek, P.L.G., Gilgenbach, R.M., Sell, J.A., and Heffelfinger, D.M., J.Appl. Phys. 68, 965-968 (1990).
35. *Laser induced vaporization of a metal surface*, Aden, M., Beyer, E., Herziger, G., and Kunze, H. Journ.Phys. D: Appl. Phys. 25, 57-65 (1992)
36. *Spallation as an effect of laser-induced shock waves*, Gilath, I., Salzmann, D., Givon, M., Daril, M., Kornblit, L., Bar-Noy, T. Journ. Mat. Sci., 23, 1825-1828 (1988)
37. *Shock and compression by TEA-CO₂-laser pulses drastically enhanced by liquid layers spread on surfaces of solids*, Siegrist, M., and Kneubuhl, M. Appl. Phys. 2, 43-44 (1973)
38. *Large-spot thermal coupling of CO₂ laser radiation to metallic surfaces*, Marcus, S., Lowder, J.E., and Mooney, D.L. J.Appl.Phys., Vol 47, 2966-2968 (1973).
39. *A study of energy conversion during Nd:YAG laser ablation of metal surfaces in air by means of a laser beam deflection probe*, Diaci, J., and Mozina, J. Journal De Physique IV, Colloque C7, Volume 4, C7-737-740 (1994)

40. *Theory of momentum transfer to a surface with a high power laser*, Pirri, A.N., Phys.Fluids 16, 1435-1440 (1973)
41. *Effect of pressure on the microstructure of an austenitic stainless steel shock-loaded by very short pulses*, Gerland, M., and Hallouin, M. Jour.Mat.Sci 29, 345-351 (1994)
42. *Experimental study of metallurgical evolutions in metallic alloys induced by laser generated high pressure shocks*, Fabbro, R., Fournier, J., Fabre, E., Leberichel, E., Hannau, Th., and Corbet, G. pg 320 of SPIE Vol 668 Laser Processing: Fundamentals, Applications, and Systems Engineering, ed. by Duley, W.W. and Weeks, R. (SPIE-The International Society of Optical Engineering, Bellingham, 1986)
43. *Dynamic Response of a Thin Disk Subjected to a Thermal Pulse*, Calder, C.A. and R.H. Cornell, R.H. Experimental Mechanics, 27, 352-358 (1987)
44. *Pulsed Laser Heating: A Tool for Studying Degradation of Materials Subjected to Repeated High-Temperature Excursions*, Goldberg, A. and Cornell, R.H., Technical Report UCRL-53074 (Lawrence Livermore National Laboratory, 1980)
45. *Simulation of Erosion/Corrosion Surface Chemical Reactions with a Laser Beam*, Price, C.W. Report UCRL-53468 (Lawrence Livermore Laboratories, Nov 1983)
46. *Shock Wave Generation in Air and in Water by CO₂ TEA Laser Radiation*, Bell, C.E., and Maccabee, B.S., Appl. Opt. 13, 605-609 (1974)
47. *Laser-induced liquid breakdown: a step-by-step account*, Felix, M.P., and Ellis, A.T., Appl. Phys. Lett. 19, 484-486 (1971).
48. *Laser-Induced High-Pressure Shock Waves in Water*, Bell, C.E., and Landt, J.A. Appl. Phys. Lett. 10, 46 (1967).
49. *Laser generation of stress waves in metal*, Masse, J-E., and Barreau, G., Surface and Coatings Technology, 70 (1995) 231-234.
50. *Laser Shock Processing of Materials. Physical Processes Involved and Examples of Applications*. Fabbro, R., and Peyre, P. Proceedings ICALEO'95 (to be published, Laser Institute of America, Orlando, 1995).
51. *Factors influencing the durability of chrome plate*, Montgomery, R.S., and Sautter, F.K. Wear, 60, 141-148 (1980)
52. *Chromium as a gun tube liner*, McCormick, M. and Dobson, S.J. Trans. Inst. Met. Finish. 66, (1), 22-27 Feb. 1988.

53. *Nondestructive evaluation of electrodeposited chromium*, Todaro, M.E., Technical Report ARCCB-TR-92046, Army Armament Research, Development, and Engineering Center, Watervliet, N.Y., 1992.
54. *Laser Treatment of Chromium Plated Steel*, R. S. Montgomery, *Wear*, **56**, 1979, 155-166.
55. *Laser Surface Treatment of Chromium Electroplate on Medium Carbon Steel*, Christodoulou, G. and Steen, W.M., in Proc. Conf. on Lasers in Materials Processing, ASM, 1983, 116-125.
56. *Characterization of Fusion Zone Defects in Laser Surface Alloying Applications*, Molian, P.A. *Scripta Metallurgica*, **17**, 1311-1314 (1983).
57. *Increasing the surface strength of carbon steel in laser deposition of chromium-bearing coatings*, Govorov, I.V., Kolesnikov, Yu.V., and Mirkin, L.I. *Fizika i Khimiya Obrabotki Materialov*, Vol 22, p 68-71 (1988).
58. O'Shea, R.P. and Watmonth, T, pg 3.2 in Proceedings of the Triservice Technical Meeting on Gun Tube Erosion and Control, Watervliet Arsenal, AD14668, February 1970, Ed. Ahmad, I., and Picard, J.P.
59. *High Temperature and Strength Material Development*, Liu, Y.H., and Kennedy, E.M., Jr., Technical Report AFATL-TR-73-54 (March 1973).
60. *Heat Transfer and Erosion in the ARES 75 mm HV Cannon*, Vassallo, F.A., Calspan Technical Report BL-564-D-1 (October 1975)
61. *Development of erosion resistant refractory metal and alloy coatings by magnetron sputtering*. Turley, D.M. *Surface and Coatings Technology*, Vol. 39/40, 135-142 (1989).
62. *Screening Gun Barrel Coating's Response to Combustion Gases*, Stobie, I.C., Kaste, R.P, Bensinger, B.D., Brosseau, T.L., Ward, J.R., Mullaly, J.R., and Allard, P.A. Technical Report ARBRL-TR-02396 (US Army Armament Research and Development Command, Aberdeen Proving Ground, Maryland, 1982).
63. Smithells Metals Reference Book, 6th Edition, Brandes, E.A., Editor (Butterworths, London, 1983), pg. 13-58.
64. *Brittle-to-ductile transition in laser-induced spall at ultrahigh strain rate in 6061-T6 aluminum alloy*, Gilath, I., Eliezser, S., Darile, M.P., and Kornblit, L. *Applied Physics Letters*, **52**, 1207 (11 April 1988)
65. *Hugoniot Measurements for Laser-Generated Shock Waves in Aluminum*, A. Ng, D. Parfeniuk, and L. DaSilva, *Physical Review Letters*, **54**, Pg 2604 (17 June 1985)

66. *Shock wave generation in dielectric liquids using Q-switched lasers*, Roach, J.F., Zagieboyhlo, W., and Davies, J.M., Proc. IEEE, XX 1693-1694 (1969).
67. *Laser-induced liquid breakdown: a step-by-step account*, Felix, M.P., and Ellis, A.T., Appl. Phys. Lett. 19, 484-486 (1971).
68. *Laser Surface Heat Treatment with Profiled Laser Beams*, Sandven, O.A., Proceedings of the First International Laser Processing Conference, Nov. 16-17, 1981, Anaheim, California (Laser Institute of America, Toledo, 1981).

Phase II - Experimental Work

I. Introduction

I.1 Background

Based on the literature survey of phase I of this project, two materials which showed promise as gun barrel coatings were pure tantalum (Ta) and a tantalum-tungsten alloy (Ta-10W). These alloys have excellent high temperature properties in many different environments. Pure Ta has excellent physical properties at temperatures up to around 2000°F (1093°C), but must be alloyed for use at temperatures up to 3500°F (1927°C). However, both materials are very difficult to clad to other metals. The gun barrel base material that we are looking at is AISI 4340 alloy steel. This material contains a high percentage of iron (Fe). When attempting to create a metallurgical bond between the two materials (ie. melting during laser weld overlaying), brittle intermetallics such as FeTa and Fe₂Ta can be formed. These intermetallics can cause cracking and spalling of the coating. If a damaged coating is used inside a gun barrel, it becomes extremely susceptible to corrosive and chemical attack, which leads to failure.

Two techniques were envisioned to minimize the possibility of the formation of harmful intermetallic materials. The first was use of laser energy for the weld overlaying. This allows careful control of the heat input which could potentially minimize the dilution between the coating and the substrate^{1,2}. The second technique for reducing the formation of Fe-Ta intermetallics is use of an interlayer.

Candidate materials for an interlayer should be metallurgically compatible with the substrate and the coating, and must have values of the thermal coefficient of expansion and melting point intermediate between those of both materials. One possible candidate for an interlayer material is titanium (Ti). It has a melting point of 1671°C, which is between iron with 0.4%C ($T_{(m)} = 1200^{\circ}\text{C}$) and tantalum ($T_{(m)} = 2996^{\circ}\text{C}$) or Ta-10W ($T_{(m)} = 3035^{\circ}\text{C}$). Titanium is 100% soluble in tantalum, which means it forms a solid solution at all compositions. Iron, however, forms intermetallics with titanium (FeTi, FeTi₂, etc.). The advantage of using Ti as interlayer material follows from the fact that its melting temperature is closer to that of steel. Laser weld overlaying of Ti may result in lower dilution than what could be achieved with overlaying of Ta due to its high melting temperature. With the low

dilution, the cracking effects of the intermetallics may not be as pronounced in the coating. In applying Ta on the Ti, lower dilution is not as significant a factor because:

- a) the melting temperatures are slightly closer so the temperature gradient between Ti and Ta will not be as high as between Fe and Ta, and
- b) dilution that does occur will not likely cause cracking due to the high solubility of Ti in Ta.

Both titanium and tantalum are extremely reactive with oxygen, nitrogen, and hydrogen at temperatures over 300°C. In order to avoid formation of oxides, nitrides, and hydrides throughout the coatings, cladding must be performed in an inert atmosphere. The use of either a vacuum, or an evacuated and argon-backfilled chamber will greatly reduce this type of contamination. A getter plate of titanium can be used to reduce atmospheric contamination. This plate could be placed in the chamber and scanned with the laser beam several times. Since Ti is so reactive with these gases, much of the remaining O, N, and H² contaminating the atmosphere may be removed and tied up with the Ti. Then, cladding of Ti, or Ta may proceed.

Methods for cladding titanium on steel plate include: sputtering, thermal spraying, vacuum thermal spraying, electron beam welding, friction welding, and explosion welding. Sputtering would only likely coat up to about 5-10 µm, and is only used for relatively small samples. Thermal spraying would be extremely contaminated, unless used in a vacuum. Vacuum spraying is also useful for only small parts, is not commonly used, and is very expensive. Electron beam welding must also be done in a specialized chamber under vacuum, and so is not practical for coating a gun barrel. Friction welding is usually only practical for rounded parts, which can be spun at high speeds to be joined, unlike this application.

Explosion welding, however, is performed on many different materials of varying shapes and sizes. It is a common method for joining such dissimilar materials as Ta to Fe, Ti to Fe, Ni to Ta, and many other normally incompatible combinations. Explosion clad titanium on steel plate is commercially produced. Due to the nature of the process, brittle intermetallics

are produced, but become surrounded by ductile base material and so do not lend themselves to coating cracking. If titanium powder is impractical to use due to either excessive price, or availability, explosion clad samples of Ti on Fe may be a viable alternative. For eventual use, explosion welding may be used to clad the inside bores of gun barrels.

I.2 Objectives

There are a number of objectives to be met in this experiment.

1. To construct a chamber capable of being used for laser weld overlaying and for thermal cycle testing.
2. To laser weld overlay a number of different materials in the chamber, all of which, might be useful coatings for gun materials.
3. To determine a method for testing these and other materials using laser thermal cycling.

Section II of this phase of the report describes the construction of the system and its use for preparation of weld overlayed samples, while Section III describes the thermal cycle testing of these materials.

Although laser weld overlaying or cladding with the CO₂ laser is a well established technology³, there is little work in the literature on cladding with the Nd:YAG laser. The Nd:YAG laser was used for the current work because of the ease of coupling the beam into the vacuum chamber in which the cladding took place. An engineering effort beyond the scope of the current project would have been required to couple the output of the CO₂ laser into the vacuum chamber. The Nd:YAG work done to date has been cladding of stellite-6 on various substrates. The work described in this report is therefore considered to be ground-breaking. However because of the limited time and effort available for both preparation and evaluation of coatings, no time was spent optimizing these coatings.

II. LASER WELD OVERLAYING

II.1 Experimental Apparatus

The vacuum chamber was modified from a piece of equipment from an earlier experiment. It was redesigned so that it could be used for laser weld overlaying with the LASAG Nd:YAG laser (Figure 1). The main body of the chamber consists of a cylinder with

two end flanges; on all three parts, there are a number of attachments, described below.

Top of the Chamber

The top of the chamber has a vacuum feed-through hole onto which a vacuum-sealed flat window is attached. This window is anti-reflection coated and is capable of efficiently transmitting light of 1064 nm wavelength (Nd:Yag light). A 300 mm focal length lens in the laser head focusses the beam. The focussing lens can be adjusted in vertical position, controlling the degree to which the beam is focussed or partly focussed on the workpiece, independently from the vacuum chamber. Also on the top of the chamber are two 10 cm diameter acrylic viewports and another vacuum feed through. This second feed-through has two T-fittings which contain a chamber-to-atmosphere valve for slowly letting the chamber back up to atmospheric pressure, a vacuum pump evacuating the chamber, and a vacuum gauge connected to a monitor which displays the chamber pressure in mtorr (millitorr).

Flange 1

At one end of the chamber, there is a variable speed motor with a mechanical feed-through. This is attached to a screw drive inside the chamber which drives the stage in a single (x) direction. The motor speed can be manually set by adjusting the voltage, which then varies the linear speed and direction (forward or backward) of the stage. The inert gas input line is also attached to this end of the chamber, with a shut-off valve between the chamber and line.

Flange 2

At the other end of the chamber, there is a pressure relief valve for relieving pressure during the inert gas backfilling operation, and a mechanical feed-through. The mechanical feed-through consists of a long rod, which can be manually moved in and out of the chamber, and a rubber friction pad. The friction pad is used to manually adjust a micrometer on the stage inside the chamber. This allows manual manipulation of the stage in the y-direction between side-by-side passes, without opening the chamber.

Operation of the System

For the laser weld overlaying operation, one end of the chamber is removed, the powder is placed on the coupon, and the coupon is placed into a holder on the stage. The flange is replaced, and the chamber is first evacuated, then backfilled with argon several times. The coupon is positioned correctly, the stage is manually started, and the laser is turned on. After each pass, the coupon is manually moved into the next position, and the process repeated.

Tests showed the system could be pumped down to a pressure of 106 mtorr. Because the available vacuum pump was relatively small, and because the vacuum chamber was constructed of mild steel (a non-ideal vacuum material), the pump down was relatively slow. On the initial pumpdown, four days were required to reach the pressure of 106 mtorr. However, the chamber could be pumped down to 830 mtorr after 24.5 minutes, which was deemed adequate, since this chamber was to be backfilled up to atmospheric pressure (760 torr) with argon. Due to the slow turn around time for the experiments, it was necessary to construct the method of translating the stage between runs without opening the system to atmosphere, as described above.

II.2 Experimental Materials

Substrate materials used in overlaying were commercially Pure Titanium, available at The Laser Institute from previous experiments, and AISI 4340 supplied by DREA. Most of the work was done using the AISI 4340 coupons, of dimension 2" x 2" x 1". Coating materials were 99.9% pure Titanium Powder and 90Ta-10W - Tantalum-Tungsten Alloy Powder. The appropriate documents (datasheets) for the powders can be found in the Appendix as Figures 2 and 3.

II.3 Experimental Procedures

The initial trials of this project were also the initial trials at cladding with the Nd:YAG laser; there was very limited data available in the literature. Since Stellite 6 is a common, and easily weld overlayed material, the initial cladding experiments were done using this material

on 4340 coupons.

Preparation of Coupons

The AISI 4340 coupons were received in 5.1 cm x 10.1 cm x 2.5 cm thick blocks. Each of these blocks was first cut down to 5.1 cm x 5.1 cm x 2.5 cm blocks, and then a 2.54 cm x 2.54 cm square groove was milled out of the center of one surface on each block to a depth of either 0.13 mm or 0.25 mm. Prior to processing, the coupons were glass bead-blasted, cleaned in soap and water, and degreased with acetone.

Determination of Laser Mode

The LASAG K-622 laser can be placed in one of 3 modes. Single cavity mode can be used to provide the smallest spot-size of the beam, but this mode sacrifices laser power. Dual cavity- simultaneous mode can be used to provide much higher power, but the minimum spot size is larger in this mode. The third mode is dual cavity - alternating mode. In this mode, the two cavities can be 'pumped' alternately. The manufacturer claims that this mode can provide quasi-continuous wave operation, where the pumping rate of the cavities is matched so that as one pulse ends, the other begins, and so on. The limitation of this mode is that there is a limitation on the frequency and pulse duration such that only a few configurations of parameters can be used.

A 300 mm focal length lens was used for all the experiments. The lens was positioned so that a standoff of 300 mm would give a 0 mm defocus. Several sets of trials were used with the lens at this position. The laser was used in dual cavity-alternating mode to provide a quasi-continuous wave-type operation. It was found that even using a fully focussed beam, inadequate average power was obtained, using the limited number of configurations available in this mode. It was conjectured that single cavity operation would not provide adequate power density for laser weld overlaying. The dual cavity-simultaneous mode was used for all laser weld overlaying.

Determine Focal Position

The lens was positioned so that a standoff of 300 mm (0 mm defocus) to 320 mm (20 mm defocus) was used. Single weld overlayed tracks were made by scanning the coupon under the beam. The beam was defocussed between tracks from 0 mm to 20 mm. Sectioning of the samples revealed that a defocus of 6.35 mm (0.25") produced a clad track of 1.53 mm (0.060") width and approximately 2% dilution. Higher defocus did not provide adequate power density to melt and fuse the Stellite powder, while lower defocus provided excessive power density which resulted in higher penetration, and highly diluted coatings.

Determination of Overlap

The optimum conditions described above were used to produce coupons with 0.25 mm (0.010") thick coatings of approximately 2.54 cm x 2.54 cm dimensions. Overlap was varied between 25% and 75%. It was determined that an overlap of 50% produced the most consistent and smooth coating, without replacing powder between passes. This required that 34 side-by-side passes be used to create a 0.27 mm thick coating which covered 2.64 cm².

II.3.1 Laser Melting of C.P. Titanium

The chamber was evacuated and backfilled with argon several times. The laser was defocussed from the surface of the coupon by 12.7 mm. This provided conditions by which nitrogen and/or oxygen could be tied up with atoms of titanium. The beam was then scanned over the surface of coupons of commercially pure titanium. Each scan was about 7 cm long, with a gap of 0.6 cm between scans.

The scans were all made under the same conditions in order to determine the ability of the Ti to be used as a getter plate. The beginning of the first scan had a black/sooty material surrounding it for about the first 3 - 4 mm; otherwise the track was shiny silver in colour. The tracks were generally silverish in appearance with the dark soot appearing once in a while. One track was created in open atmosphere. It was dull grey in colour, with white soot coating the track. This white material indicated the presence of oxygen (likely in the form of TiO₂). The gold colour indicative of TiN was not present. The track was terminated prematurely because smoke rings were continually being created which could possibly

damage the optical window.

II.3.2 Laser Weld Overlaying of Titanium on AISI 4340

The AISI 4340 coupons were installed in the chamber. Titanium powder was placed in the 0.25 mm deep groove on the surface, and levelled. The chamber was then sealed, evacuated and backfilled with argon 3 times. Several sets of experiments were performed, varying speed, pulse length and energy, and focus. These samples were then sectioned, polished, and etched, in order to determine the amount of dilution in the coating. The lowest dilution possible should be used to avoid the formation of brittle inter-metallics, especially for the coupons on which the 90Ta-10W alloy will be weld overlayed. Once the correct parameters were found (Table I), side-by-side scans were performed in order to coat a larger area. Eight coupons were made with an area coverage of 6.7 cm² (1.0 in²). The surface of the coatings was relatively smooth (Figure 4). The amount of dilution of the coating is unknown.

Table I. Parameters for Laser Weld Overlaying

Task	Base Material	Overlay Material	Thickness (mm)	Frequency (Hz)	Pulse Length (ms)	Energy/Pulse (J)	Speed (ipm)
II.3.1	Ti	None	----	50	1.0	7.5	9
II.3.2	4340	Ti	0.25	50	1.0	7.5	5
II.3.3	Ti	Ta-W	0.25	50	1.0	7.5	10
II.3.4	Ti /4340	Ta-W	0.25	50	1.0	7.5	10

II.3.3 Laser Weld Overlaying of Tantalum-Tungsten Alloy on C.P. Titanium

A similar method to that described in II.3.2 was used for weld overlaying a 90% tantalum - 10% tungsten alloy on commercially pure titanium substrates. The coupons were installed in the chamber, and the tantalum-tungsten alloy powder was placed on the surface, and levelled to 0.25 mm (0.010") using powder depth gages. The chamber was then sealed,

and evacuated and backfilled with argon several times.

Several sets of experiments were performed, varying speed, pulse length and energy, and focus. These samples were then visually inspected to determine the best parameters to be used for the coating. Using 7.5 to 9.5 J/pulse of energy and a speed of 5 ipm, a smooth coating was produced, but it was expected that this coating was highly diluted with the titanium. The laser radiation reflected from the molten Ta cracked and destroyed the optical window in the chamber after about 30 passes. Due to this problem with the optics, the energy was dropped back to 7.5 J/pulse, corresponding to an average power of about 375 watts, and the speed was increased to 10 ipm. The cover glasses did not fail under these conditions, but a smooth coating could not be produced. The coatings were not contiguous and contained large surface 'craters', as shown in Figure 5.

Once the parameters were determined, side-by-side scans were used to coat a larger area. Four coupons were made with 90Ta-10W coatings, covering an area of 6.7 cm² (1.0 in²).

II.3.4 Laser Weld Overlaying of Tantalum on LWO Titanium (on AISI4340)

Coupons of titanium on AISI 4340, produced in task II.3.2, were used as substrate materials. The surfaces were cleaned with acetone, but otherwise used as deposited. The tantalum-tungsten alloy powder was spread over the surface and levelled to the same thicknesses as in tasks II.3.2 and II.3.3. The chamber was then prepared as before, and the the same parameters used in task II.3.3 were used for laser weld overlaying the tantalum-tungsten alloy on the titanium interlayer on 3 coupons. The coatings were similar to the 90Ta-10W on Ti, but 2 of the 3 coupons contained lack of fusion defects. It was likely that the as-welded Ti surface was smoother and less absorptive of the laser radiation than the as cast Ti plates used in task II.3.3. The higher reflection did not allow the coatings to be completely metallurgically bonded to the titanium (Figure 6).

II.4 Description of Coatings

Stellite Coated A36 Steel

The surface appeared relatively smooth (Figure 7). Semicircular solidification lines and structure due to side by side passes was clearly visible. Isolated cracks, generally perpendicular to the solidification semicircles, did not seem to cross from one pass to the next. There was a number of balls of a size 1/20 to 1/5 mm in diameter adhered to the surface, probably spatter.

Titanium Coated 4340

The titanium coated 4340 steel was relatively smooth, with a number of semicircular solidification lines (Figure 4). There were small regions in which the coating had somewhat beaded up, and the solidification lines were absent. The beads were 1/2 to one millimetre in extent. There were a number of cracks on the surface, which went in random directions with respect to the solidification lines. Some cracks passed from one pass to the adjacent pass, but the majority stopped at the boundary between successive passes.

Tantalum-Tungsten Coated Titanium

The surface was very rough (Figure 5). There were deep pits which seemed to extend through the entire thickness of the coating and even into the base metal. In other regions there was material that seemed to project from the surface. The pits had a range of sizes from approximately 0.3 mm to 0.6 mm. The coating appeared silvery. No cracks were found. There was no change of texture that made successive cladding passes discernable when observed through the stereomicroscope, although the successive passes were visible to the unaided eye.

Tantalum-Tungsten on Titanium Coated 4340

The laser clad tantalum on titanium on 4340 steel surface was very irregular (Figure 6). There were regions of considerable buildup, but also deep pits in the surface that seemed to extend down to the original titanium coating. The pits were a variety of shapes and sizes, with typical dimensions varying from a quarter to one millimetre. Approximately 1/4 of the surface was comprised of the pits, and the rest of the applied coating. The top surface of the clad area was quite textured and bumpy, but the bottom of the pits, even those not extending through the entire thickness of the clad, was generally smooth and reflective. There was no

cracks in the cladding. The tantalum clad was a greyish-straw colour.

III. THERMAL CYCLE TESTING

Uncoated and coated materials, prepared as described in the previous section, were subjected to a series of pulses from the Nd:YAG to simulate the effect of the heat flow into the material from the firing of the gun. For these trials, the laser was partly focussed on the surface, to avoid the drilling action that would result if the beam was completely focussed. For some of the trials, the test material was coated with graphite, to induce carbon absorption into the substrate similar to that observed in the gun. In other trials, the material was coated with vacuum oil which would be decomposed by heat of the laser pulse, resulting in a crude simulation of the complex chemical environment resulting from the detonation of the explosive charge in the gun.

This work also included a calculation of the temperature versus time and depth in the irradiated material.

III.1 Initial Trials

The first set of experiments were performed in open atmosphere, without the apparatus, and using single shot bursts. Austenitic stainless steel shim stock (0.005" or 0.125mm thick) was sprayed with graphite to increase the absorptivity of the surface. A 47 J/pulse (5 ms duration, 150 watts average power) beam was defocussed to determine the threshold intensity to deform the surface of these coupons. It was found that the fully focussed beam (0 mm defocus) simply drilled through the material. For successive pulses, the workpiece was moved progressively further out of focus, with respect to the beam. As the beam was defocussed, drilling continued until melting occurred with a melt diameter of about 5 mm. On later shots, as the beam was further defocussed, less melting occurred, and the plate was only thermally deformed (6.3 mm). Eventually, the beam was defocussed to the point where no damage could occur on the surface due to low intensity (beam diameter of about 10 mm).

Similar experiments were carried out on AISI 4140 coupons coated with graphite spray. In this case, a 5 ms pulse at 65 J/pulse was used to determine the damage threshold. A series of shots were undertaken, with the beam defocussed from a diameter of 2.8 mm to 8 mm. Up to 5.0 mm in diameter, the intensity was high enough to cause melting. Above 5.8

mm diameter, the intensity was low enough that the graphite was barely marked. The threshold for the transition from melting to no-observable-damage, was between 5.0 mm and 5.8 mm. These numbers were then used for calculations of thermal profiles.

III.2 Calculation of Thermal Profiles

Introduction

To assist in understanding the effect of firing on gun steel and the effect of the test sequence on coupons, the temperature versus time of the steel was evaluated, at the request of government scientific personnel. The basis is the calculation is similar to that considered for laser transformation hardening⁴. When the surface is irradiated by a sequence of pulses, it has been shown that the resulting temperature distribution can be found by superimposing single pulse solutions from the heat flow equations⁵. A "Basic" program was written to evaluate the equations describing the heat flow, with the output of the program in a form that could be drawn into a spreadsheet. The spreadsheet was used to prepare graphs showing the temperature variation as a function of depth.

Assumptions

The calculation performed here has a number of assumptions incorporated. These are as follows:

1. One dimensional heat flow is assumed; that is, the surface of a surface is irradiated, with subsequent cooling by conduction into the depth of the material. This is the case when there is uniform irradiation over a surface. If nonuniform irradiation occurs, the evaluation would be meaningful if the results are evaluated only for distances into the solid that are small with respect to the transverse scale of distance in which significant fluctuations in beam intensity occur. At greater distances, the results presented here would overestimate the temperature that would occur if three-dimensional heat conduction was taken into account.
2. A semi-infinite solid is assumed. Consequently the results are meaningful only if evaluated for time scales short compared for the time for the heat incident on one surface to be

conducted through to the back surface.

3. Thermal properties of AISI 4340 steel were not readily available. Data for AISI 4140 was used instead, but the difference of the properties for different grades of steels is not significant.

4. The calculation assumes that material parameters such as the specific heat and thermal conductivity are constant. In actual fact, the thermal conductivity of steels decreases with increasing temperature and the specific heat decreases⁶. This means a given amount of energy results in a smaller temperature increase at high temperature than at lower temperature, but that the energy is conducted more slowly in the bulk of the material. The calculations are performed using material parameters that are an average over the temperature range.

5. The calculation neglects the time dependence of the laser beam, but assumes a constant output during a time period which is one of the inputs to the program. For time periods long compared to the laser on time, this assumption has a negligible effect.

6. The calculation does not take into account vaporization or melting of the material. Motion of the molten pool can dramatically effect the heat transfer, but this is neglected in the calculation. The calculation loses accuracy if the melting temperature is increased.

7. Factors which influence the absorption of the beam into material are ignored. Thus pulse energies quoted in the results refer to the energy absorbed into the material, not the energy incident on the material.

Results

Figures 8 to 10 show the calculated temperature increase at the surface and at various distances under the surface for a metal irradiated with a burst of five pulses at 120 ppm. Each pulse is 50J spread over a diameter of 0.4 cm, in a 5 millisecond pulse. Figure 8 shows the temperature over a five second time period. Peak temperatures approaching but not quite reaching the melting point are reached, but after five seconds the temperature has decreased

to about 100 degrees (above ambient temperature). After a few seconds, there is a minimal temperature variation with depth, and in the rate of a temperature gradient the rate of heat conduction decreases. Figure 9 shows the temperature profile produced by the first pulse in the sequence, over the time period extending to the beginning of the second pulse.

Figure 10 shows the temperature dependence in the first 50 milliseconds following the first pulse. The shape of the temperature versus time curve at the surface is determined by the assumption of a constant energy flux during the laser on period of 5 millisecond; if a different pulse shape was assumed, the temperature versus time dependence in this time period would be somewhat modified, and more rounded. The curve is not dissimilar, however, to the recorded bore surface temperatures shown in Figure 2 of the Literature Survey in Phase I (pg. 18). Here a peak temperature of approximately 890°C was observed, four to five milliseconds after the temperature first started to decrease, and the surface temperature fell to approximately one quarter of its peak value after 50 milliseconds.

Comparison of simulation with first set of irradiation experiments

The initial set of experiments had been performed with single pulses from the Nd:YAG laser directed at a sample of 4140 steel coated with colloidal graphite. A number of shots were taken for given laser conditions (pulse energy and duration) with the beam moved with respect to the sample for each shot. The threshold for damaging the surface via surface melting was discovered in this way. The diameter of the beam at each location was found by observing the area from which the graphite was removed. In this way, it was found that 65J, 5 ms pulses partly focussed to a 5.0 mm diameter did not cause surface melting, but a beam focussed to a smaller diameter to 4.1 mm did. When 65J, 10 ms pulses were used, a beam for 4.2 mm diameter charred the graphite but did not melt the steel, but a beam of smaller diameter did melt the steel. In the latter case, the fluence (Energy per unit area) striking the surface is the same, but the peak intensity (Energy per unit time per unit area) is smaller by a factor of two.

Figure 11 shows the peak temperature reached for different depths underneath the

surface. The calculation, made with the various assumptions listed above, shows a 65 J pulse focussed to 0.41 cm produces a surface temperature approximately equal to the melting point, whereas pulses focussed to a smaller diameter cause the melting point to be exceeded. This is regarded as very satisfactory agreement with the experimental work, in view of the assumptions detailed above. In particular, the calculation assumes uniform irradiance with an intensity level of

$$65\text{J}/[5\text{ ms} * \pi (0.41\text{ cm})^2 / 4] = 10^5\text{ Watts/cm}^2.$$

In fact the intensity is a function of position and time, which when averaged over the duration of the pulse and its spatial extent would produce the above value. The peak value may be considerably in excess of this, however. Consequently, the fact that melting occurs at a beam radius value that the calculation says the melting point should be approached but not exceeded is not regarded as a significant discrepancy. Rather, the model is considered generally successful at predicting the behaviour.

The calculation shows when melting does not occur, the A3 temperature of the 4140 steel is exceeded for a depth of 50 to 100 μm into the material. Thus, careful polishing of samples which have not undergone surface melting would be required to show a heat affected area. This has not been performed to the current time.

III.3 Experimental Apparatus

Although the chamber could be pressurized to just over 760 torr with a carbon rich gas such as carbon dioxide, it was decided to use an open chamber to perform the thermal cycle experiments (Figure 12). Carbon was provided to the sample by spraying graphite on the surface after each burst of shots. A 300 mm focal length lens was used so that the lens-to-workpiece distance was great enough to avoid contamination of the lens (which would be likely if a 100 mm focal length lens was used). To further protect the lens, nitrogen gas was used coaxially with the beam to keep combustion products (vapor and smoke) away from the lens. The system is capable of pulsing over 2000 times, but a practical number of 50 shots was used for the experiments.

Originally, thermocouples were to be used to monitor temperature. Unfortunately, a thermocouple could not be used near the beam, as a direct hit from the beam would likely melt the leads due to the high instantaneous temperature. The best location would be a thermocouple drilled into the side of the coupon, just below the surface. The closest practical location would be about 1 mm below the surface of the coupon. Based on the cooling curves, it was determined that at 1 mm below the surface, the temperature would likely only increase by 220°C after 5 pulses at 50 J/pulse and 5 ms duration/pulse. This temperature would be reached after about 2 seconds, but after 5 seconds, would reach equilibrium at about 100°C. Due to the limited response time, and the lack of information that could be gathered on the actual surface temperature, no thermocouples were used.

III.4 Experimental Procedures

The firing rate of the Otto-Malera 76 mm gun was simulated. This gun is capable of firing at a rate of 120 rounds per minute, but with only 5 shot bursts separated by enough time to reach equilibrium. 120 rounds per minute corresponds to one shot every 0.5 seconds. If the frequency is set at 2 Hz (2 shots per second) and the shutter is opened for 2.5 seconds, there will be 5 shots at the correct rate of firing. According to the cooling curves, the surface (and material up to several mm below the surface) reaches equilibrium temperatures after about 5 seconds. A 10 second delay between bursts allows sufficient time for steady state temperatures to be reached.

First, the following conditions were chosen to be used for the experiments:

Frequency = 2 Hz

Pulse Duration = 5 ms

Energy = 45 J / pulse

An AISI 4340 coupon was painted flat black and single pulses were used to irradiate the surface. The beam was defocussed from 2 mm to 10 mm in diameter. Single pulses indicated that melting occurred up to about 5.4 mm. This defocus was chosen as the experimental defocus.

The surface was prepared by using one or more of the following conditions: a)coat with graphite; b)coat with vacuum oil; or c)uncoated. A single shot burst was allowed to irradiate the surface by opening the beam shutter for 0.5 seconds. In a new location on the sample block, the surface was irradiated by a burst of 5 shots by opening the shutter for 2.5 seconds. In a third location on the block, the surface was subjected to 10 bursts of 5 shots per burst, with a 10 second delay between. Graphite was reapplied to the surface between bursts, but not between individual pulses.

For most materials, three shots or pulse sequences were used. The first pulse sequence was a single laser pulse on the surface. The second pulse sequence was (usually) a series of five pulses at 120 ppm. Occasionally, six rather than five pulses may have occurred. The third pulse sequence was ten series of five (occasionally six) individual shots, with each series of shots separated by 10 seconds. Each of these sequences was applied to each of the samples. Most samples, as indicated, were DAG coated before irradiation and recoated between sequences of pulses. The DAG was cleaned off before the samples were examined.

The following sample materials were tested using this technique:

Sample	Base Material	Metal Coating	Surface Prep.
1	A36 Boiler Plate	Stellite 6	Graphite (DAG)
2	A36 Boiler Plate	-----	Uncoated
3	A36 Boiler Plate	-----	Graphite
4	AISI 4140	-----	Uncoated
5	AISI 4340	-----	Uncoated
6	AISI 4340	-----	Vacuum Oil
7	AISI 4340	-----	Graphite
8	AISI 4340	-----	Graphite
9	Titanium	-----	Graphite
10	Titanium	90Ta-10W	Graphite
11	Titanium	90Ta-10W	Graphite
12	AISI 4340	Ti	Graphite
13	Ti on AISI4340	90Ta-10W	Graphite

III.5 Experimental Results and Observations

Sample 1: DAG coated Stellite samples.

Examination before cleaning DAG:

First shot: physically smooth, signs of interpass cladding have disappeared

Second shot: The surface is roughened and pitted

Third shot: The surface has melted to the point that beading has occurred.

Examination after cleaning DAG off the surface:

First shot: The surface is much smoother than before the irradiation, with both lines due to

successive passes and the solidification lines having disappeared. The bulk of the region is a dark, matte grey colour, but part of it is silvery grey. There was an extensive network of fine cracks through both regions, seeming to originate at a number of points from which the cracks spread out.

Second shot: The surface was very rough, with relatively smooth and featureless areas interspersed with deep pits and grooves. Cracks extended through the smooth areas.

Third shot: The melted area now consisted of relatively large (half to one millimetre) beads that were relatively smooth but had a fine texture to the surface. The beads were separated by pits and grooves. Whereas the top of the beads appeared shiny, the grooves appeared dull. The number of cracks had dramatically decreased.

Sample 2: Uncoated boiler plate (A36)

First shot: Machining marks are still visible. The material was discoloured with a mottled pattern of different shades of blue, with patches of brown. There was no sign of surface melting.

Second shot: The centre part of the irradiated region was a silvery blue colour, surrounded by a region that was dark grey. Machining marks were visible through the majority of the region. There were however three region of diameter 0.2 mm with a shiny melt bead, surrounded by a ring shaped area of outside diameter 0.4 to 0.8 mm. The ring was brownish and appeared to be depressed below the surface. There were also some smaller melt beads.

Third shot: The area of most intense irradiation had melted and formed a large bead. This was surrounded by an area which had melted but the various small melt areas had not joined to form a large bead. No cracks were found.

Sample 3: DAG coated boiler plate (A36)

First shot: The most intense portion of the irradiated region had turned brown. It was largely a textured surface in which the machining marks were not visible, but there was irregularly shaped spots of dimensions roughly 0.1 to 0.5 millimetres that had a smooth textured surface.

Second shot: The irradiated region was brown, but the machining marks were still visible. There was a patch of blue surface, with small brown inclusions, in which the machining marks were not visible, and a patch with two different shades of light brown with no

machining marks visible. These regions had a smooth surface texture, and it was thought that melting had taken place. No cracking was visible.

Third shot: The irradiated region was brown in colour. It appeared to be depressed and smooth textured in the region of most intense irradiation, and raised and coarse textured at the periphery. Some microcracks in the melt, perhaps indicative of carbon being absorbed into the melt, and subsequent embrittlement.

Sample 4: Uncoated 4140

First shot: Extensive discoloration; the surface was cleaned by the shot. The spot where the laser hit is a lighter shade of grey than the surrounding area, with a tinge of brown on the fringe.

Second shot: Extensive discoloration; the most intensely irradiated area has turned blue; this is surrounded by a brown fringe. There are perhaps small areas (0.2 mm diameter) of localized melting.

Third shot: Melting and beading had occurred over the most intensely irradiated area, perhaps 1/5 of the irradiated area. A 38°C Templestik applied immediately (<1/2 second) after the end of the laser pulse did not melt.

Sample 5: Uncoated 4340

First shot: Machining marks are still visible. The material was discoloured with a mottled pattern of different shades of blue, with patches of brown. There was two regions of approximately 1/2 mm in size in which localized melting had taken place. There was another region about 1/10 mm in size surrounded by a darker area of blue, with a number of very minor cracks extending away.

Second shot: The area of greatest intensity was a variety of shades of light brown. It was surrounded by a blue area of extent 0.1 mm, with the rest of the irradiated area being a greyish brown colour. No microcracks were visible. The machining marks had disappeared from the central brownish area.

Third shot: The majority of the laser irradiated area had melted and was blackened. there was two types of blackened surface, however, one being glossy and the other matte.

Sample 6: Oil coated 4340

First shot: No physical change to the material, machining marks are still intact. Perhaps very minor regions of melting on top of the machining marks. The oil was apparently cleaned off by the shot.

Second shot: Discoloration. An area of light brown which is smooth; the machining marks have disappeared indicating melting had taken place. This is surrounded by a darker brown area in which machining marks are still visible, but there appears to be small glassy patches.

Third shot: Extensive melting and beading over a shape similar to that discoloured in the second shot. Very small cracking at edge of melt.

Sample 7: DAG coated 4340 #1.

First shot: After the DAG had been removed, the majority of the area that had been laser irradiated appeared black (but shiny with the incident light irradiation through the stereomicroscope). With higher power examination through the stereomicroscope, the shiny area consisted of shiny melt pools interspersed with the machining marks. In the centre, the machining marks had disappeared with the formation of larger melt pools.

Second shot: Surprisingly, this irradiated area was less obvious than the area that had seen only a single laser pulse. There was very small ($\approx 1/20$ mm) regions of localized melting over part of the irradiated area.

Third shot: The machining marks had disappeared from about half of the laser irradiated area, and replaced with a flat melt pool. In spite of the melting, no substantial beading had taken place.

Sample 8: DAG Coated 4340 #2

First shot: The irradiated region is visible on the surface as a minor change in texture; the surface of the steel is a slightly shinier silver colour than the surrounding area. Machining marks are still clearly visible. The stereomicroscope examination showed areas of melt interspersed with the machining marks.

Second shot: The irradiated region appears visually black, with a brownish central region. The area of greatest intensity was a variety of shades of light brown. The rest of the irradiated

area was a greyish brown colour. No microcracks were visible. The machining marks had disappeared from the central brownish area.

Third shot: The majority of the irradiated region was melted. Some of the melted region was shiny and silvery, but other areas were mottled and brownish. Around the melted region, there was a blackened region of width ≈ 0.2 mm which appeared pebbled. The machining marks were still visible in this region, but under high magnification there was a finer sets of marks interrupting the surface. This area was not removed by repeated washing and did not flake off when scraped with a screwdriver with sufficient force to mark the surrounding metal.

Sample 9: DAG Coated Titanium

First shot: the whole of the irradiated region had changed colour, being a much darker grey than the untreated titanium. A centre portion had turned black, with some grey circles remaining, and had a smoother texture than either the untreated region or the darkened grey region. Yet another region, approximately 1.5×0.5 mm, was a lighter grey colour and had a smoother surface texture. Second shot: The whole of the irradiated region was very dark grey, but the centre portion, perhaps 20% of the overall area, was gold coloured. The gold colour is typical of Titanium nitride, indicating that perhaps the first shot in the sequence removed the graphite coating and subsequent shots heated the surface causing it to react with the surrounding air. Laser induced nitriding of titanium is a phenomenon described in the technical literature, and some previous work on this has been conducted at The Laser Institute.

Third shot: As before, the whole of the irradiated region was a dark grey, but the centre portion appeared like gravel, with particles perhaps $1/20$ mm in size imbedded in a smoother background.

Sample 10: Tantalum-Tungsten on C.P. Titanium, DAG Coated

First and Second shot: Before the DAG was removed, a visual examination showed that the area of irradiation was barely visible, indicating a very minor change in the texture of the surface. Under the stereomicroscope, however, the areas of irradiation could not be identified. After the DAG was removed by soaking in acetone, the irradiated area was visible because all but the largest globules of metal had become blackened and rough on the surface, whereas the

samples unirradiated globules remained shiny. On the second shot, the centre of the irradiated region had turned brown.

Third shot: The coarse structure typical of the clad tantalum had become much finer and with considerably fewer peaks and dips, although the surface was not smooth. It appeared "gravelly", with lumps about 1/20 mm in size scattered over the surface, similar to the surface of laser irradiated Titanium. No cracks were visible.

Sixth shot (100 laser pulses): Generally similar to the third, but the centre of the irradiated region was now brown. There was a series of microcracks on the outer fringes of the irradiated region.

Sample 11: Tantalum-Tungsten on Titanium, partly smoothed by grinding and coated with DAG before irradiation

The surface had areas where it had been made flat by the grinding operation. This had deep irregularly-shaped pits of dimension 0.2 to 1 mm scattered through it, which had been too deep to be removed by the grinding.

First shot: The ground area was darker grey colour where it had been irradiated. the centre portion was a brownish colour. There was no cracking.

Second shot: Similar, but here the most intensely irradiated region had splotches of a grey-brown colour and splotches of blue.

Third shot: Similar, but here the brown was paler and the blue less prominent. The surface at the bottom of the pits had also turned brown. Small areas that appeared shiny where the tantalum appeared to have melted.

Fourth shot (100 laser pulses): small areas that appeared shiny under the stereomicroscope where it appeared that the tantalum melted.

Fifth shot (250 laser pulses): Somewhat larger areas where the tantalum appeared to have melted. No cracks were visible.

Sample 12: Titanium on 4340, Coated with DAG

First shot: The region where the greatest intensity was incident on the sample had a considerable change in surface texture prior to the irradiation. It was considerably smoother,

but less glossy and had occasional pits of diameter 0.1 to 0.3 mm. There were a number of cracks in the surface, greater than the number in the as clad surface. A stereomicroscope photograph was taken, but it failed to clearly show the cracks.

Second shot: The irradiated region was covered with a network of cracks, and was coloured deep blue, light brown, and dark brown. Regions of the different colours frequently had cracks on the edge, so there was a sharp rather than a gradual transition from one colour to the next. As before, there were pits in the surface.

Third shot: The surface was now largely dark brown, and was very rough with projections extending from the surface. The region was crack free except near the perimeter. There was a region that looked like a solidified bead, and another region that looked gravelly.

Sample 13: Tantalum-Tungsten on Titanium on 4340, DAG Coated

First shot: The laser irradiated region was a dirty grey colour, with one splotch of burgundy and blue. There were frequent cracks in the clad portion, and occasional cracks in the bottom of the pits. The texture of the clad portion seemed smoother than that in the unirradiated region.

Second shot: The laser irradiated region was largely a charcoal grey colour. There was one patch of burgundy, and one region of 0.7 x 0.9 mm had a shiny black featureless surface. The charcoal grey area seemed smoother than the surrounding unirradiated region, and was crack

free although there were cracks on its periphery.

Third shot: This region was approximately half the dirty grey colour and half the charcoal grey colour, and had a number of pits. Some regions (of both colours) had a smooth texture and were crack free, although the remainder of the area had a number of cracks.

IV. Recommendations

Laser Weld Overlaying Titanium

The coatings appeared to be relatively smooth and contamination-free. Future work should include measuring the dilution of the coating in order to reduce Fe-Ti intermetallic formation, and measurement of the amount of oxygen and nitrogen in the coatings. Flowability of the melt pool was good enough to create a continuous coating, but it is possible that either powder injection or wire injection may produce even better quality coatings with minimal dilution. A system would have to be designed to provide the material injection inside the chamber.

Tantalum-Tungsten Alloy

This material is not commonly weld overlayed due to its high reactivity with oxygen and nitrogen at relatively low temperatures. With the system constructed during this contract, a layer of tantalum was created which was metallurgically bonded over portions of the coating. A much more in-depth study needs to be done with this material. Due to the poor flowability of the molten material, and the precise heat input required to allow melting of the alloy and not the base material, it is possible that pre-placed powder is not the best method for applying the alloy. As with the titanium, a fine wire (0.25 mm diameter) injection of powder may produce better coatings.

This material can also be roll-bonded or explosion weld-bonded. In a future study, the merits of using these techniques versus laser weld overlaying should be addressed.

Thermal Cycle Testing

It is safe to say that this project has only scratched the surface of the capability of using lasers for simulation the thermal, mechanical, and chemical interactions inside a gun barrel. In this experiment, only thermal effects were addressed. The thermal testing was limited to 10 cycles (and in a few cases 20 or 50 cycles). A future study should look at causing surface damage/melting after about 2000 pulses (400 cycles) on AISI 4340. The damage should then be qualified and quantified. The parameters used for this should be used on a variety of materials with the same surface finish. To start with, a comparison of as-rolled materials with similar compositions to the potential coatings could be used. This would ensure that a similar surface finish would be used for all materials. Any coatings would have to be continuous and as defect-free as possible. The number of cycles required to cause the same amount of damage (possibly measured with a surface roughness tester) should be counted, and a comparison chart could be made up. The same experiments could be repeated for a variety of between-burst coatings (such as graphite, oil, or acetone) that might simulate the chemical effects inside a gun barrel.

It was determined that for the scope of this project, the simulation of mechanical damage through the use of a laser-induced shock wave could not be addressed. It is possible that this may be pursued.

The actual temperatures being reached at the surface should be monitored and recorded on computer. Thermocouples may not give enough information, as they could not be placed in the path of the beam, and so must be installed just below the surface. The temperature modelling done during this project indicated that the temperatures even at 0.5 mm below the surface would only be a fraction of the peak surface temperatures. A calibrated infrared pyrometer with a fast response time (0.05ms) could be used, but would have to be connected to either a computer or a recording oscilloscope.

V. Conclusions

1. A chamber was modified and found to be useful for both laser weld overlaying of coatings, and thermal cycle testing with a pulsed Nd:YAG laser. The laser beam passed through a BK7 glass window onto a sample mounted on a motorized stage inside the chamber. A vacuum could be used to remove/reduce the air pressure and either inert or other gases could be used to backfill the chamber.
2. Laser melting of titanium coupons indicated that the chamber could provide an extremely inert atmosphere. Laser melted scans in an evacuated, then argon backfilled chamber were silverish in color, indicating a low level of contamination of oxygen and nitrogen. Scans done without the argon atmosphere gave off a plume of smoke and combustion products, and the scans were white in color, likely indicating the presence of titanium oxides/sub-oxides.
3. A 0.005" thick layer of titanium could be weld overlayed on AISI 4340 steel using 0.010" of preplaced powder, 1 ms pulses at a frequency of 50 Hz, an energy of 7.5 J/pulse, and a speed of 5 ipm. This could not previously have been done without the chamber, due to contamination from inadequate gas shielding. The coating appeared relatively smooth.
4. A 0.010" thick layer of 90tantalum-10tungsten alloy could be weld overlayed on commercially pure titanium using 0.010" of preplaced powder, 1 ms pulses at a frequency of 50 Hz, an energy of 7.5 J/pulse, and a speed of 10 ipm. Although the coating was non-continuous due to incomplete melting, there may be promise for laser weld overlaying this difficult to weld material using laser energy.
5. Using a 0.005" thick laser weld overlayed layer of titanium as an interlayer, the 90Ta-10W alloy was also laser weld overlayed on AISI4340 using the same parameters. The coating was also non-continuous and in some cases contained lack of fusion. However, some portions of the coating appeared to be intact.
6. The action of a 120 rounds/minute, 5 burst pattern gun barrel was simulated using laser thermal cycling. Possible chemical effects inside the barrel from combustion products of the charge were simulated by using a graphite spray on the surface of the material. Using 45 J/pulse, 2 pulses per second, and burst of 5 pulses/cycle, obvious melting and deformation of the surface of AISI 4340 occurred after 10 cycles (50 shots).
7. The same burst pattern was used to test A36 mild steel, AISI 4140, commercially pure titanium, A36 laser weld overlayed with Stellite 6, AISI 4340 laser weld overlayed with titanium, commercially pure titanium laser weld overlayed with tantalum-tungsten alloy, and AISI 4340 laser weld overlayed with tantalum-tungsten alloy (with a laser weld overlayed titanium interlayer). After 10 rounds (while coating with graphite between bursts), the tantalum-tungsten alloy coatings appeared to have the least amount of deformation due to melting, while the A36 contained the most damage.

8. Without the use of graphite or any other coating, the damage/melting was minimized, likely due to the reflection of the surfaces without the aid of the dark graphite to help laser absorption.

9. AISI 4340 coated with vacuum oil (light hydrocarbon) appeared to have more carbon on the surface of the coupons than the graphite coated coupons.

10. This system could be used to thermally fatigue a variety of materials and could be used to simulate well over 2000 rounds.

VI. References

1. *Laser Cladding for Surface Protection*, J.A. Hewitt and V.E. Merchant, presented at The 2nd CF/CRAD Meeting on Naval Applications of Materials Technology, Halifax, Nova Scotia, May 2-4th, 1995.
2. *Laser Welding of Nickel Electroplate onto Zr-2.5%Nb Pressure Tubes*, K.H. Magee and V.E. Merchant, Laser Applications for Improved CANDU Reactors, COG-90-53, Ed. by K.F. Amouzouvi, pg. 25-28 (Whiteshell Laboratories, Atomic Energy of Canada Ltd, 1991).
3. *The Applications and Technology of Laser Weld Overlaying*, K.H. Magee, DREA CR/92/419.
4. *Laser Surface Transformation Hardening*, O. Sandven, in Metals Handbook, Ninth Edition, Volume 4 Heat Treating (American Society of Metals, Metals Park Ohio, 1981)
5. White, R.M., J. Appl. Phys. **34**, 2123 and 3559 (1963)
6. Metals Handbook, Ninth Edition, Volume 1, Properties and Selection: Irons and Steel (American Society of Metals, Metals Park Ohio, 1978), pg 148

Appendix: Figures

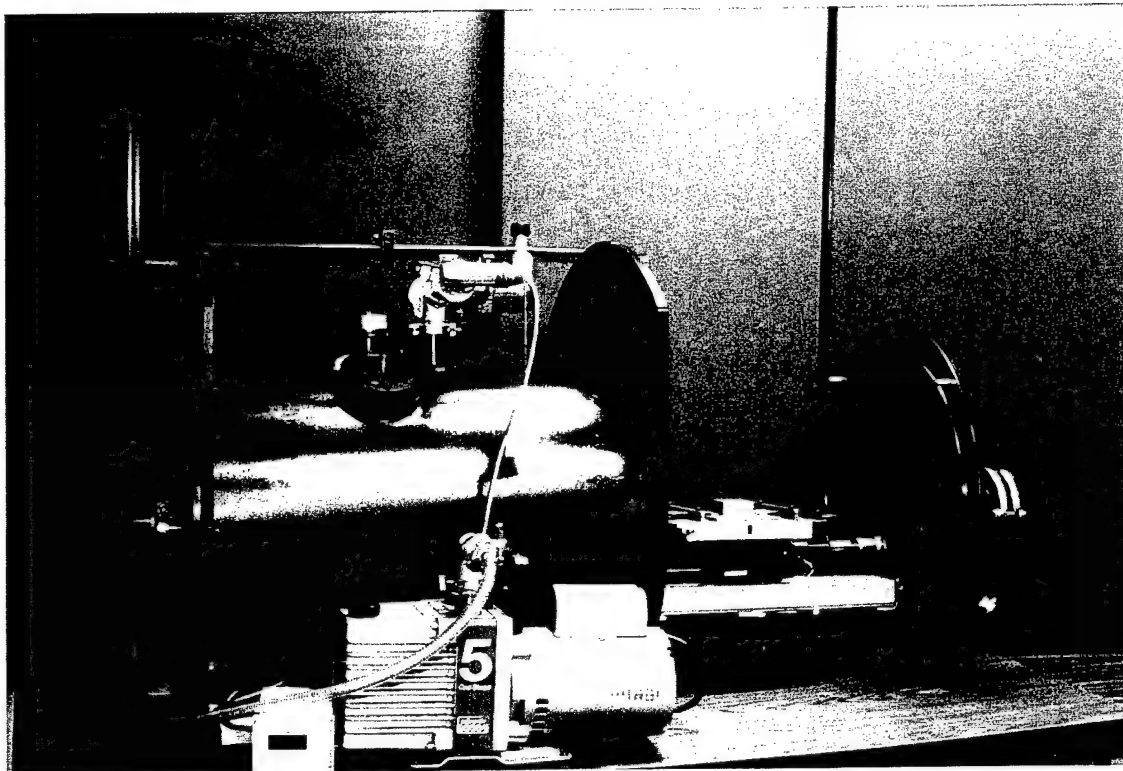


Figure 1: Chamber used for laser weld overlaying materials can be evacuated and back filled with an inert gas, such as argon. Inside is a motorized, linear stage.


April 1, 1996

p. 2 of 2
retr 0.9035

CERTIFICATE OF ANALYSIS

Product: Titanium Metal Powder
Grade: K-020-1050
Lot number: sl 455
Quantity shipped: 5 kgs
Customer: Alloy Sales - Edmonton
Purchase Order: E5028

Iron (Fe)	0.07 %
Oxygen (O2)	0.32 %
Nitrogen (N2)	0.02 %
Specific gravity	4.54 g/cm ³
App density	21.3 g/in ³
Screen analysis:	
+ 80 mesh	trace
80/100 mesh	0.1 %
100/200 mesh	36.6 %
200/325 mesh	26.3 %
-325 mesh	37.0 %


Josef Otto
Quality Engineer

We hereby certify that all materials used in the manufacturing of the product identified above conform to the Kennametal metallurgical and manufacturing specifications.

Kennametal Inc. does not guarantee merchantability, performance, or fitness for any particular purpose or use, nor does Kennametal Inc. accept the responsibility for any failure due to misuse or improper application of this product, or for any incidental or consequential damages arising out of the use of this product.

Figure 2: Datasheet for titanium powder used for laser weld overlaying.



Abnahmeprüfzeugnis 3.1.B
Inspection Certificate 3.1.B

gemäß EN 10204

Datum/Date 20.9.94

H.C. Starck GmbH & Co. KG

Inspection 2540
D 38615 Goslar
Reaktion 0 53 247 51-0

Kunde/Customer

Laser Institute

Produkt/Product

Amperit 990.003

Ta + W 90/10

Blend, -45/+10

Ihre Bestell-Nr./Your Order No. Dated

PO # 003702

Unsere Auftrags-Nr./Our Order No

Liefermenge/Quantity Delivered
5 lbs.

Lot-Nr./Lot No.
PRQ(-325)A.C
10051/96

Analysenergebnisse/Analytical Results

Analysenergebnisse nach vorschriftsmäßiger Probenahme und Prüfung/Analytical results by specified sampling and testing

Chemical	Ta	W
	PQR (-325)A.C	10051/96
Al	< 10 ppm	< 10 ppm
Ca	< 2 ppm	< 10 ppm
Cr	< 5 ppm	< 20 ppm
Cu	< 5 ppm	< 5 ppm
Fe	< 5 ppm	< 80 ppm
Ni	< 5 ppm	< 10 ppm
O	1070 ppm	220 ppm
N	42 ppm	< 10 ppm
C	9 ppm	< 10 ppm
W	< 40 ppm	Balance
Ta	Balance	n.a.

Microtrac I:

10 %	= 8.21 µm
50 %	= 19.93 µm
90 %	= 60.55 µm

Alpine Air Jet Screening

+45 µm	= 0.4%
-45/+10 µm	= 98.5%
-10 µm	= 1.1%

Bemerkungen/Remarks

Always mix well before using.

H.C. Starck GmbH & Co. KG

H.C. Starck gehört zur Bayer-Gruppe
H.C. Starck is an affiliate of Bayer AG, Germany.

Figure 3: Datasheet for tantalum-tungsten alloy used for laser weld overlaying.

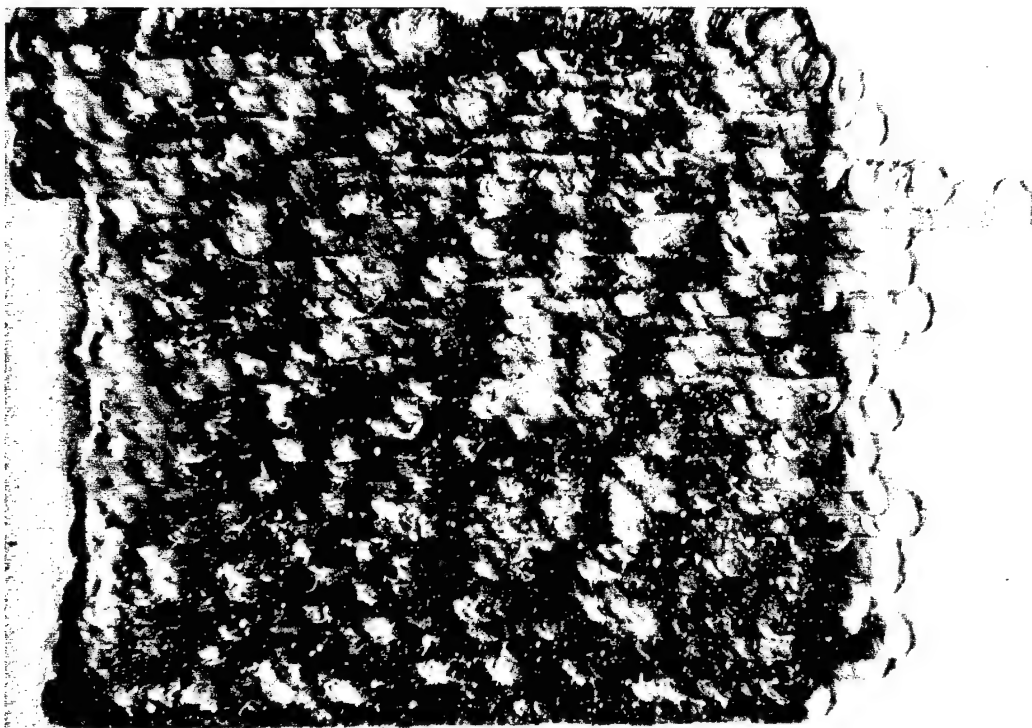


Figure 4: Photo of surface of AISI 4340 laser overlay in the chamber with 0.010" of titanium.

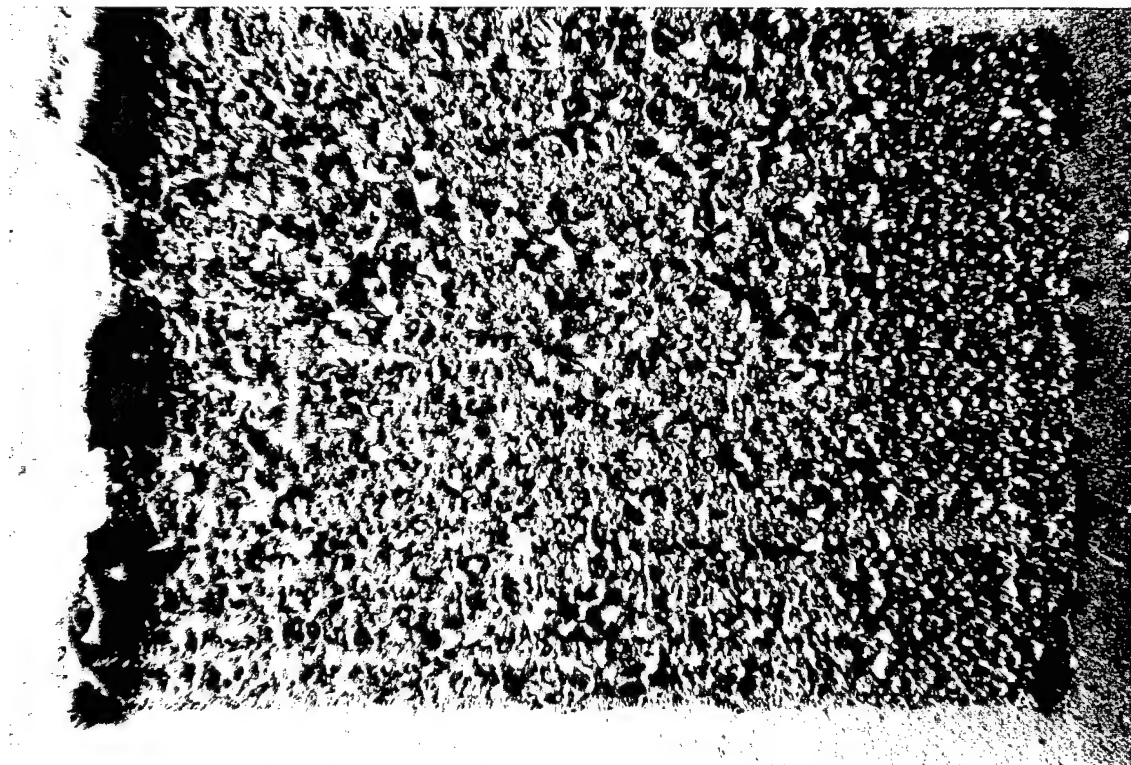


Figure 5: Photo of c.p. Ti laser weld overlayed with 90Ta-10W alloy.

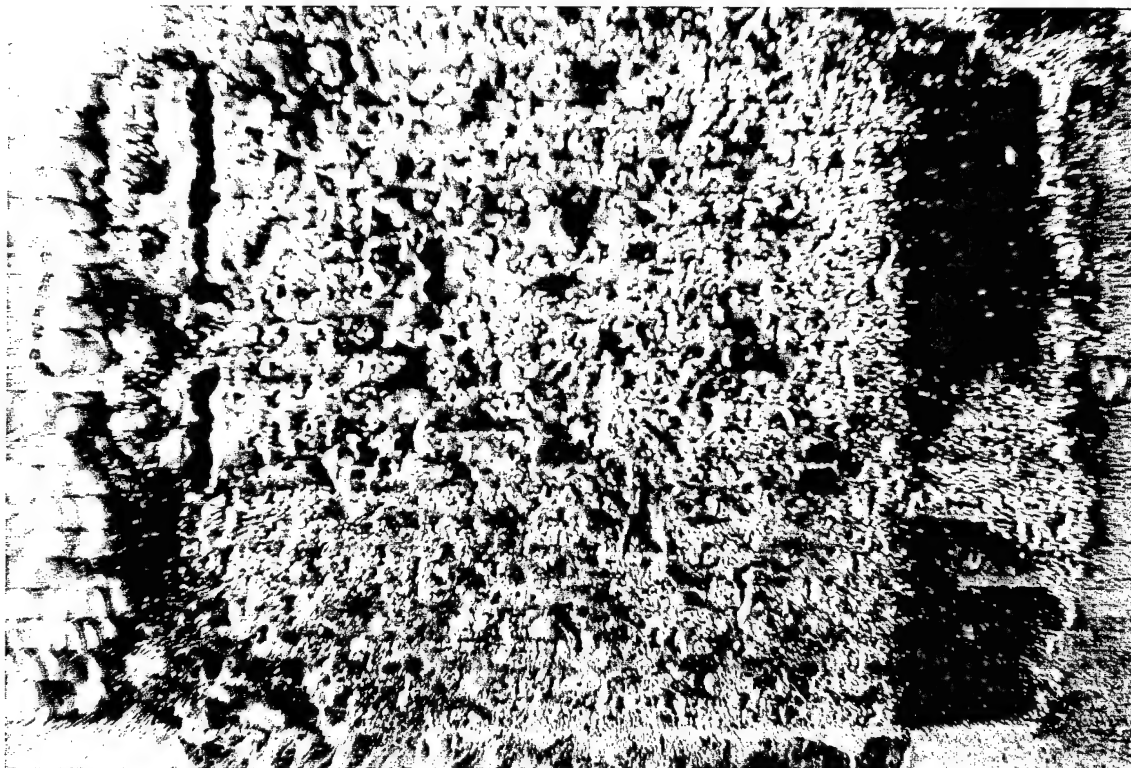


Figure 6: Photo of 90Ta-10W alloy laser weld overlayed on a layer of Ti which in turn had been laser weld overlayed on AISI 4340.

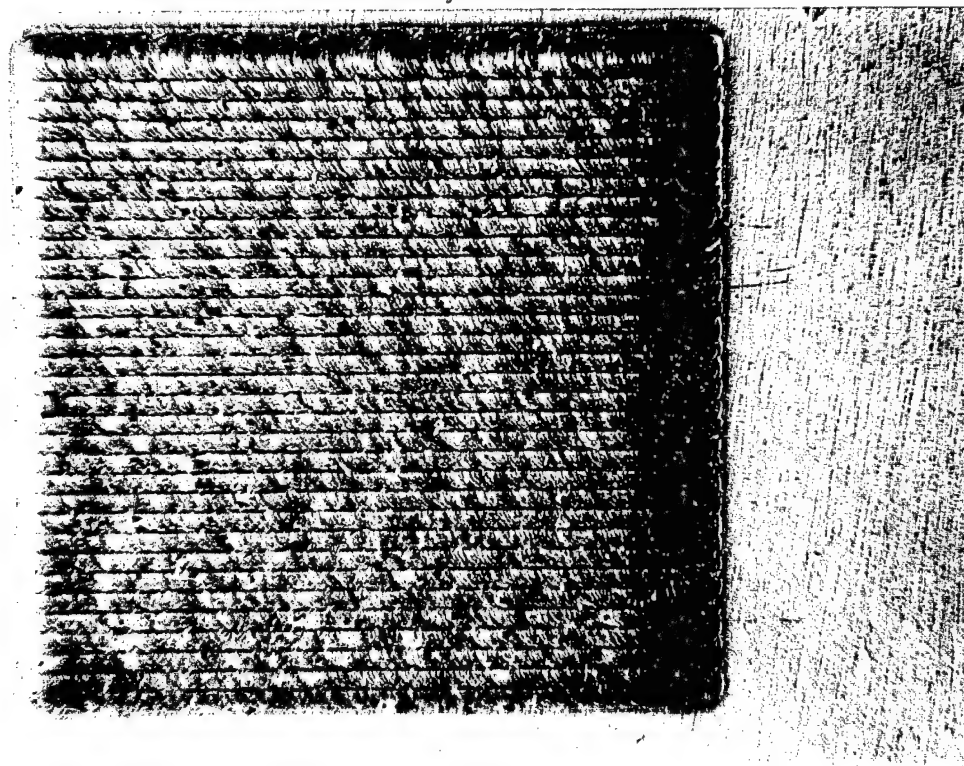


Figure 7: Stellite 6 laser weld overlayed on A36 steel.

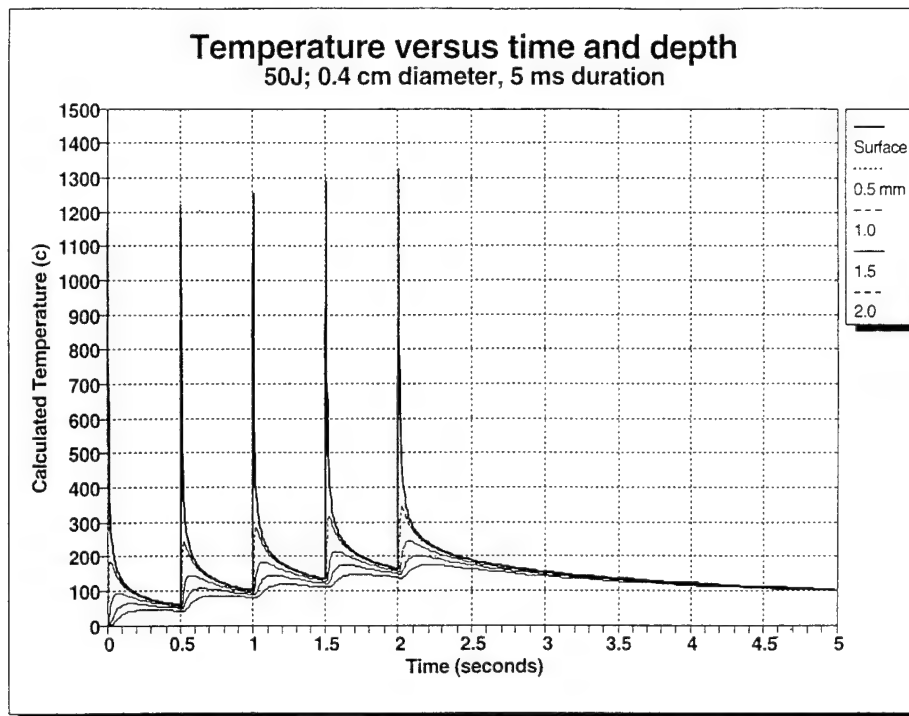


Figure 8: Temperature versus time and depth in AISI4140 irradiated with a burst of 5 pulses (5 second period - all 5 pulses).

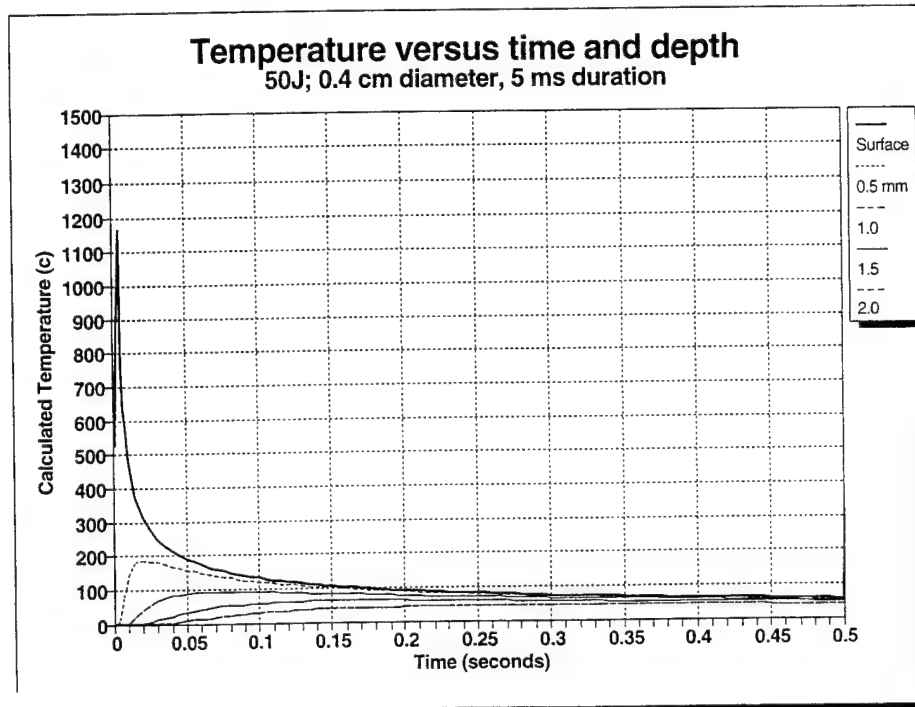


Figure 9: Temperature versus time and depth in AISI4140 irradiated with a burst of 5 pulses (0.5 second period - 1 pulse).

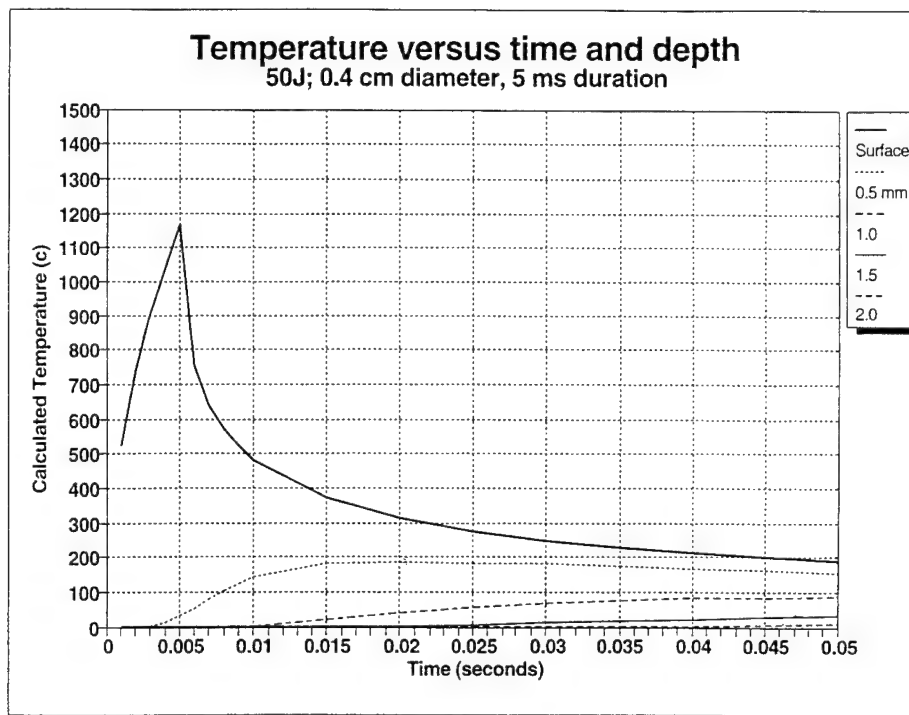


Figure 10: Temperature versus time and depth in AISI4140 irradiated with a burst of 5 pulses (0.05 second period - portion of 1 pulse).

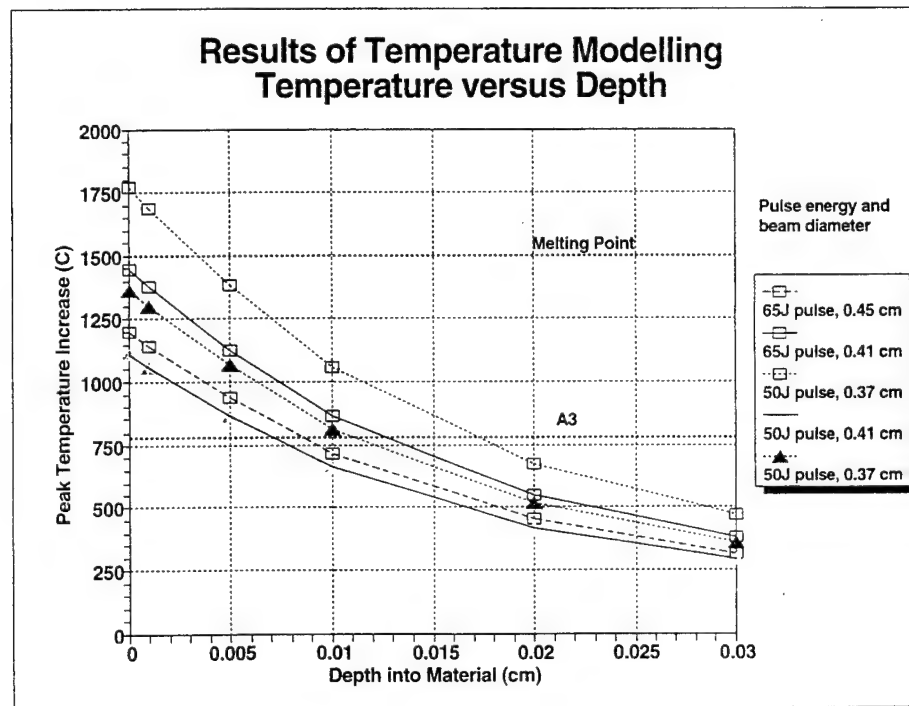


Figure 11: Temperature modelling using various heat inputs and beam diameters.

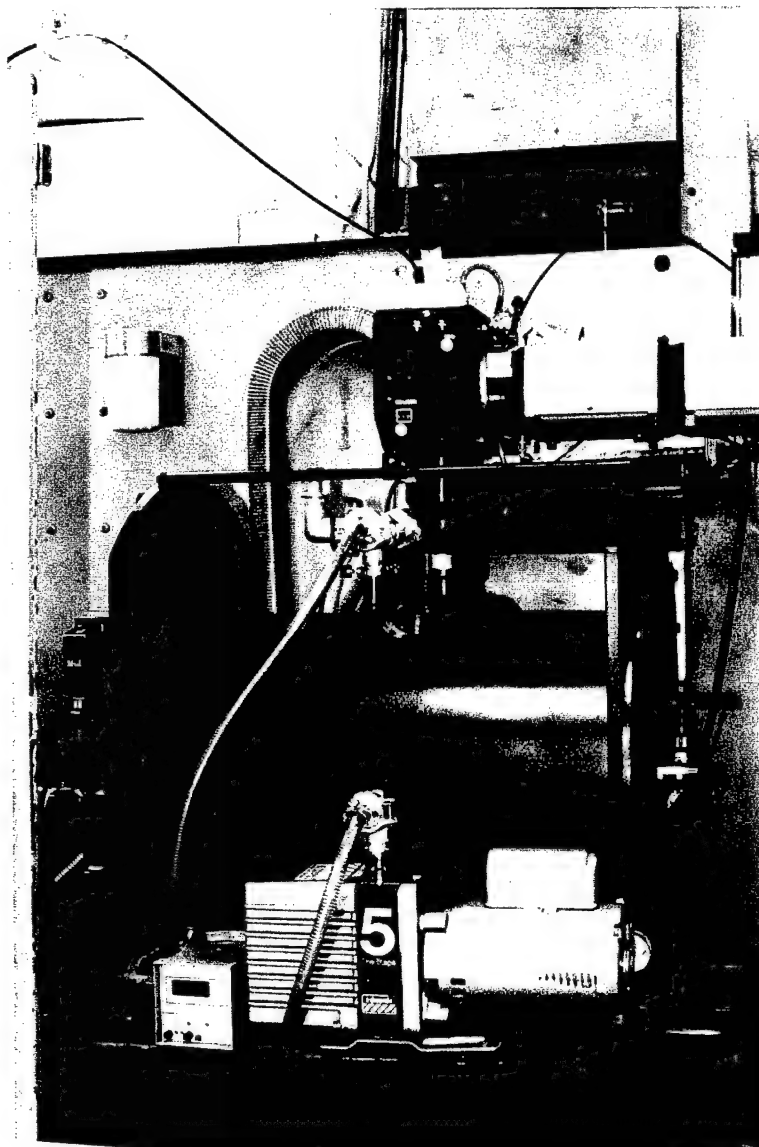


Figure 12: Chamber set up for thermal cycle testing.

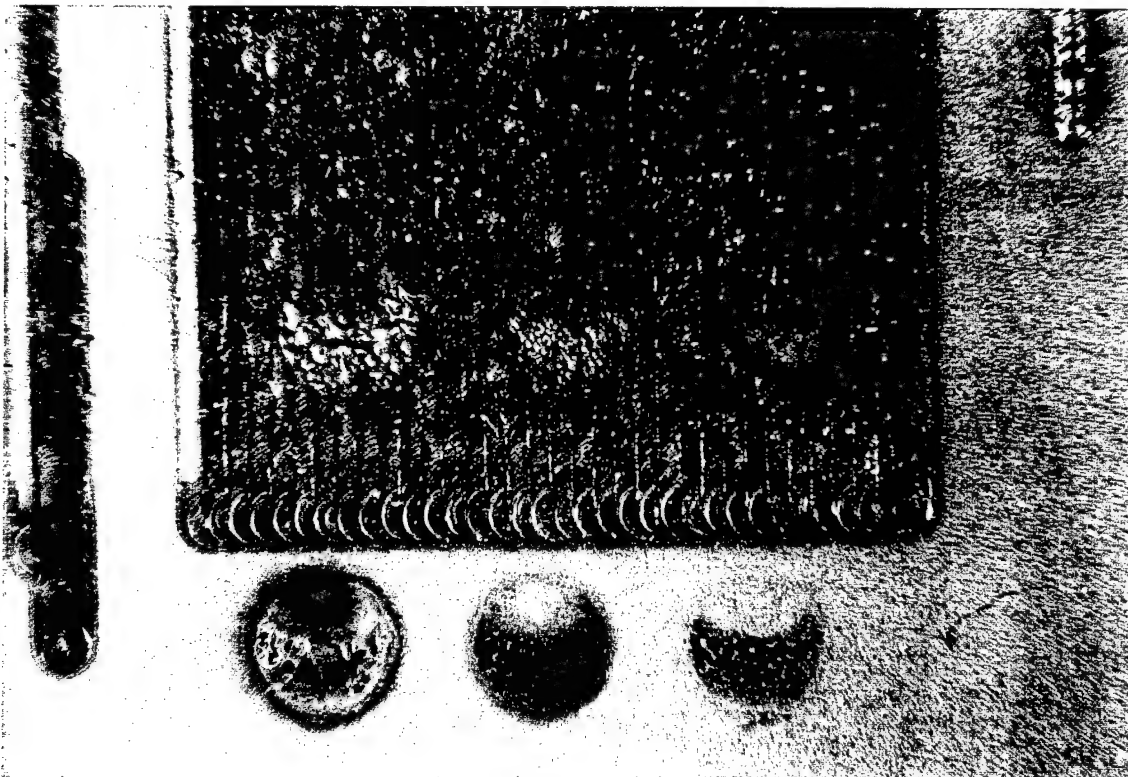


Figure 13: Stellite 6 on A36 mild steel. Hit with 1 pulse, 5 pulses, and 50 pulses on both the Stellite 6 and the A36 Graphite coated before thermal cycle testing.

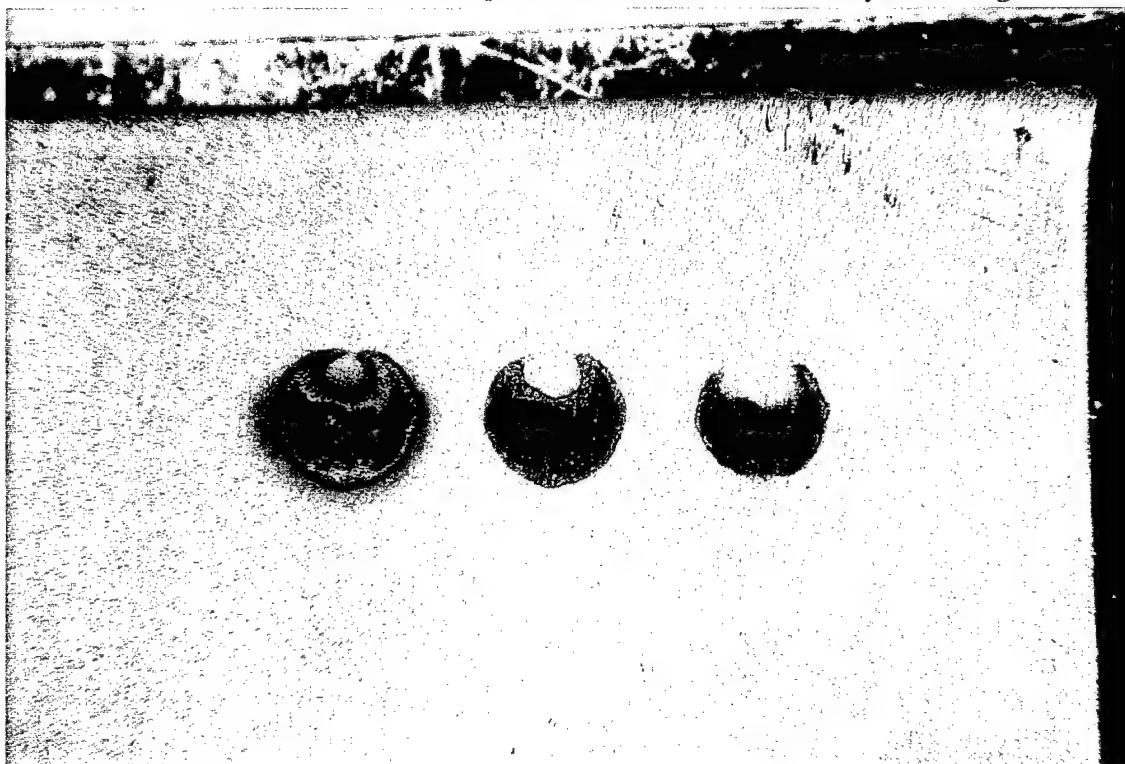


Figure 14: A36 mild steel hit with 1 pulse, 5 pulses, and 50 pulses and not coated before thermal cycle testing.

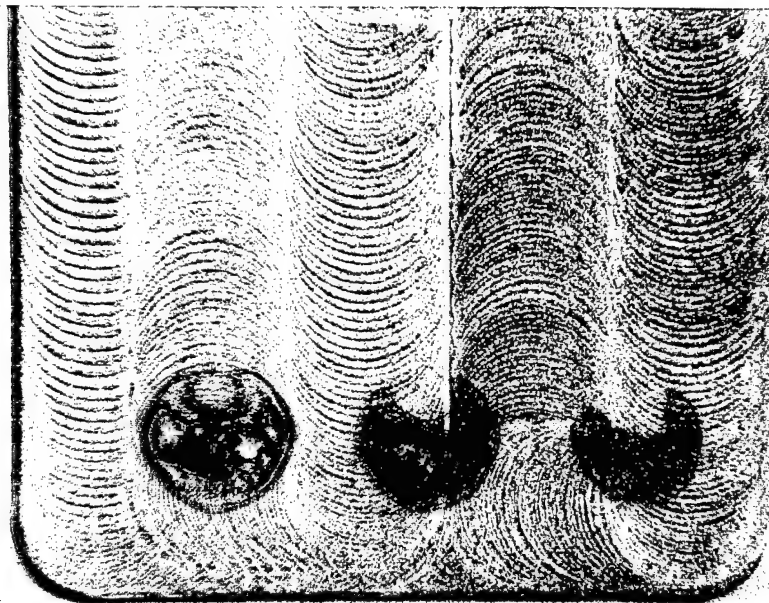


Figure 15: AISI 4340 uncoated before thermal cycle testing.

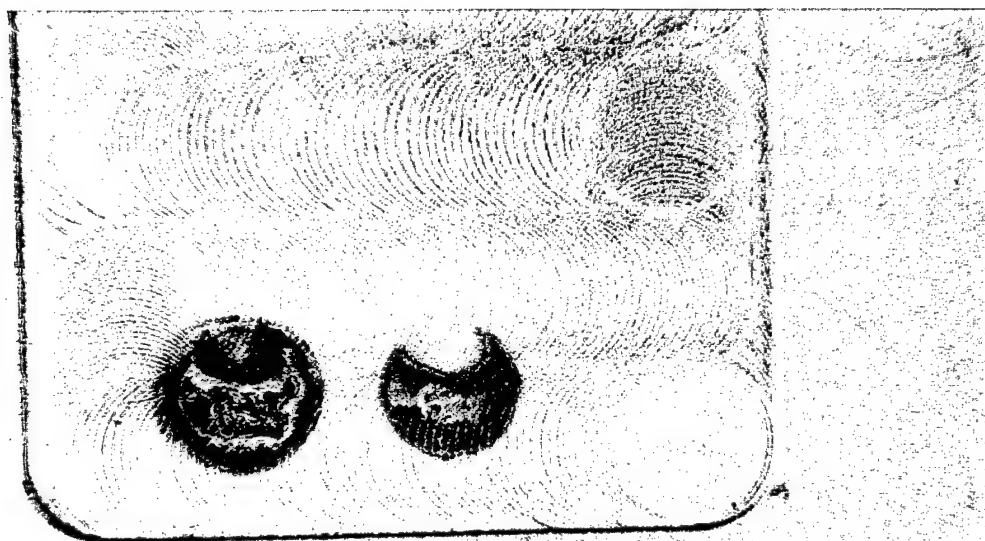


Figure 16: AISI 4340 coated with vacuum oil before thermal cycle testing.

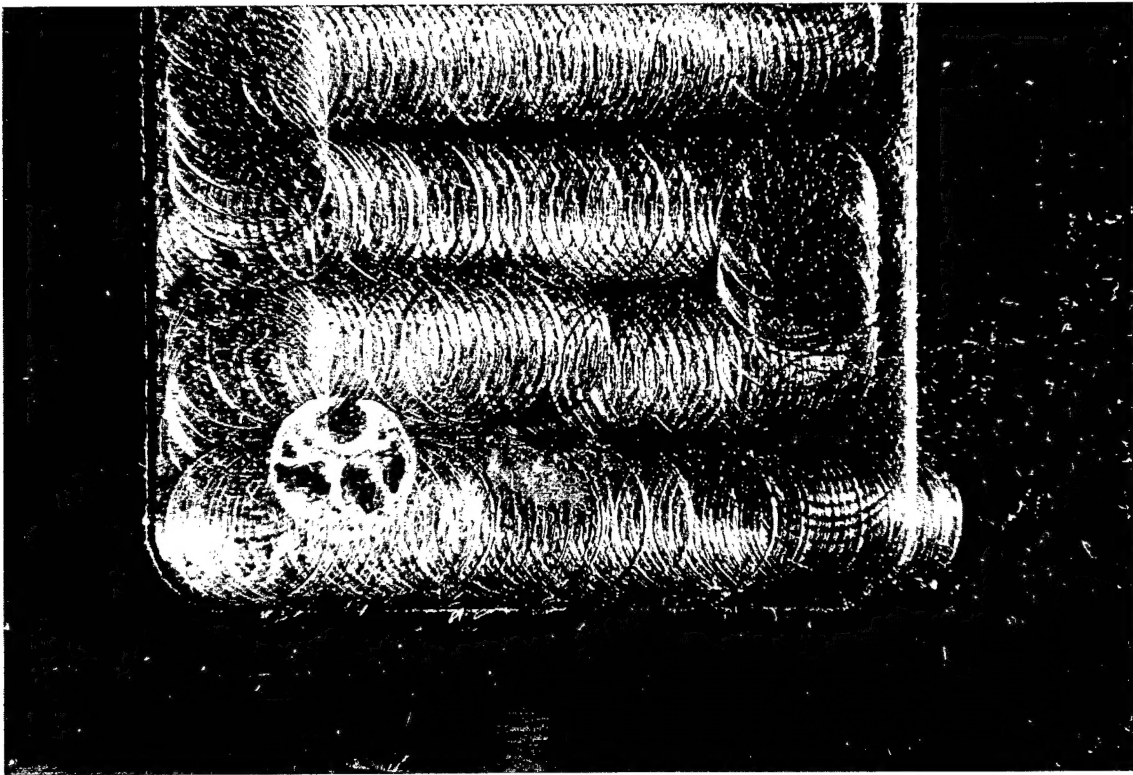


Figure 17: AISI 4340 coated with graphite before thermal cycle testing.

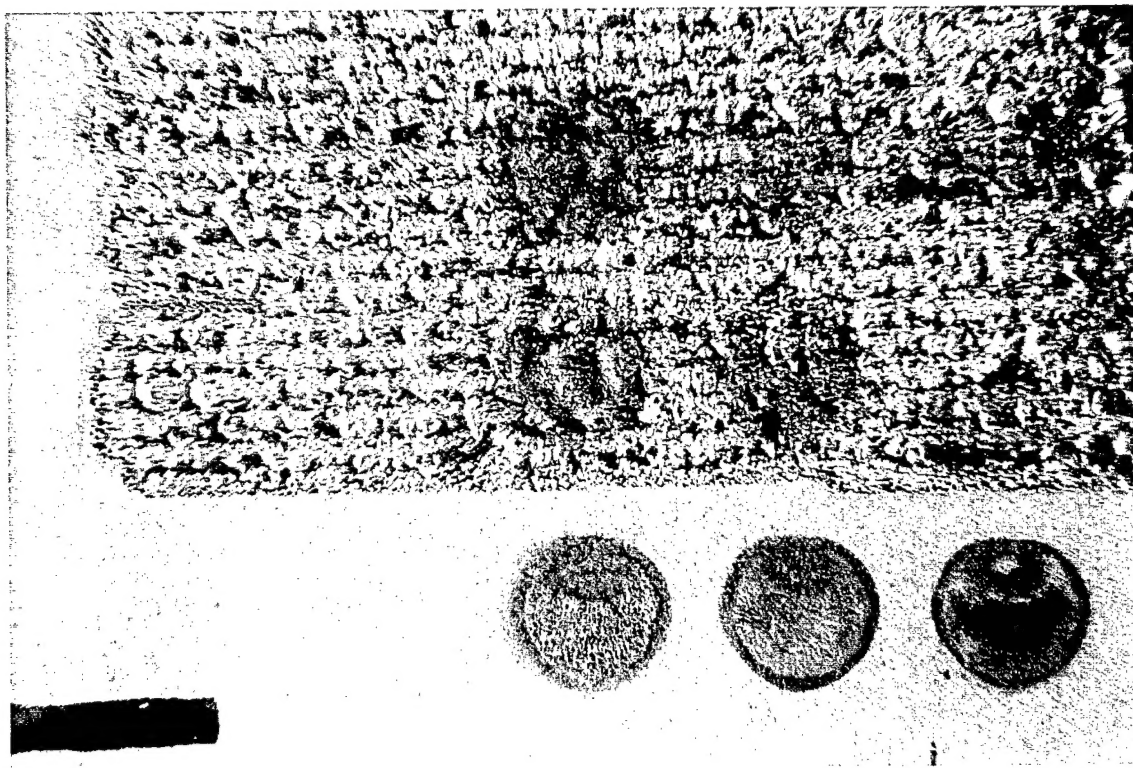


Figure 18: Titanium laser weld overlayed with 90Ta-10W and coated with graphite before thermal cycle testing. Upper left has 250 shots, centre left has 50 shots.

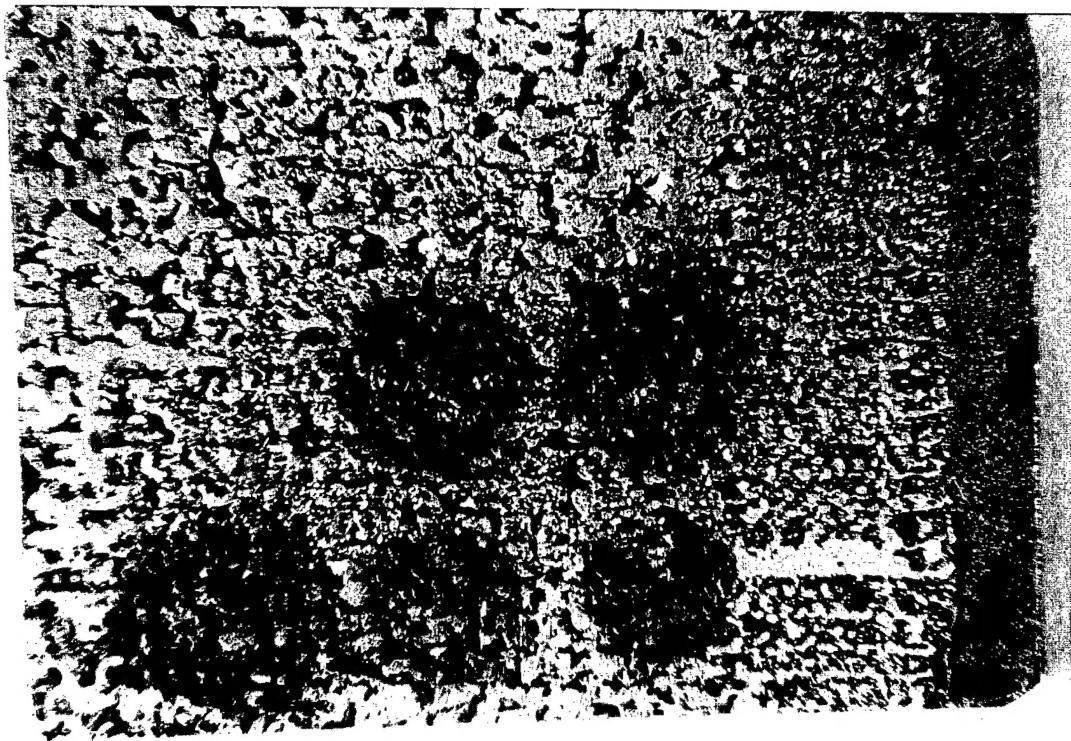


Figure 19: Titanium laser weld overlayed with 90Ta-10W. Surface ground and coated with graphite before thermal cycle testing. Upper left has 250 shots, centre left has 50 shots.

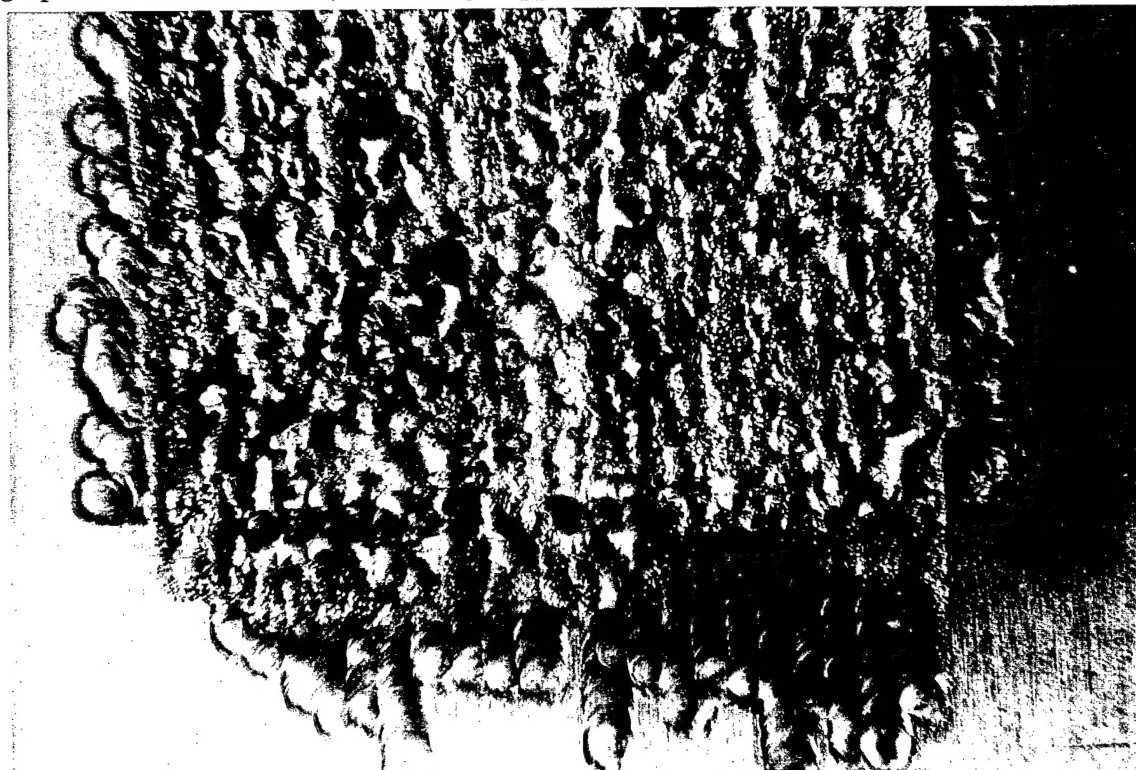


Figure 20: AISI 4340 with laser weld overlayed Ti, with laser weld overlayed 90Ta-10W and coated with graphite before thermal cycle testing.

UNCLASSIFIED

SECURITY CLASSIFICATION OF FORM
(highest classification of Title, Abstract, Keywords)

DOCUMENT CONTROL DATA		
(Security classification of title, body of abstract and indexing annotation must be entered when the overall document is classified)		
1. ORIGINATOR (The name and address of the organization preparing the document. Organizations for whom the document was prepared, e.g. Establishment sponsoring a contractor's report, or tasking agency, are entered in section 8.) The Laser Institute 9924-45 Avenue Edmonton, Alberta, Canada, T6E 5J1		2. SECURITY CLASSIFICATION (Overall security of the document including special warning terms if applicable.) <p style="text-align: center;">UNCLASSIFIED</p>
3. TITLE (The complete document title as indicated on the title page. Its classification should be indicated by the appropriate abbreviation (S,C,R or U) in parentheses after the title.) <p style="text-align: center;">Laser Based Method of Evaluating the Behavior of Surfaces and Surface Treatments at Transient High Temperatures and Pressures.</p>		
4. AUTHORS (Last name, first name, middle initial. If military, show rank, e.g. Doe, Maj. John E.) <p style="text-align: center;">V.E. Merchant and J.A. Hewitt</p>		
5. DATE OF PUBLICATION (Month and year of publication of document.) <p style="text-align: center;">March 1997</p>	6a. NO. OF PAGES (Total containing information. Include Annexes, Appendices, etc.) <p style="text-align: center;">109</p>	6b. NO. OF REFS. (Total cited in document.) <p style="text-align: center;">74</p>
6. DESCRIPTIVE NOTES (The category of the document, e.g. technical report, technical note or memorandum. If appropriate, enter the type of report, e.g. interim, progress, summary, annual or final. Give the inclusive dates when a specific reporting period is covered.) <p style="text-align: center;">DREA Contractor Report</p>		
8. SPONSORING ACTIVITY (The name of the department project office or laboratory sponsoring the research and development. Include the address.) Defence Research Establishment Atlantic P.O. Box 1012, Dartmouth, N.S. B2Y 3Z7		
9a. PROJECT OR GRANT NUMBER (If appropriate, the applicable research and development project or grant number under which the document was written. Please specify whether project or grant.) <p style="text-align: center;">Project 1.g.h.</p>	9b. CONTRACT NUMBER (If appropriate, the applicable number under which the document was written.) <p style="text-align: center;">W7707-5-3295/01-HAL</p>	
10a. ORIGINATOR'S DOCUMENT NUMBER (The official document number by which the document is identified by the originating activity. This number must be unique to this document.)	10b. OTHER DOCUMENT NUMBERS (Any other numbers which may be assigned this document either by the originator or by the sponsor.) <p style="text-align: center;">DREA CR 97/408</p>	
11. DOCUMENT AVAILABILITY (Any limitations on further dissemination of the document, other than those imposed by security classification) <div style="margin-left: 20px;"> <input checked="" type="checkbox"/> Unlimited distribution <input type="checkbox"/> Distribution limited to defence departments and defence contractors; further distribution only as approved <input type="checkbox"/> Distribution limited to defence departments and Canadian defence contractors; further distribution only as approved <input type="checkbox"/> Distribution limited to government departments and agencies; further distribution only as approved <input type="checkbox"/> Distribution limited to defence departments; further distribution only as approved <input type="checkbox"/> Other (please specify): </div>		
12. DOCUMENT ANNOUNCEMENT (Any limitation to the bibliographic announcement of this document. This will normally correspond to the Document Availability (11). However, where further distribution (beyond the audience specified in 11) is possible, a wider announcement audience may be selected.)		

UNCLASSIFIED

SECURITY CLASSIFICATION OF FORM

DDO3 2/06/87

UNCLASSIFIED
SECURITY CLASSIFICATION OF FORM

13. **ABSTRACT** (a brief and factual summary of the document. It may also appear elsewhere in the body of the document itself. It is highly desirable that the abstract of classified documents be unclassified. Each paragraph of the abstract shall begin with an indication of the security classification of the information in the paragraph (unless the document itself is unclassified) represented as (S), (C), (R), or (U). It is not necessary to include here abstracts in both official languages unless the text is bilingual).

A set of experiments were performed in order to test the ability of a laser based system to simulate the chemical and thermal effects inside a gun barrel. It is expected that a laser based system would be a relatively inexpensive method for testing various materials and coatings for eventual gun barrel use, and to the present time, there are no publically documented systems capable of such testing. An extensive literature review revealed that simulation of the mechanical effects would not be possible under the scope of this project, but thermal and chemical simulations could be done. A chamber was constructed to be used for both laser weld overlaying in an inert atmosphere, and for the simulations. Laser melting of titanium indicated that the chamber could provide an inert atmosphere in which no visual contamination of the titanium occurred. Parameters were developed to weld overlay titanium on AISI 4340 using 0.25 mm of preplaced powder, 1 ms pulses at a frequency of 50 Hz, and energy of 7.5 J/pulse, and a speed of 2.1 mm/s. This coating was then used as an interlayer for weld overlaying a 90tantalum-10tungsten alloy. Since titanium has a melting temperature close to the alloy steel, it was conjectured (correctly) that it could be more easily laser weld overlayed than the high melting temperature tantalum-tungsten alloy. Since Ta-Ti form a solid solution, rather than intermetallics formed by Ta-Fe, this was the best interlayer. The 90Ta- 10W alloy was overlayed using 0.25 mm of preplaced powder, 1 ms pulses at a frequency of 50 Hz, and energy of 7.5 J/pulse, and a speed of 5.2 mm/s. The coating was not continuous, but did appear to be melted and bonded in several locations. Other coatings were produced, including 0.25 mm of Stellite 6 on A36 mild steel, and 90 Ta-10W on commercially pure titanium. These coatings and their base materials were then subjected to thermal cycle testing.

The testing involved using a frequency of 2 Hz corresponding to a firing rate of 120 rounds/minute, a pulse duration of 5 ms (typical of a gun), 5 shot bursts at 45 J/shot. A waiting period of 10 s between bursts was necessary for equilibrium temperatures to be reached. The process was calibrated using AISI14340. Although the system was capable of over 2000 shots (400 cycles), the parameters were based on 10 cycles (50 shots) to cause visible melting on the surface. After 10 cycles, the poorest material was the A36 mild steel which contained extensive melting. The 90Ta- 10W alloy seemed to perform the best, with little visible damage after 10 cycles (50 shots). After 20 cycles (100 shots), damage/melting was more evident, but did not worsen up to 50 cycles (250 shots).

14. **KEYWORDS, DESCRIPTORS or IDENTIFIERS** (technically meaningful terms or short phrases that characterize a document and could be helpful in cataloguing the document. They should be selected so that no security classification is required. Identifiers, such as equipment model designation, trade name, military project code name, geographic location may also be included. If possible keywords should be selected from a published thesaurus. e.g. Thesaurus of Engineering and Scientific Terms (TEST) and that thesaurus-identified. If it not possible to select indexing terms which are Unclassified, the classification of each should be indicated as with the title).

UNCLASSIFIED
SECURITY CLASSIFICATION OF FORM